

**MODAL INTERACTIONS IN THE DYNAMIC RESPONSE OF ISOTROPIC AND  
COMPOSITE PLATES**

by

Mohammad Jafar Hadian

Dissertation submitted to the Faculty of the  
Virginia Polytechnic Institute and State University  
in partial fulfillment of the requirements for the degree of  
Doctor of Philosophy  
in  
Engineering Mechanics

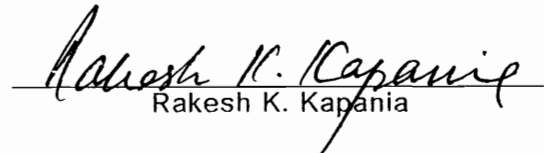
APPROVED:

  
Ali H. Nayfeh, Chairman

  
Dean T. Mook

  
Scott L. Hendricks

  
Junuthula N. Reddy

  
Rakesh K. Kapania

May, 1991

Blacksburg, Virginia

# **MODAL INTERACTIONS IN THE DYNAMIC RESPONSE OF ISOTROPIC AND COMPOSITE PLATES**

by

Mohammad Jafar Hadian

Ali H. Nayfeh, Chairman

Engineering Mechanics

(ABSTRACT)

Hamilton's principle and a third-order shear-deformation theory are used to derive a set of five coupled partial-differential equations governing the nonlinear response of composite plates. The reduction of these equations by using classical plate theory is discussed and the corresponding partial-differential equations governing both rectangular and circular plates are derived.

Generalized Levy-type solutions are obtained for the problem of linear free vibrations and linear stability of shear-deformable cross-ply laminated plates. The governing equations are transformed into a set of first-order linear ordinary-differential equations with constant coefficients. The general solution of these equations is obtained by using the state-space concept. Then, the application of the boundary conditions yields equations for the natural frequencies and critical loads. However, a straightforward application of the state-space concept yields numerically ill-conditioned problems as the plate thickness is reduced. Various methods for overcoming this problem are discussed. An initial-value method with orthonormalization is selected. It is shown that this method not only yields results that are in excellent agreement with the results in the literature, but it also converges fast and gives all the frequencies and buckling loads regardless of the plate

thickness. Further It is shown that the application of classical plate theory to thick plates yields inaccurate results.

The influence of modal interactions on the response of harmonically excited plates is investigated in detail. The case of a two-to-one autoparametric resonance in shear-deformable composite laminated plates is considered. Four first-order ordinary-differential equations describing the modulation of the amplitudes and phases of the internally resonant modes are derived using the averaged Lagrangian when the higher mode is excited by a primary resonance. The fixed-point solutions are determined using a homotopy algorithm and their stability is analyzed. It is shown that besides the single-mode solution, two-mode solutions exist for a certain range of parameters. It is further shown that in the multi-mode case the lower mode, which is indirectly excited through the internal resonance may dominate the response. For a certain range of parameters, the fixed points lose stability via a Hopf bifurcation, thereby giving rise to limit cycle solutions. It is shown that these limit-cycles undergo a series of period-doubling bifurcations, culminating in chaos.

Finally, the case of a combination resonance involving the first three modes of axisymmetric circular plates is studied. The method of multiple scales is used to determine a set of ordinary-differential equations governing the modulation of phases and amplitudes. It is shown that the internal resonance is responsible for coupling of the modes involved and that the excited mode is not necessarily the dominant one. Furthermore, it is shown that for a choice of parameters the multi-mode response loses stability through a Hopf bifurcation, resulting in periodically or chaotically modulated motions of the plate.

## Acknowledgements

I would like to express my appreciation and gratitude to my advisor Professor Ali H. Nayfeh for his guidance and support. Special thanks also go to the members of my committee: Professors Dean T. Mook, Scott L. Hendricks, Junuthula N. Reddy, and Rakesh K. Kapania. Their comments and valuable advice were valuable for completing this work.

I appreciate the friendship and assistance of fellow graduate students: Raouf Raouf, Balakumar Balachandran, Marwan Bikdash, Jamal Nayfeh, Jamal Masad, Tariq Nayfeh, and Frank Pai.

Thanks are also due to the Army Research Office for supporting this research under Grant No. DAAL03-89-K-0180 and the Center for Innovative Technology under Contract No. MAT-91-013.

I wish to express my appreciation to my family for their continuous support and encouragement. Special thanks go to my wife, Sayeh, for her unselfish patience, understanding, and support.

Finally, it is a pleasure to acknowledge the excellent typing skills and friendly helpfulness of Mrs. Sally Shrader during the preparation of part of this dissertation.

# Table of Contents

**1. INTRODUCTION ..... 1**

1.1. Isotropic Plates ..... 2

1.2. Composite Plates ..... 5

1.3. Nonlinear Systems ..... 8

1.4. Modal Interactions ..... 10

1.5. Objectives and Scope of the Dissertation ..... 14

**2. THE GOVERNING EQUATIONS OF LAMINATED PLATES ..... 16**

2.1. The Displacement Field ..... 17

2.2. Strain-Displacement Relations ..... 18

2.3. Constitutive Relations ..... 20

2.4. The Lagrangian ..... 21

    2.4.1. Kinetic energy ..... 22

    2.4.2. Potential energy ..... 23

2.5. Equations of Motion ..... 25

2.6. Simplifications by Using CPT ..... 32

    2.6.1. Rectangular plates ..... 33

    2.6.2. Axisymmetric circular plates ..... 36

**3. LINEAR FREE VIBRATIONS AND BUCKLING OF CROSS-PLY LAMINATED PLATES ... 43**

3.1. Free Vibration .....	46
3.2. Stability .....	49
3.3. Method of Solution .....	49
3.4. Numerical Results .....	55
 <b>4. MODAL INTERACTION IN THE RESPONSE OF COMPOSITE RECTANGULAR PLATES .</b>	<b>74</b>
4.1. Solution Procedure .....	75
4.2. Autoparametric Resonance .....	79
4.2.1. Polar form .....	82
4.2.2. Cartesian form .....	84
4.3. Numerical Results .....	86
4.3.1. Single-mode solutions .....	88
4.3.2. Two-modes solutions .....	90
4.3.2.1. Fixed point solutions of the averaged equations and their stability ..	90
4.3.2.2. Periodic solutions of the averaged equations and their stability .....	92
 <b>5. MODAL INTERACTION IN CIRCULAR PLATES .....</b>	<b>109</b>
5.1. Nondimensionalization .....	109
5.2. Method of Solution .....	112
5.3. Numerical Results .....	121
 <b>6. SUMMARY AND RECOMMENDATIONS FOR FUTURE WORK .....</b>	<b>136</b>
6.1. Present Study .....	136
6.2. Recommendations for Future Work .....	138
 <b>References .....</b>	<b>140</b>
 <b>Appendix A. The elements of the coefficient matrix in equation (3.10): free vibrations ..</b>	<b>155</b>

**Appendix B. The elements of boundary coefficient matrices in equation (3.11): free vibrations . . . . . 157**

**Appendix C. The elements of the coefficient matrix in equation (3.10): stability . . . . . 159**

**Appendix D. The elements of boundary coefficient matrices in equation (3.11): stability . 161**

**Appendix E. The constant coefficients in equation (4.16) . . . . . 163**

**Appendix F. The elements of the Jacobian matrices . . . . . 166**

**VITA . . . . . 168**

# 1. INTRODUCTION

The interaction of modes in plates is of interest in connection with various structures. Such a phenomenon may occur when the linear natural frequencies of some modes are commensurate or nearly commensurate. This phenomenon which is due to internal resonances have led to undesirable and sometimes catastrophic events in the past because engineers and scientists were not aware of the possibility of modal interactions. Therefore, it is our interest to study modal interactions in plates.

Because composite materials are extensively used in airspace, missile, shipbuilding, and many other industries, we investigate the influence of nonlinearities on the response of composite plates. In particular, we study two-to-one modal interactions in composite plates using the the third-order shear-deformation plate theory of Reddy. As a numerical example we choose a simply-supported cross-ply laminated plate. As a first step in the nonlinear analysis, one needs the linear solution. Thus, we discuss Levy-type solutions.

Moreover, we analyze modal interactions in isotropic circular plates. Because shear deformations in thin isotropic plates are known to be small and negligible, we



use the classical plate theory and the method of multiple scales (Nayfeh, 1973, 1981) to study the response of isotropic circular plates to external excitation in the presence of a combination internal resonance.

Next, some previous work on plate mechanics and dynamics of relevant nonlinear systems is presented.

## ***1.1. Isotropic Plates***

The fundamental assumptions of the small deflection theory of bending or the so-called classical theory for thin plates, known as the Kirchhoff hypotheses, can be stated as follows:

1. The deflection of the midsurface is small compared with the thickness of the plate.
2. The midplane remains unstrained and neutral during bending.
3. Plane sections initially normal to the midsurface of the plate remain plane and normal to that surface after bending. This means that the transverse shear strains are negligible.
4. The normal stresses in the direction transverse to the midsurface of the plate are small compared with the other stress components and may be neglected.

These assumptions are extensions of those made in the simple bending theory of beams.

When the deflections are not small the bending of plates is accompanied by strains in the midsurface, and the first two assumptions are not applicable any longer. The governing differential equations for large deflections of thin plates were obtained and introduced by von Karman (1910). Analytical solutions to these coupled partial differential equations may be a formidable task. Among the books with approximate solutions for plates of simple regular shapes, we quote those of Timoshenko and Woinowsky-Krieger (1959) and Sokolnikoff and Redheffer (1966). Banerjee (1982, 1983) presented approximate solutions for large deflections of isotropic circular plates of variable thickness using the Galerkin method. He used a one-term expansion for the deflection. Berger (1955) used a variational principle and ignored the second invariant in the energy term to obtain simplified governing equations for plates.

The dynamic problem of large deflections of plates has attracted the attention of many researchers in recent decades. Wah (1963) extended the approximation suggested by Berger and reduced the coupled fourth-order partial-differential equations of von Karman to a single fourth-order partial-differential equation. Nash and Modeer (1959) followed the Berger approximation and derived the dynamic analog of Berger's equations. They showed that the application of these equations to simply-supported plates leads to results that are in excellent agreement with those obtained by using the dynamic analogue of von Karman equations. Huang and Al-Khattat (1977) considered the vibration of a circular plate and showed that solutions based on the Berger hypothesis are accurate at low amplitudes of vibration but that the accuracy decreases as the amplitude increases. They also showed that the Berger hypothesis is entirely unsuitable for plates with movable edges. Nowinski

and Ohnabe (1972) also pointed out that the Berger hypothesis may lead to inaccurate and even meaningless results for plates without the inplane restraint.

The dynamic analogue of von Karman equations, which take into account the stretching of the midsurface, were used by several investigators to study the response of plates to harmonic excitations. Chia (1980) gave a comprehensive review of the literature through 1979. Some early experimental results were obtained by Tobias (1958) for main-resonant vibrations of free circular plates. Yamaki (1967) obtained approximate solutions for rectangular and circular plates with various boundary conditions. He used a single-term Galerkin expansion. Kung and Pao (1972) used a combination of the Galerkin method and the method of harmonic balance to analyze axisymmetric vibrations of circular plates. Rehfield (1974) proposed a new method for investigating single-mode main resonances of structures in which Hamilton's principle is combined with a perturbation procedure; he applied the method to beams and rectangular plates. Easley (1964) used a combination of the Galerkin method with the Lindstedt-Poincare technique to investigate the main-resonant vibration of buckled rectangular plates.

Huang and Sandman (1971) used the Kantorovich method to study axisymmetric vibrations of circular plates. They used a numerical technique to solve the resulting two-point boundary-value problems; Huang (1973) used the same approach to study the main-resonant vibration of an axisymmetric orthotropic circular plate. None of these studies considered multi-mode solutions.

Sridhar et al. (1975, 1978) and Lobitz et al. (1977) investigated primary resonant responses of a circular isotropic plate. They considered the interaction of modes and the possibility of multi-mode solutions.

## **1.2. Composite Plates**

The fundamentals of the mechanics of composite materials can be found in the books by Jones (1975), Christensen (1979), and Tsai and Hahn (1980). Bennett (1971) considered the response of simply-supported rectangular laminated plates. He used a four-term Galerkin expansion. Chandra and Raju (1975) and Chandra (1976) investigated the nonlinear response of cross-ply laminated plates. They employed the Galerkin method to reduce the governing nonlinear partial-differential equations to an ordinary-differential equation, which they solved using perturbation techniques and a Runge-Kutta numerical scheme. Chia and Prabhakara (1976, 1978) employed the approach used by Chandra (1976) to study the nonlinear responses of cross-ply and angle-ply laminated rectangular plates. Eslami and Kandil (1989) used a combination of the Galerkin method and the method of multiple scales (Nayfeh, 1973, 1981) to analyze the nonlinear forced and damped responses of rectangular orthotropic plates to uniformly distributed harmonic transverse loads.

A composite plate is weak in shear because its elastic modulus is much larger than its shear modulus is weak in shear. The classical theory of plates (CPT) neglects transverse shear strains and hence does not lead to accurate results for thick laminated plates. Srinivas et al. (1970) showed that the vibration analysis of homogeneous thick laminated plates carried out without considering transverse shear deformations is highly inaccurate. Pagano (1969, 1970) demonstrated the deficiencies of classical plate theory for thick laminated plates by comparing his exact solutions for cylindrical bending of a simply-supported rectangular plate subjected to a distributed harmonic transverse load with the results obtained by CPT.

These works clearly illustrate the need for including the transverse shear effects in the analysis of thick composite plates.

A number of improved theories have been proposed by various authors. Reissner (1945) and Mindlin (1951) were the first to provide first-order shear-deformation theories that account for variations of stresses and displacements through the thickness of the plate, respectively. These theories when applied to isotropic plates yield a system of sixth-order partial-differential equations that allow the specification of three boundary conditions at each edge. Medwadowski (1958) extended Reissner's theory to orthotropic plates. He used the von Karman type nonlinearity for isotropic plates and included the effects of transverse shear and rotary inertia for orthotropic plates. Stavsky (1965) is the first to apply the first-order shear-deformation theory to laminated isotropic plates.

Noor and Hartley (1977) included the effect of transverse shear and used a finite-element method to investigate the nonlinear response of composite plates. Reddy and Chao (1981a) formulated a quadratic finite element to study large displacements and large-amplitude free vibrations of laminated composite plates. Their formulation has been extended for the study of the nonlinear vibration behavior of sandwich plates by Rajgopal et al. (1986). Among the many other works on the nonlinear analysis of plates, including the effect of transverse shear, we quote those of Schmidt (1977), Wu and Vinson (1969a,b), Singh, Sundararajan, and Das (1974), Sathyamoorthy (1978, 1979, 1984a), Sathyamoorthy and Chia (1980), and Prathap and Pandalai (1979). Wu and Vinson (1971) used the Berger approach and discussed the effect of transverse shear deformations on the nonlinear response of cross-ply laminated plates. Sathyamoorthy (1981) suggested an improved version of Berger-type theory for the dynamic analysis of rectilinearly orthotropic moderately thick circular plates. Sathyamoorthy (1984b) used the Berger approach to investigate

the effect of transverse shear deformations, geometrical nonlinearity, and modal interactions on the dynamic behavior of moderately thick orthotropic circular plates clamped along the boundary. He compared the results with those he obtained by using the von Karman-type theory and validated the Berger approximation for moderately thick plates. Sathyamoorthy and Prasad (1983) conducted a multi-mode analysis of isotropic circular plates and showed the significance of modal interactions, especially for moderately thick plates.

Lo, Christensen, and Wu (1977a,b) developed a higher-order plate theory in which the transverse and inplane displacements were expanded as quadratic and cubic functions of the transverse coordinate, respectively. Levinson (1980) considered similar expansions for the inplane displacements. In these higher-order shear-deformation theories there is no need for a shear-correction factor, which is a necessity in the first-order refined theories. Reddy (1984a,b) developed a refined plate theory in which the expanded displacement field is similar to that of Levinson (1980) and Murthy (1981). He used the method of virtual displacements to derive the equations of motion. The higher-order shear-deformation theory (HSDT) of Reddy accounts for quadratic distributions of the transverse shear strains through the thickness. In addition to being variationally consistent, Reddy's modification satisfies the condition of zero transverse shear stresses on the top and bottom surfaces of the plates. A similar third-order shear-deformation theory was also proposed by Bhimaraddi and Stevens (1984) in which the generalized variables are slightly different from those of Reddy. A review and discussion of the relationship of all third-order shear-deformation theories of plates is presented by Reddy (1990).

### **1.3. Nonlinear Systems**

Nonlinear systems have taken the attention of many mathematicians and scientists in the recent decades. In the area of dynamics of plates the prime target of most authors was the calculation of the nonlinear frequencies. Chia and Prabhakara (1978), Prabhakara and Chia, (1977), and Sivakumaran and Chia (1985) investigated the dependence of the nonlinear frequencies of rectangular plates on the amplitude of vibration. They used Fourier series in space and the method of harmonic balance in time. Reddy and Chao (1981b) included the effects of shear deformation and rotary inertia and studied free vibrations of rectangular laminated plates. They used finite elements in space and numerical integration in time. Chu and Herman (1956), Yamaki (1967), and Rao et. al (1976) used classical plate theory while Wah (1963) and Mei (1973) used Berger's approximation to calculate the nonlinear frequencies of the same isotropic rectangular plate. These results are represented and compared with in the work of Reddy and Chao (1981b). However, none of the above studied the qualitative nonlinear behavior of plates. They did not consider nonlinear phenomena, such as modal interactions, which are inherent in physical systems with nonlinear governing differential equations and/or nonlinear boundary conditions.

The equations governing the nonlinear dynamics of plates and several other physical systems share many qualitative behaviors. A comprehensive literature survey and discussion of nonlinear systems can be found in the excellent book by Nayfeh and Mook (1979). In addition to a survey of mathematical models exhibiting chaotic vibrations, a variety of theoretical and experimental tools for characterizing chaos are given by Moon (1987). Among other books in the field, we quote those of

Hale (1963), Urabe (1967), Marsden and McCracken (1976), Jordan and Smith (1977), Iooss and Joseph (1980), Hassard, Kazarinoff, and Wan (1981), Chow and Hale (1982), Vanderbauwhede (1982), Guckenheimer and Holmes (1983), Thompson and Stewart (1986), and Seydel (1988).

Nayfeh (1988) discussed the existence of various nonlinear responses, such as saturation, jumps, period-doubling bifurcations, and chaos in nonlinear systems. Evan-Iwanowski (1976), Ibrahim (1985), and Schmidt and Tondl (1986) gave comprehensive reviews of parametric excitations. Zavodney and Nayfeh (1988) studied the response of one-degree-of-freedom systems with quadratic and cubic nonlinearities to a fundamental harmonic parametric excitation. They used the method of multiple scales to obtain a second-order solution. They showed that the system exhibits complicated behavior, including period-multiplying and demultiplying bifurcations and chaos. Kojima et al. (1985) investigated the nonlinear forced vibration of a beam with a mass to parametric excitations and found superharmonic and subharmonic vibrations of order two and one-half, respectively. Gurgoze (1986) studied parametric vibrations of a restrained beam with mass at one end and a displacement excitation at the other end. He used a one-mode Galerkin approximation and reduced the governing partial-differential equation to a Mathieu equation containing cubic nonlinearities. He obtained an approximate solution for the case of a principal parametric resonance. HaQuang (1986) studied the nonlinear response of one- and two-degree-of-freedom systems having quadratic and cubic nonlinearities to external, parametric, and combined external and parametric excitations. He found period-multiplying bifurcations and chaotic responses. Szemplinska-Stupnicka (1978) studied the response of parametrically excited systems. She used the method of harmonic balance and validated her results by using an analog computer.



Awrejcewicz (1989) presented an analysis of the transition from regular to chaotic motions in a van der Pol-Duffing oscillator with time delay after a Hopf bifurcation. He determined conditions for the occurrence of the Hopf bifurcation by means of an approximate method.

## ***1.4. Modal Interactions***

The interaction of modes may take place in multi-degree-of-freedom systems. Nayfeh et al. (1973) and Mook et al. (1974) applied the method of multiple scales to analyze the response of a system of two coupled oscillators with quadratic nonlinearities to a harmonic excitation. Their system models the interaction of pitch and roll modes of a ship. They considered the cases of primary and secondary resonances when the linear natural frequency of the pitch mode is approximately twice that of the roll mode. They showed that when the excitation frequency is near the frequency of the higher mode (pitch mode) the system exhibits a saturation phenomenon, and when the excitation frequency is near the frequency of the lower mode (roll mode) an amplitude- and phase-modulated motion becomes possible. Later Yamamoto and Yasuda (1977) applied the method of harmonic balance to study the forced response of systems with quadratic and cubic nonlinearities to a harmonic excitation when one frequency is twice the other. They used analog-computer simulations and obtained amplitude- and phase-modulated steady-state responses for the case of primary resonance of either mode. Hatwal, Mallik, and Ghosh (1983a, 1983b) investigated the forced nonlinear oscillation of a two-degree-of-freedom

system. They showed that the motion of the system may be periodic or chaotic in the presence of a two-to-one autoparametric resonance.

Haddow, Barr, and Mook (1984) investigated modal interactions in a two-degree-of-freedom beam structure under a harmonic external excitation. They conducted an experiment and verified the saturation phenomenon. Balachandran and Nayfeh (1990) studied the planar dynamic response of a flexible L-shaped beam-mass structure with a two-to-one internal resonance to a primary resonance. They obtained the equations governing the modulations of the amplitudes and phases by averaging the Lagrangian of the system over the period of the primary oscillation. They experimentally verified the analytical solutions.

Pai and Nayfeh (1991a,b) investigated the response of composite beams having two-to-one internal resonances to subharmonic and superharmonic excitations. They considered elastic bending-torsion coupling and identified chaotic motions.

Maganty and Bickford (1988) used the method of multiple scales to study the nonlinear response of a circular ring. Yasuda and Kushida (1984) studied axisymmetric responses of shallow spherical shells to primary resonant excitation of a higher flexural mode. They performed an experiment in the presence of a two-to-one internal resonance and observed periodic responses of the shell. Raouf and Nayfeh (1990b) studied the nonlinear axisymmetric response of spherical shells to radial harmonic excitation. Nayfeh, Raouf, and Nayfeh (1990) studied the response of cylindrical shells to a subharmonic radial excitation in the presence of two-to-one internal resonance. Nayfeh and Raouf (1987) studied the nonlinear response of an infinitely long circular cylindrical shell to primary resonant excitations of the breathing and flexural modes in the presence of a two-to-one internal resonance. They used the method of multiple scales and obtained differential equations governing the amplitudes and phases whose solutions exhibit jumps, the saturation

phenomenon, and Hopf bifurcations, leading to amplitude- and phase-modulated motions.

Nayfeh and Zavodney (1986) studied the response of two-degree-of-freedom systems with quadratic nonlinearities to combination parametric resonances. They presented steady-state solutions and their stability. They also presented limit-cycle solutions and period-doubling bifurcations using numerical techniques. Streit, Bajaj, and Krousgrill (1988) studied a similar system and found Hopf bifurcations and limit-cycle solutions. They showed that the limit cycles undergo a cascade of period-doubling bifurcations culminating in chaos.

Miles (1984a) studied the case of perfectly tuned two-to-one internal resonances in surface waves. He considered the case of principal parametric resonance of the lower mode and found no Hopf bifurcations. He concluded that there are no limit-cycle or chaotic solutions of the modulation equations. Nayfeh (1987a,b) used the method of multiple scales to analyze the problem studied by Miles (1984a, 1985). He relaxed the assumption of perfectly tuned internal resonance and found Hopf bifurcations and period-multiplying bifurcations culminating in chaos.

Miles (1984b) used the method of averaging to study the response of two internally resonant coupled oscillators with quadratic nonlinearities to a harmonic excitation. He investigated the stability of the analytical solutions and presented numerical results that demonstrate periodically and chaotically modulated motions when the excitation frequency is near the lower frequency. Nayfeh (1987a) studied a parametrically excited double pendulum in the presence of two-to-one internal resonances. He found that the response exhibits a Hopf bifurcation leading to amplitude- and phase-modulated motions. Furthermore, he showed that the periodic motions of the averaged equations may undergo period-doubling bifurcations leading to chaos.

Shaw and Shaw (1989) investigated the dynamic response of a two-degree-of-freedom impacting system consisting of an inverted pendulum with motion limiting stops. They attached this system to a sinusoidally excited mass-spring system. They found several types of periodic motions and discussed the stability of two types of motion. They also found chaotic motions and concluded that a great care should be taken in the design of an inverted pendulum with an unstable central position as an absorber.

Nayfeh and Pai (1989) used the method of multiple scales to study the case of one-to-one internal resonance between the inplane and out-of-plane motions of beams. They found Hopf bifurcations and periodically and chaotically modulated motions. Feng and Sethna (1989) studied symmetry-breaking bifurcations of surface waves in nearly square containers subjected to a vertical excitation. For the case of one-to-one internal resonance, they showed that the system may exhibit periodic, quasi-periodic, or chaotically modulated motions. Raouf and Nayfeh (1990a) investigated the nonlinear response of infinitely long cylindrical shells to a harmonic excitation. They considered a one-to-one internal resonance and used the method of multiple scales to derive the modulation equations. They obtained both periodic and periodically- and chaotically-modulated motions of the shells.

Yasuda and Torri (1986) used the method of multiple scales to analyze the nonlinear forced response of a string. They studied the multi-mode responses near the first, third, and fourth primary resonance points. They performed an experiment with a thin steel strip to validate their theoretical results.

## ***1.5. Objectives and Scope of the Dissertation***

In this thesis, we analyze modal interactions in isotropic circular and rectangular composite laminated plates. We use the method of multiple scales to derive nonlinear equations governing the modulation of the amplitudes and phases of the interacting modes. These modulation equations are used to investigate and trace some nonlinear phenomenon. We demonstrate the existence of periodic motions, jumps, Hopf and period-doubling bifurcations, and chaotically-modulated motions in the response of rectangular and circular plates to harmonic excitation. These modal interactions, quasiperiodic motions, period-doubling bifurcations, and chaotic behaviors of plates have never been studied in depth prior to the present work.

For rectangular cross-ply laminated plates, both Navier- and Levy-type solutions are investigated. For the Levy-type case, the problem is reduced to the solution of a set of linear first-order ordinary differential-equations, which can be solved using the state-space concept. Several methods for obtaining the numerical of this problem are discussed and an initial value method with orthonormalization is selected. The latter yields all the natural frequencies regardless of the plate thickness (Chapter 3).

Rectangular composite plates are treated in Chapter 4. The case of two-to-one internal resonance is considered. The two-to-one internal resonance is due to the quadratic terms. Modulation equations governing the amplitudes and phases of the interacting modes are obtained by averaging the Lagrangian of the motion over the fast time. These modulation equations contain both quadratic and cubic terms. The cubic terms cause a shift in frequency. It is found that the plates exhibit single-mode and two-mode periodic motions in addition to periodically and chaotically modulated motions.

In the study of the axisymmetric response of circular isotropic plates, the method of multiple scales is used to derive the modulation equations. The nonlinearities in the modulation equations are cubic. The internal resonance considered is a combination resonance involving the lowest three modes. In this case, similar to the case of shear-deformable composite rectangular plates, single-mode and multi-mode (three-mode) solutions are possible (Chapter 5). Some of the multi-mode solution may correspond to periodically- or chaotically-modulated motions.

## **2. THE GOVERNING EQUATIONS OF LAMINATED PLATES**

In this chapter we present the nonlinear equations of motion of shear-deformable composite plates based on a combination of the higher-order shear-deformation theories of plates given by Reddy (1984a-c) and Bhimaraddi and Stevens (1984). The strain-displacement relations are assumed to be nonlinear in the von Karman sense. Hamilton's principle is used to derive five coupled nonlinear partial-differential equations governing the displacements of laminated plates constructed from orthotropic layers of general orientations.

In Section 2.6 the governing equations of isotropic rectangular and circular plates based on the classical plate theory are presented. A coordinate transformation is used to transform the governing equations of rectangular plates into those governing circular plates in a cylindrical coordinate system. A stress function is defined and the governing equations in the absence of shear deformations and rotary inertias are combined into two coupled fourth-order nonlinear partial-differential equations in terms of the transverse deflection and the stress function.

## 2.1. The Displacement Field

A rectangular coordinate system  $xyz$  is chosen such that the  $x$ - $y$  plane coincides with the midsurface of the plate before deformation. The higher-order shear-deformation theory (HSDT) of Reddy assumes that the inplane components of the displacements are cubic functions of the transverse coordinate  $z$ . Hence, the transverse shear distribution is assumed to be a quadratic function of  $z$ . Requiring the stresses to vanish at the top and bottom surfaces, one can express the displacement field as

$$\begin{aligned}u_1(x,y,z,t) &= u(x,y,t) - z \frac{\partial w}{\partial x} + z \left[ 1 - \frac{4}{3} \left( \frac{z}{h} \right)^2 \right] \phi(x,y,t) \\u_2(x,y,z,t) &= v(x,y,t) - z \frac{\partial w}{\partial y} + z \left[ 1 - \frac{4}{3} \left( \frac{z}{h} \right)^2 \right] \psi(x,y,t) \\u_3(x,y,z,t) &= w(x,y,t)\end{aligned}\tag{2.1}$$

where  $u_1$ ,  $u_2$ , and  $u_3$  denote the components of the displacement in the  $x$ ,  $y$ , and  $z$  directions, respectively. Here,  $u$ ,  $v$ ,  $w$ ,  $\phi$ , and  $\psi$  are the generalized coordinates of a point  $(x,y)$  on the midplane at time  $t$  (see Figure 2.1). The plate is assumed to have a total thickness  $h$  and the dimensions  $a$  and  $b$  in the  $x$  and  $y$  directions, respectively. Like CPT, it is assumed that the plate thickness remains the same and hence the transverse component of the displacement is not a function of  $z$ . When  $\phi$  and  $\psi$ , which measure the effect of shear deformation, are set equal to zero, the displacement field reduces to its counterpart in CPT. The coefficients of  $\phi$  and  $\psi$  in equations (2.1) are the most simple functions of  $z$  that identically satisfy the conditions of zero shear stress at the top and bottom surfaces. These coefficients



vanish at the midsurface and reach their maxima on the top and bottom surfaces of the plate.

## 2.2. Strain-Displacement Relations

The deflections are assumed to be large in comparison with the plate thickness but are nevertheless small compared with the other dimensions. The von Karman approximation of the nonlinear Lagrangian strain tensor is used, where squares and products of  $\frac{\partial w}{\partial x}$  and  $\frac{\partial w}{\partial y}$  are the only nonlinear terms retained. These strains are

$$\begin{aligned}
 \varepsilon_1 &= \frac{\partial u_1}{\partial x} + \frac{1}{2} \left( \frac{\partial w}{\partial x} \right)^2 \\
 \varepsilon_2 &= \frac{\partial u_2}{\partial y} + \frac{1}{2} \left( \frac{\partial w}{\partial y} \right)^2 \\
 \varepsilon_3 &= 0 \\
 \varepsilon_4 &= \frac{\partial u_2}{\partial z} + \frac{\partial w}{\partial y} \\
 \varepsilon_5 &= \frac{\partial u_1}{\partial z} + \frac{\partial w}{\partial x} \\
 \varepsilon_6 &= \frac{\partial u_1}{\partial y} + \frac{\partial u_2}{\partial x} + \frac{\partial w}{\partial x} \frac{\partial w}{\partial y}
 \end{aligned} \tag{2.2}$$

According to the displacement field (2.1) these strains can be written as

$$\begin{aligned}
\varepsilon_1 &= \varepsilon_1^0 + z\kappa_1^0 + z^3\kappa_1^2 \\
\varepsilon_2 &= \varepsilon_2^0 + z\kappa_2^0 + z^3\kappa_2^2 \\
\varepsilon_3 &= 0 \\
\varepsilon_4 &= \varepsilon_4^0 + z^2\kappa_4^2 \\
\varepsilon_5 &= \varepsilon_5^0 + z^2\kappa_5^2 \\
\varepsilon_6 &= \varepsilon_6^0 + z\kappa_6^0 + z^3\kappa_6^2
\end{aligned} \tag{2.3}$$

where

$$\begin{aligned}
\varepsilon_1^0 &= \frac{\partial u}{\partial x} + \frac{1}{2} \left( \frac{\partial w}{\partial x} \right)^2, \quad \kappa_1^0 = \frac{\partial \phi}{\partial x} - \frac{\partial^2 w}{\partial x^2}, \quad \kappa_1^2 = \frac{-4}{3h^2} \frac{\partial \phi}{\partial x} \\
\varepsilon_2^0 &= \frac{\partial v}{\partial y} + \frac{1}{2} \left( \frac{\partial w}{\partial y} \right)^2, \quad \kappa_2^0 = \frac{\partial \psi}{\partial y} - \frac{\partial^2 w}{\partial y^2}, \quad \kappa_2^2 = \frac{-4}{3h^2} \frac{\partial \psi}{\partial y} \\
\varepsilon_4^0 &= \psi, \quad \kappa_4^2 = -\frac{4}{h^2} \psi \\
\varepsilon_5^0 &= \phi, \quad \kappa_5^2 = -\frac{4}{h^2} \phi \\
\varepsilon_6^0 &= \frac{\partial u}{\partial y} + \frac{\partial v}{\partial x} + \frac{\partial w}{\partial x} \frac{\partial w}{\partial y}, \\
\kappa_6^0 &= \frac{\partial \phi}{\partial y} + \frac{\partial \psi}{\partial x} - 2 \frac{\partial^2 w}{\partial x \partial y}, \quad \kappa_6^2 = -\frac{4}{3h^2} \left( \frac{\partial \phi}{\partial y} + \frac{\partial \psi}{\partial x} \right)
\end{aligned} \tag{2.4}$$

In equations (2.3) the  $\varepsilon_i^0$  represent the midsurface strains, the  $\kappa_i^0$  represent the curvatures, and the  $\kappa_i^2$  are contributions of the third-order shear-deformation theory used.

### 2.3. Constitutive Relations

The constitutive equations of an orthotropic layer, in material-symmetry axes, are given by

$$\begin{bmatrix} \bar{\sigma}_1 \\ \bar{\sigma}_2 \\ \bar{\sigma}_6 \end{bmatrix} = \begin{bmatrix} \bar{Q}_{11} & \bar{Q}_{12} & 0 \\ \bar{Q}_{12} & \bar{Q}_{22} & 0 \\ 0 & 0 & \bar{Q}_{66} \end{bmatrix} \begin{bmatrix} \bar{\varepsilon}_1 \\ \bar{\varepsilon}_2 \\ \bar{\varepsilon}_6 \end{bmatrix}, \quad \begin{bmatrix} \bar{\sigma}_4 \\ \bar{\sigma}_5 \end{bmatrix} = \begin{bmatrix} \bar{Q}_{44} & 0 \\ 0 & \bar{Q}_{55} \end{bmatrix} \begin{bmatrix} \bar{\varepsilon}_4 \\ \bar{\varepsilon}_5 \end{bmatrix} \quad (2.5)$$

where the  $\bar{Q}_{ij}$  are the plane-strain reduced elastic constants

$$\begin{aligned} \bar{Q}_{11} &= E_1/(1 - \nu_{12}\nu_{21}), \quad \bar{Q}_{12} = \nu_{12}E_2/(1 - \nu_{12}\nu_{21}), \quad \bar{Q}_{22} = E_2/(1 - \nu_{12}\nu_{21}) \\ \bar{Q}_{44} &= G_{23}, \quad \bar{Q}_{55} = G_{13}, \quad \bar{Q}_{66} = G_{12} \end{aligned} \quad (2.6)$$

Here, the  $E_i$ ,  $G_{ij}$ , and  $\nu_{ij}$  are the Young's moduli, shear moduli, and Poisson's ratios, respectively. The stress-strain relationships in equation (2.5) can be transformed into the principal laminate coordinates as follows:

$$\begin{bmatrix} \sigma_1 \\ \sigma_2 \\ \sigma_6 \end{bmatrix} = \begin{bmatrix} Q_{11} & Q_{12} & Q_{16} \\ Q_{12} & Q_{22} & Q_{26} \\ Q_{16} & Q_{26} & Q_{66} \end{bmatrix} \begin{bmatrix} \varepsilon_1 \\ \varepsilon_2 \\ \varepsilon_6 \end{bmatrix}, \quad \begin{bmatrix} \sigma_4 \\ \sigma_5 \end{bmatrix} = \begin{bmatrix} Q_{44} & Q_{45} \\ Q_{45} & Q_{55} \end{bmatrix} \begin{bmatrix} \varepsilon_4 \\ \varepsilon_5 \end{bmatrix} \quad (2.7)$$

where the  $Q_{ij}$  are the transformed reduced stiffnesses and are given by

$$\begin{aligned}
Q_{11} &= \bar{Q}_{11} \cos^4 \theta + 2(\bar{Q}_{12} + 2\bar{Q}_{66}) \sin^2 \theta \cos^2 \theta + \bar{Q}_{22} \sin^4 \theta \\
Q_{12} &= (\bar{Q}_{11} + \bar{Q}_{22} - 4\bar{Q}_{66}) \sin^2 \theta \cos^2 \theta + \bar{Q}_{12}(\sin^4 \theta + \cos^4 \theta) \\
Q_{22} &= \bar{Q}_{11} \sin^4 \theta + 2(\bar{Q}_{12} + 2\bar{Q}_{66}) \sin^2 \theta \cos^2 \theta + \bar{Q}_{22} \cos^4 \theta \\
Q_{16} &= (\bar{Q}_{11} - \bar{Q}_{12} - 2\bar{Q}_{66}) \sin \theta \cos^3 \theta + (\bar{Q}_{12} - \bar{Q}_{22} + 2\bar{Q}_{66}) \sin^3 \theta \cos \theta \\
Q_{26} &= (\bar{Q}_{11} - \bar{Q}_{12} - 2\bar{Q}_{66}) \sin^3 \theta \cos \theta + (\bar{Q}_{12} - \bar{Q}_{22} + 2\bar{Q}_{66}) \sin \theta \cos^3 \theta \\
Q_{66} &= (\bar{Q}_{11} + \bar{Q}_{22} - 2\bar{Q}_{12} - 2\bar{Q}_{66}) \sin^2 \theta \cos^2 \theta + \bar{Q}_{66}(\sin^4 \theta + \cos^4 \theta) \\
Q_{44} &= \bar{Q}_{44} \cos^2 \theta + \bar{Q}_{55} \sin^2 \theta \\
Q_{45} &= (\bar{Q}_{55} - \bar{Q}_{44}) \sin \theta \cos \theta \\
Q_{55} &= \bar{Q}_{55} \cos^2 \theta + \bar{Q}_{44} \sin^2 \theta
\end{aligned} \tag{2.8}$$

Here  $\theta$  is the rotation angle measured from the laminate coordinates to the lamina principal material coordinates.

## 2.4. The Lagrangian

In this section, the Lagrangian for a general laminated rectangular plate is formulated. Lagrange's equations of motion are derived using Hamilton's principle in the next section. It is necessary at this stage to obtain the Lagrangian which will be the basis for more general treatments. The Lagrangian approach provides an elegant and powerful technique for solving a variety of nonlinear physical systems, as we shall see in the subsequent chapters.

### 2.4.1. Kinetic energy

The expression for the plate kinetic energy is

$$T = \frac{1}{2} \int_{-h/2}^{h/2} \int_0^b \int_0^a \rho \left[ \left( \frac{\partial u_1}{\partial t} \right)^2 + \left( \frac{\partial u_2}{\partial t} \right)^2 + \left( \frac{\partial u_3}{\partial t} \right)^2 \right] dx dy dz \quad (2.9)$$

where  $\rho$  is the density of the plate. Substituting the expressions for  $u_1$ ,  $u_2$ , and  $u_3$  from equations (2.1) into equation (2.9) and integrating over the thickness of the plate, we obtain

$$\begin{aligned} T = \frac{1}{2} \int_0^b \int_0^a \left\{ I_1 \left[ \left( \frac{\partial u}{\partial t} \right)^2 + \left( \frac{\partial v}{\partial t} \right)^2 + \left( \frac{\partial w}{\partial t} \right)^2 \right] + I_3 \left[ \left( \frac{\partial^2 w}{\partial x \partial t} \right)^2 + \left( \frac{\partial^2 w}{\partial y \partial t} \right)^2 \right] \right. \\ \left. + \bar{I}_3 \left[ \left( \frac{\partial \phi}{\partial t} \right)^2 + \left( \frac{\partial \psi}{\partial t} \right)^2 \right] - 2I_2 \left( \frac{\partial^2 w}{\partial x \partial t} \frac{\partial u}{\partial t} + \frac{\partial^2 w}{\partial y \partial t} \frac{\partial v}{\partial t} \right) \right. \\ \left. + 2\bar{I}_2 \left( \frac{\partial u}{\partial t} \frac{\partial \phi}{\partial t} + \frac{\partial v}{\partial t} \frac{\partial \psi}{\partial t} \right) - 2\bar{I}_0 \left( \frac{\partial^2 w}{\partial x \partial t} \frac{\partial \phi}{\partial t} + \frac{\partial^2 w}{\partial y \partial t} \frac{\partial \psi}{\partial t} \right) \right\} dx dy \end{aligned} \quad (2.10)$$

where the  $I_i$  are generalized inertias and are defined as

$$I_i = \int_{-h/2}^{h/2} \rho z^{i-1} dz \quad (i = 1, 2, 3, 4, 5, 7) \quad (2.11)$$

and

$$\begin{aligned}
\bar{l}_0 &= l_3 - \frac{4}{3h^2} l_5 \\
\bar{l}_2 &= l_2 - \frac{4}{3h^2} l_4 \\
\bar{l}_5 &= l_5 - \frac{4}{3h^2} l_7 \\
\bar{l}_3 &= l_3 - \frac{4}{3h^2} (l_5 + \bar{l}_5)
\end{aligned} \tag{2.12}$$

### 2.4.2. Potential energy

The potential energy consists of the strain energy of the elastic plate and the conservative work done by the external transverse distributed load,  $q$ . The potential energy is

$$V = \frac{1}{2} \int_{-h/2}^{h/2} \int_0^b \int_0^a (\sigma_1 \varepsilon_1 + \sigma_2 \varepsilon_2 + \sigma_3 \varepsilon_3 + \sigma_4 \varepsilon_4 + \sigma_5 \varepsilon_5 + \sigma_6 \varepsilon_6) dx dy dz - \int_0^b \int_0^a q w dx dy \tag{2.13}$$

Substituting equations (2.2) and (2.7) into equation (2.13) and integrating over the thickness of the plate, we obtain the following expression for the potential energy:

$$\begin{aligned}
V = \frac{1}{2} \int_0^b \int_0^a \left\{ N_1 \left[ \frac{\partial u}{\partial x} + \frac{1}{2} \left( \frac{\partial w}{\partial x} \right)^2 \right] + N_2 \left[ \frac{\partial v}{\partial y} + \frac{1}{2} \left( \frac{\partial w}{\partial y} \right)^2 \right] \right. \\
+ N_6 \left( \frac{\partial u}{\partial y} + \frac{\partial v}{\partial x} + \frac{\partial w}{\partial x} \frac{\partial w}{\partial y} \right) + \hat{Q}_1 \phi + \hat{Q}_2 \psi \\
+ \hat{M}_1 \frac{\partial \phi}{\partial x} + \hat{M}_2 \frac{\partial \psi}{\partial y} + \hat{M}_6 \left( \frac{\partial \phi}{\partial y} + \frac{\partial \psi}{\partial x} \right) - q w \\
\left. - M_1 \frac{\partial^2 w}{\partial x^2} - M_2 \frac{\partial^2 w}{\partial y^2} - 2M_6 \frac{\partial^2 w}{\partial x \partial y} \right\} dx dy
\end{aligned} \tag{2.14}$$

where the stress resultants  $N_i$ ,  $M_i$ ,  $P_i$ ,  $Q_i$ ,  $R_i$ ,  $\hat{M}_i$ , and  $\hat{Q}_i$  are defined as

$$\begin{aligned}
 (N_i, M_i, P_i) &= \int_{-h/2}^{h/2} \sigma_i(1, z, z^3) dz \quad (i = 1, 2, 6) \\
 (Q_2, R_2) &= \int_{-h/2}^{h/2} \sigma_4(1, z^2) dz \\
 (Q_1, R_1) &= \int_{-h/2}^{h/2} \sigma_5(1, z^2) dz \\
 \hat{M}_i &= M_i - \frac{4}{3h^2} P_i \quad (i = 1, 2) \\
 \hat{Q}_i &= Q_i - \frac{4}{h^2} R_i \quad (i = 1, 2)
 \end{aligned} \tag{2.15}$$

These stress resultants are related to the strains and curvatures in equations (2.4)

by the following relations:

$$\begin{bmatrix} N_1 \\ N_2 \\ N_6 \\ M_1 \\ M_2 \\ M_6 \\ P_1 \\ P_2 \\ P_6 \end{bmatrix} = \begin{bmatrix} A_{11} & A_{12} & A_{16} & B_{11} & B_{12} & B_{16} & E_{11} & E_{12} & E_{16} \\ & A_{22} & A_{26} & & B_{22} & B_{26} & & E_{22} & E_{26} \\ & \text{sym} & A_{66} & & B_{66} & & \text{sym} & & E_{66} \\ & & & D_{11} & D_{12} & D_{16} & F_{11} & F_{12} & F_{16} \\ & & & & D_{22} & D_{26} & & F_{22} & F_{26} \\ & & & & \text{sym} & D_{66} & & \text{sym} & F_{66} \\ & & & & & & H_{11} & H_{12} & H_{16} \\ & & & & & & & H_{22} & H_{26} \\ & \text{sym} & & & & & \text{sym} & & H_{66} \end{bmatrix} \begin{bmatrix} \varepsilon_1^0 \\ \varepsilon_2^0 \\ \varepsilon_6^0 \\ \kappa_1^0 \\ \kappa_2^0 \\ \kappa_6^0 \\ \kappa_1^2 \\ \kappa_2^2 \\ \kappa_6^2 \end{bmatrix} \tag{2.16}$$

$$\begin{bmatrix} Q_2 \\ Q_1 \\ R_2 \\ R_1 \end{bmatrix} = \begin{bmatrix} A_{44} & A_{45} & D_{44} & D_{45} \\ \text{sym} & A_{55} & \text{sym} & D_{55} \\ & & F_{44} & F_{45} \\ \text{sym} & & \text{sym} & F_{55} \end{bmatrix} \begin{bmatrix} \varepsilon_4^0 \\ \varepsilon_5^0 \\ \kappa_4^2 \\ \kappa_5^2 \end{bmatrix} \quad (2.17)$$

Here, the  $A_{ij}$ ,  $B_{ij}$ ,  $D_{ij}$ ,  $E_{ij}$ ,  $F_{ij}$ , and  $H_{ij}$  are the plate stiffnesses defined by

$$\begin{aligned} (A_{ij}, B_{ij}, D_{ij}, E_{ij}, F_{ij}, H_{ij}) &= \int_{-h/2}^{h/2} Q_{ij}(1, z, z^2, z^3, z^4, z^6) dz \quad (i, j = 1, 2, 6) \\ (A_{ij}, D_{ij}, F_{ij}) &= \int_{-h/2}^{h/2} Q_{ij}(1, z^2, z^4) dz \quad (i, j = 4, 5) \end{aligned} \quad (2.18)$$

The Lagrangian  $L$  is the difference between the kinetic and potential energies given in equations (2.10) and (2.14), respectively; that is,

$$L = T - V \quad (2.19)$$

## 2.5. Equations of Motion

Hamilton's principle is used instead of an equilibrium approach to derive the equations of motion of laminated plate. The principle is stated as

$$\delta \int_{t_1}^{t_2} L dt = 0 \quad (2.20)$$



where  $\delta$  stands for the first variation. Substituting for  $L$  in equations (2.19) and (2.20), we obtain

$$\begin{aligned}
0 = \int_{t_1}^{t_2} \int_0^b \int_0^a \left\{ & + I_1 \left( \frac{\partial u}{\partial t} \delta \frac{\partial u}{\partial t} + \frac{\partial v}{\partial t} \delta \frac{\partial v}{\partial t} + \frac{\partial w}{\partial t} \delta \frac{\partial w}{\partial t} \right) \right. \\
& + 2\bar{I}_2 \left( \frac{\partial u}{\partial t} \delta \frac{\partial \phi}{\partial t} + \frac{\partial v}{\partial t} \delta \frac{\partial \psi}{\partial t} + \frac{\partial \phi}{\partial t} \delta \frac{\partial u}{\partial t} + \frac{\partial \psi}{\partial t} \delta \frac{\partial v}{\partial t} \right) \\
& + I_3 \left( \frac{\partial^2 w}{\partial x \partial t} \delta \frac{\partial^2 w}{\partial x \partial t} + \frac{\partial^2 w}{\partial y \partial t} \delta \frac{\partial^2 w}{\partial y \partial t} \right) + \bar{I}_3 \left( \frac{\partial \phi}{\partial t} \delta \frac{\partial \phi}{\partial t} + \frac{\partial \psi}{\partial t} \delta \frac{\partial \psi}{\partial t} \right) \\
& - 2\bar{I}_0 \left( \frac{\partial \phi}{\partial t} \delta \frac{\partial^2 w}{\partial x \partial t} + \frac{\partial \psi}{\partial t} \delta \frac{\partial^2 w}{\partial y \partial t} + \frac{\partial^2 w}{\partial x \partial t} \delta \frac{\partial \phi}{\partial t} + \frac{\partial^2 w}{\partial y \partial t} \delta \frac{\partial \psi}{\partial t} \right) \\
& - 2I_2 \left( \frac{\partial u}{\partial t} \delta \frac{\partial^2 w}{\partial x \partial t} + \frac{\partial v}{\partial t} \delta \frac{\partial^2 w}{\partial y \partial t} + \frac{\partial^2 w}{\partial x \partial t} \delta \frac{\partial u}{\partial t} + \frac{\partial^2 w}{\partial y \partial t} \delta \frac{\partial v}{\partial t} \right) \quad (2.21) \\
& - N_1 \left( \delta \frac{\partial u}{\partial x} + \frac{\partial w}{\partial x} \delta \frac{\partial w}{\partial x} \right) - N_2 \left( \delta \frac{\partial v}{\partial y} + \frac{\partial w}{\partial y} \delta \frac{\partial w}{\partial y} \right) \\
& - N_6 \left( \delta \frac{\partial u}{\partial y} + \delta \frac{\partial v}{\partial x} + \frac{\partial w}{\partial x} \delta \frac{\partial w}{\partial y} + \frac{\partial w}{\partial y} \delta \frac{\partial w}{\partial x} \right) \\
& - \hat{Q}_1 \delta \phi - \hat{Q}_2 \delta \psi + M_1 \delta \frac{\partial^2 w}{\partial x^2} + M_2 \delta \frac{\partial^2 w}{\partial y^2} + 2M_6 \delta \frac{\partial^2 w}{\partial x \partial y} \\
& \left. - \hat{M}_1 \delta \frac{\partial \phi}{\partial x} - \hat{M}_2 \delta \frac{\partial \psi}{\partial y} - \hat{M}_6 \left( \delta \frac{\partial \phi}{\partial y} + \delta \frac{\partial \psi}{\partial x} \right) + q \delta w \right] dx dy dt
\end{aligned}$$

Performing the integration by parts and setting each of the coefficients of  $\delta u$ ,  $\delta v$ ,  $\delta w$ ,  $\delta \phi$ , and  $\delta \psi$  independently equal to zero, we obtain the following equations of motion:

$$\frac{\partial N_1}{\partial x} + \frac{\partial N_6}{\partial y} = I_1 \frac{\partial^2 u}{\partial t^2} + \bar{I}_2 \frac{\partial^2 \phi}{\partial t^2} - I_2 \frac{\partial^3 w}{\partial x \partial t^2} \quad (2.22)$$

$$\frac{\partial N_2}{\partial y} + \frac{\partial N_6}{\partial x} = I_1 \frac{\partial^2 v}{\partial t^2} + \bar{I}_2 \frac{\partial^2 \psi}{\partial t^2} - I_2 \frac{\partial^3 w}{\partial y \partial t^2} \quad (2.23)$$

$$\begin{aligned}
& \frac{\partial^2 M_1}{\partial x^2} + \frac{\partial^2 M_2}{\partial y^2} + 2 \frac{\partial^2 M_6}{\partial x \partial y} + \frac{\partial}{\partial x} \left( N_1 \frac{\partial w}{\partial x} + N_6 \frac{\partial w}{\partial y} \right) \\
& + \frac{\partial}{\partial y} \left( N_2 \frac{\partial w}{\partial y} + N_6 \frac{\partial w}{\partial x} \right) = I_1 \frac{\partial^2 w}{\partial t^2} - q \\
& + I_2 \left( \frac{\partial^3 u}{\partial x \partial t^2} + \frac{\partial^3 v}{\partial y \partial t^2} \right) - I_3 \left( \frac{\partial^4 w}{\partial x^2 \partial t^2} + \frac{\partial^4 w}{\partial y^2 \partial t^2} \right) \\
& + \bar{I}_0 \left( \frac{\partial^3 \phi}{\partial x \partial t^2} + \frac{\partial^3 \psi}{\partial y \partial t^2} \right)
\end{aligned} \tag{2.24}$$

$$\frac{\partial \hat{M}_1}{\partial x} + \frac{\partial \hat{M}_6}{\partial y} - \hat{Q}_1 = \bar{I}_2 \frac{\partial^2 u}{\partial t^2} - \bar{I}_0 \frac{\partial^3 w}{\partial x \partial t^2} + \bar{I}_3 \frac{\partial^2 \phi}{\partial t^2} \tag{2.25}$$

$$\frac{\partial \hat{M}_2}{\partial y} + \frac{\partial \hat{M}_6}{\partial x} - \hat{Q}_2 = \bar{I}_2 \frac{\partial^2 v}{\partial t^2} - \bar{I}_0 \frac{\partial^3 w}{\partial y \partial t^2} + \bar{I}_3 \frac{\partial^2 \psi}{\partial t^2} \tag{2.26}$$

The boundary conditions associated with equations (2.22)-(2.26) are the specification of one factor from the following groups:

at  $x = 0, a$ :

$$\begin{aligned}
& N_1, u; \quad N_3, v; \quad \hat{M}_1, \phi; \quad \hat{M}_3, \psi; \quad M_1, \frac{\partial w}{\partial x}; \\
& w, \left( I_2 \frac{\partial u}{\partial t^2} + \bar{I}_0 \frac{\partial \phi}{\partial t^2} - I_3 \frac{\partial^3 w}{\partial x \partial t^2} - N_1 \frac{\partial w}{\partial x} - N_3 \frac{\partial w}{\partial y} - \frac{\partial M_1}{\partial x} - 2 \frac{\partial M_3}{\partial y} \right)
\end{aligned} \tag{2.27}$$

at  $y = 0, b$ :

$$\begin{aligned}
& N_2, v; \quad N_3, u; \quad \hat{M}_2, \psi; \quad \hat{M}_3, \phi; \quad M_2, \frac{\partial w}{\partial y}; \\
& w, \left( I_2 \frac{\partial v}{\partial t^2} + \bar{I}_0 \frac{\partial \psi}{\partial t^2} - I_3 \frac{\partial^3 w}{\partial y \partial t^2} - N_2 \frac{\partial w}{\partial y} - N_3 \frac{\partial w}{\partial x} - \frac{\partial M_2}{\partial y} - 2 \frac{\partial M_3}{\partial x} \right)
\end{aligned} \tag{2.28}$$

Many of the inertia terms in equations (2.22)-(2.26) vanish for certain types of laminates. For example, for symmetric and antisymmetric laminate plates, where the terms  $I_2$  and  $\bar{I}_2$  are zero, the rotary inertia terms in equations (2.22) and (2.23) and the inplane inertia terms in equations (2.25) and (2.26) as well as the inplane rotary inertia terms in equation (2.24) vanish. However, the inplane inertia terms in equations (2.22) and (2.23) and the transverse inertia term in equation (2.24) are always present.

Substituting for the  $N_i$ ,  $M_i$ ,  $\hat{M}_i$ , and  $\hat{Q}_i$  in equations (2.22)-(2.26), we obtain the governing equations of the plate in terms of the field variables as

$$\begin{aligned}
& A_{11} \frac{\partial^2 u}{\partial x^2} + 2A_{16} \frac{\partial^2 u}{\partial x \partial y} + A_{66} \frac{\partial^2 u}{\partial y^2} + A_{16} \frac{\partial^2 v}{\partial x^2} + (A_{12} + A_{66}) \frac{\partial^2 v}{\partial x \partial y} + A_{26} \frac{\partial^2 v}{\partial y^2} \\
& + \hat{B}_{11} \frac{\partial^2 \phi}{\partial x^2} + 2\hat{B}_{16} \frac{\partial^2 \phi}{\partial x \partial y} + \hat{B}_{66} \frac{\partial^2 \phi}{\partial y^2} + \hat{B}_{16} \frac{\partial^2 \psi}{\partial x^2} + (\hat{B}_{12} + \hat{B}_{66}) \frac{\partial^2 \psi}{\partial x \partial y} + \hat{B}_{26} \frac{\partial^2 \psi}{\partial y^2} \\
& - B_{11} \frac{\partial^3 w}{\partial x^3} - 3B_{16} \frac{\partial^3 w}{\partial x^2 \partial y} - (B_{12} + 2B_{66}) \frac{\partial^3 w}{\partial x \partial y^2} - B_{26} \frac{\partial^3 w}{\partial y^3} \\
& + \frac{\partial w}{\partial x} \left( A_{11} \frac{\partial^2 w}{\partial x^2} + 2A_{16} \frac{\partial^2 w}{\partial x \partial y} + A_{66} \frac{\partial^2 w}{\partial y^2} \right) \\
& + \frac{\partial w}{\partial y} \left( A_{16} \frac{\partial^2 w}{\partial x^2} + (A_{12} + A_{66}) \frac{\partial^2 w}{\partial x \partial y} + A_{26} \frac{\partial^2 w}{\partial y^2} \right) \\
& = I_1 \frac{\partial^2 u}{\partial t^2} + \bar{I}_2 \frac{\partial^2 \phi}{\partial t^2} - I_2 \frac{\partial^3 w}{\partial x \partial t^2}
\end{aligned} \tag{2.29}$$

$$\begin{aligned}
& A_{16} \frac{\partial^2 u}{\partial x^2} + (A_{12} + A_{66}) \frac{\partial^2 u}{\partial x \partial y} + A_{26} \frac{\partial^2 u}{\partial y^2} + A_{66} \frac{\partial^2 v}{\partial x^2} + 2A_{26} \frac{\partial^2 v}{\partial x \partial y} + A_{22} \frac{\partial^2 v}{\partial y^2} \\
& + \hat{B}_{16} \frac{\partial^2 \phi}{\partial x^2} + (\hat{B}_{12} + \hat{B}_{66}) \frac{\partial^2 \phi}{\partial x \partial y} + \hat{B}_{26} \frac{\partial^2 \phi}{\partial y^2} + \hat{B}_{66} \frac{\partial^2 \psi}{\partial x^2} + 2\hat{B}_{26} \frac{\partial^2 \psi}{\partial x \partial y} + \hat{B}_{22} \frac{\partial^2 \psi}{\partial y^2} \\
& - B_{16} \frac{\partial^3 w}{\partial x^3} - (B_{12} + 2B_{66}) \frac{\partial^3 w}{\partial x^2 \partial y} - 3B_{26} \frac{\partial^3 w}{\partial x \partial y^2} - B_{22} \frac{\partial^3 w}{\partial y^3} \\
& + \frac{\partial w}{\partial x} \left( A_{16} \frac{\partial^2 w}{\partial x^2} + (A_{12} + A_{66}) \frac{\partial^2 w}{\partial x \partial y} + A_{26} \frac{\partial^2 w}{\partial y^2} \right) \\
& + \frac{\partial w}{\partial y} \left( A_{66} \frac{\partial^2 w}{\partial x^2} + 2A_{26} \frac{\partial^2 w}{\partial x \partial y} + A_{22} \frac{\partial^2 w}{\partial y^2} \right) \\
& = I_1 \frac{\partial^2 v}{\partial t^2} + \bar{I}_2 \frac{\partial^2 \psi}{\partial t^2} - I_2 \frac{\partial^3 w}{\partial y \partial t^2}
\end{aligned} \tag{2.30}$$

$$\begin{aligned}
& B_{11} \frac{\partial^3 u}{\partial x^3} + 3B_{16} \frac{\partial^3 u}{\partial x^2 \partial y} + (B_{12} + 2B_{66}) \frac{\partial^3 u}{\partial x \partial y^2} + B_{26} \frac{\partial^3 u}{\partial y^3} \\
& + B_{16} \frac{\partial^3 v}{\partial x^3} + (B_{12} + 2B_{66}) \frac{\partial^3 v}{\partial x^2 \partial y} + 3B_{26} \frac{\partial^3 v}{\partial x \partial y^2} + B_{22} \frac{\partial^3 v}{\partial y^3} \\
& + \tilde{D}_{11} \frac{\partial^3 \phi}{\partial x^3} + 3\tilde{D}_{16} \frac{\partial^3 \phi}{\partial x^2 \partial y} + (\tilde{D}_{12} + 2\tilde{D}_{66}) \frac{\partial^3 \phi}{\partial x \partial y^2} + \tilde{D}_{26} \frac{\partial^3 \phi}{\partial y^3} \\
& + \tilde{D}_{16} \frac{\partial^3 \psi}{\partial x^3} + (\tilde{D}_{12} + 2\tilde{D}_{66}) \frac{\partial^3 \psi}{\partial x^2 \partial y} + 3\tilde{D}_{26} \frac{\partial^3 \psi}{\partial x \partial y^2} + \tilde{D}_{22} \frac{\partial^3 \psi}{\partial y^3} \\
& + \frac{\partial^2 w}{\partial x^2} \left[ \hat{B}_{11} \frac{\partial \phi}{\partial x} + \hat{B}_{12} \frac{\partial \psi}{\partial y} + \hat{B}_{16} \left( \frac{\partial \phi}{\partial y} + \frac{\partial \psi}{\partial x} \right) + A_{11} \frac{\partial u}{\partial x} + A_{12} \frac{\partial v}{\partial y} + A_{16} \left( \frac{\partial u}{\partial y} + \frac{\partial v}{\partial x} \right) \right] \\
& + \frac{\partial^2 w}{\partial y^2} \left[ \hat{B}_{12} \frac{\partial \phi}{\partial x} + \hat{B}_{22} \frac{\partial \psi}{\partial y} + \hat{B}_{26} \left( \frac{\partial \phi}{\partial y} + \frac{\partial \psi}{\partial x} \right) + A_{12} \frac{\partial u}{\partial x} + A_{22} \frac{\partial v}{\partial y} + A_{26} \left( \frac{\partial u}{\partial y} + \frac{\partial v}{\partial x} \right) \right] \\
& + 2 \frac{\partial^2 w}{\partial x \partial y} \left[ \hat{B}_{16} \frac{\partial \phi}{\partial x} + \hat{B}_{26} \frac{\partial \psi}{\partial y} + \hat{B}_{66} \left( \frac{\partial \phi}{\partial y} + \frac{\partial \psi}{\partial x} \right) + A_{16} \frac{\partial u}{\partial x} + A_{26} \frac{\partial v}{\partial y} + A_{66} \left( \frac{\partial u}{\partial y} + \frac{\partial v}{\partial x} \right) \right]
\end{aligned}$$

$$\begin{aligned}
& -D_{11} \frac{\partial^4 w}{\partial x^4} - 4D_{16} \frac{\partial^4 w}{\partial x^3 \partial y} - 2(D_{12} + 2D_{66}) \frac{\partial^4 w}{\partial x^2 \partial y^2} - 4D_{26} \frac{\partial^4 w}{\partial x \partial y^3} - D_{22} \frac{\partial^4 w}{\partial y^4} \\
& + 2(B_{66} - B_{12}) \left[ \frac{\partial^2 w}{\partial x^2} \frac{\partial^2 w}{\partial y^2} - \left( \frac{\partial^2 w}{\partial x \partial y} \right)^2 \right] \\
& + \frac{\partial w}{\partial x} \left( B_{11} \frac{\partial^3 w}{\partial x^3} + 3B_{16} \frac{\partial^3 w}{\partial x^2 \partial y} + (B_{12} + 2B_{66}) \frac{\partial^3 w}{\partial x \partial y^2} + B_{26} \frac{\partial^3 w}{\partial y^3} \right) \\
& + \frac{\partial w}{\partial y} \left( B_{16} \frac{\partial^3 w}{\partial x^3} + (B_{12} + 2B_{66}) \frac{\partial^3 w}{\partial x^2 \partial y} + 2B_{26} \frac{\partial^3 w}{\partial x \partial y^2} + B_{22} \frac{\partial^3 w}{\partial y^3} \right) \\
& + \frac{\partial^2 w}{\partial x^2} \left[ \frac{1}{2} A_{11} \left( \frac{\partial w}{\partial x} \right)^2 + \frac{1}{2} A_{12} \left( \frac{\partial w}{\partial y} \right)^2 + A_{16} \frac{\partial w}{\partial x} \frac{\partial w}{\partial y} \right] \\
& + \frac{\partial^2 w}{\partial y^2} \left[ \frac{1}{2} A_{12} \left( \frac{\partial w}{\partial x} \right)^2 + \frac{1}{2} A_{22} \left( \frac{\partial w}{\partial y} \right)^2 + A_{26} \frac{\partial w}{\partial x} \frac{\partial w}{\partial y} \right] \\
& + \frac{\partial^2 w}{\partial x \partial y} \left[ A_{16} \left( \frac{\partial w}{\partial x} \right)^2 + A_{26} \left( \frac{\partial w}{\partial y} \right)^2 + 2A_{66} \frac{\partial w}{\partial x} \frac{\partial w}{\partial y} \right] \\
& = -q + I_1 \left( \frac{\partial^2 w}{\partial t^2} - \frac{\partial w}{\partial x} \frac{\partial^2 u}{\partial t^2} - \frac{\partial w}{\partial y} \frac{\partial^2 v}{\partial t^2} \right) \\
& + I_2 \left( \frac{\partial^3 u}{\partial x \partial t^2} + \frac{\partial^3 v}{\partial y \partial t^2} + \frac{\partial w}{\partial x} \frac{\partial^3 w}{\partial x \partial t^2} + \frac{\partial w}{\partial y} \frac{\partial^3 w}{\partial y \partial t^2} \right) \\
& - I_3 \left( \frac{\partial^4 w}{\partial x^2 \partial t^2} + \frac{\partial^4 w}{\partial y^2 \partial t^2} \right) + \bar{I}_0 \left( \frac{\partial^3 \phi}{\partial x \partial t^2} + \frac{\partial^3 \psi}{\partial y \partial t^2} \right) - \bar{I}_2 \left( \frac{\partial w}{\partial x} \frac{\partial^2 \phi}{\partial t^2} + \frac{\partial w}{\partial y} \frac{\partial^2 \psi}{\partial t^2} \right)
\end{aligned} \tag{2.31}$$

$$\begin{aligned}
& \hat{B}_{11} \frac{\partial^2 u}{\partial x^2} + 2\hat{B}_{16} \frac{\partial^2 u}{\partial x \partial y} + \hat{B}_{66} \frac{\partial^2 u}{\partial y^2} + \hat{B}_{16} \frac{\partial^2 v}{\partial x^2} + (\hat{B}_{12} + \hat{B}_{66}) \frac{\partial^2 v}{\partial x \partial y} + \hat{B}_{26} \frac{\partial^2 v}{\partial y^2} \\
& + \hat{D}_{11} \frac{\partial^2 \phi}{\partial x^2} + 2\hat{D}_{16} \frac{\partial^2 \phi}{\partial x \partial y} + \hat{D}_{66} \frac{\partial^2 \phi}{\partial y^2} + D_{55}^* \phi \\
& + \hat{D}_{16} \frac{\partial^2 \psi}{\partial x^2} + (\hat{D}_{12} + \hat{D}_{66}) \frac{\partial^2 \psi}{\partial x \partial y} + \hat{D}_{26} \frac{\partial^2 \psi}{\partial y^2} + D_{45}^* \psi \\
& - \tilde{D}_{11} \frac{\partial^3 w}{\partial x^3} - 3\tilde{D}_{16} \frac{\partial^3 w}{\partial x^2 \partial y} - (\tilde{D}_{12} + 2\tilde{D}_{66}) \frac{\partial^3 w}{\partial x \partial y^2} - \tilde{D}_{26} \frac{\partial^3 w}{\partial y^3} \\
& + \frac{\partial w}{\partial x} \left( \hat{B}_{11} \frac{\partial^2 w}{\partial x^2} + 2\hat{B}_{16} \frac{\partial^2 w}{\partial x \partial y} + \hat{B}_{66} \frac{\partial^2 w}{\partial y^2} \right) \\
& + \frac{\partial w}{\partial y} \left( \hat{B}_{16} \frac{\partial^2 w}{\partial x^2} + (\hat{B}_{12} + \hat{B}_{66}) \frac{\partial^2 w}{\partial x \partial y} + \hat{B}_{26} \frac{\partial^2 w}{\partial y^2} \right) \\
& = \bar{I}_2 \frac{\partial^2 u}{\partial t^2} + \bar{I}_3 \frac{\partial^2 \phi}{\partial t^2} - \bar{I}_0 \frac{\partial^3 w}{\partial x \partial t^2}
\end{aligned} \tag{2.32}$$

$$\begin{aligned}
& \hat{B}_{16} \frac{\partial^2 u}{\partial x^2} + (\hat{B}_{12} + \hat{B}_{66}) \frac{\partial^2 u}{\partial x \partial y} + \hat{B}_{26} \frac{\partial^2 u}{\partial y^2} + \hat{B}_{66} \frac{\partial^2 v}{\partial x^2} + 2\hat{B}_{26} \frac{\partial^2 v}{\partial x \partial y} + \hat{B}_{22} \frac{\partial^2 v}{\partial y^2} \\
& + \hat{D}_{16} \frac{\partial^2 \phi}{\partial x^2} + (\hat{D}_{12} + \hat{D}_{66}) \frac{\partial^2 \phi}{\partial x \partial y} + \hat{D}_{26} \frac{\partial^2 \phi}{\partial y^2} + D_{45}^* \phi \\
& + \hat{D}_{66} \frac{\partial^2 \psi}{\partial x^2} + 2\hat{D}_{26} \frac{\partial^2 \psi}{\partial x \partial y} + \hat{D}_{22} \frac{\partial^2 \psi}{\partial y^2} + D_{44}^* \psi \\
& - \tilde{D}_{16} \frac{\partial^3 w}{\partial x^3} - (\tilde{D}_{12} + 2\tilde{D}_{66}) \frac{\partial^3 w}{\partial x^2 \partial y} - 3\tilde{D}_{26} \frac{\partial^3 w}{\partial x \partial y^2} - \tilde{D}_{22} \frac{\partial^3 w}{\partial y^3} \\
& + \frac{\partial w}{\partial x} \left( \hat{B}_{16} \frac{\partial^2 w}{\partial x^2} + (\hat{B}_{12} + \hat{B}_{66}) \frac{\partial^2 w}{\partial x \partial y} + \hat{B}_{26} \frac{\partial^2 w}{\partial y^2} \right) \\
& + \frac{\partial w}{\partial y} \left( \hat{B}_{66} \frac{\partial^2 w}{\partial x^2} + 2\hat{B}_{26} \frac{\partial^2 w}{\partial x \partial y} + \hat{B}_{22} \frac{\partial^2 w}{\partial y^2} \right) \\
& = \bar{I}_2 \frac{\partial^2 v}{\partial t^2} + \bar{I}_3 \frac{\partial^2 \psi}{\partial t^2} - \bar{I}_0 \frac{\partial^3 w}{\partial y \partial t^2}
\end{aligned} \tag{2.33}$$

where

$$\hat{B}_{ij} = B_{ij} - \frac{4}{3h^2} E_{ij}$$

$$\hat{D}_{ij} = D_{ij} - \frac{8}{3h^2} F_{ij} + \frac{16}{9h^4} H_{ij}$$

$$\tilde{D}_{ij} = D_{ij} - \frac{4}{3h^2} F_{ij}$$

$$D_{ij}^* = \frac{8}{h^2} D_{ij} - A_{ij} - \frac{16}{h^4} F_{ij}$$

## 2.6. Simplifications by Using CPT

The classical plate theory, which does not account for shear deformations, leads to serious errors in calculating the responses of thick composite plates. Many investigators use the classical plate theory to treat thin isotropic plates because the number of equations and labor involved are greatly reduced when CPT is used. As is shown in Chapter 3, the errors in the results obtained by using CPT are reduced as the plates become thinner. Further simplifications can be obtained by ignoring the inplane and rotary inertias. The governing equations of isotropic rectangular and circular plates are derived in the following sections.

### 2.6.1. Rectangular plates

The displacement field used in CPT is

$$\begin{aligned} u_1(x,y,z,t) &= u(x,y,t) - z \frac{\partial w}{\partial x} \\ u_2(x,y,z,t) &= v(x,y,t) - z \frac{\partial w}{\partial y} \\ u_3(x,y,z,t) &= w(x,y,t) \end{aligned} \quad (2.34)$$

The only difference between equations (2.1) and (2.34) is that the shear-deformation terms  $\phi$  and  $\psi$  are dropped in equations (2.34). This simplifies the strain-displacement relations in equations (2.3) by dropping  $\kappa_i^2$  and setting the transverse shear strains  $\varepsilon_4$  and  $\varepsilon_5$  equal to zero. Therefore, the strain-displacement relations are

$$\begin{aligned} \varepsilon_1 &= \varepsilon_1^0 - z \frac{\partial^2 w}{\partial x^2} \\ \varepsilon_2 &= \varepsilon_2^0 - z \frac{\partial^2 w}{\partial y^2} \\ \varepsilon_6 &= \varepsilon_6^0 - 2z \frac{\partial w}{\partial x} \frac{\partial w}{\partial y} \end{aligned} \quad (2.35)$$

Differentiating  $\varepsilon_1$  twice with respect to  $y$ ,  $\varepsilon_2$  twice with respect to  $x$ ,  $\varepsilon_6$  with respect to  $x$  and  $y$ , and using equations (2.4) and (2.35), we obtain

$$\frac{\partial^2 \varepsilon_1}{\partial y^2} + \frac{\partial^2 \varepsilon_2}{\partial x^2} - \frac{\partial^2 \varepsilon_6}{\partial x \partial y} = \left( \frac{\partial^2 w}{\partial x \partial y} \right)^2 - \frac{\partial^2 w}{\partial x^2} \frac{\partial^2 w}{\partial y^2} \quad (2.36)$$

which is known as the compatibility equation.

The reduced stiffnesses of isotropic plates are



$$Q_{11} = \frac{E}{1 - \nu^2}, \quad Q_{12} = \nu \frac{E}{1 - \nu^2}, \quad Q_{22} = \frac{E}{1 - \nu^2}, \quad Q_{66} = G \quad (2.37)$$

while the other reduced stiffnesses  $Q_{ij}$  are zero. Here,  $E$ ,  $G$ , and  $\nu$  are the Young modulus, shear modulus, and Poisson's ratio, respectively.

The nonzero terms in equations (2.18) can be written as

$$\begin{aligned} A_{11} &= \frac{Eh}{1 - \nu^2}, \quad A_{12} = \frac{\nu Eh}{1 - \nu^2}, \quad A_{22} = \frac{Eh}{1 - \nu^2}, \quad A_{66} = Gh, \\ D_{11} &= D, \quad D_{12} = \nu D, \quad D_{22} = D, \quad D_{66} = \frac{1 - \nu}{2} D \end{aligned} \quad (2.38)$$

where  $D$  is the bending rigidity of the plate and is defined by

$$D = \frac{Eh^3}{12(1 - \nu^2)} \quad (2.39)$$

The elements of the Piola-Kirchhoff stress tensor can be obtained by substituting equations (2.35) and (2.37) into equations (2.7). These stress components are

$$\begin{aligned} \sigma_1 &= \frac{E}{1 - \nu^2} \left[ \frac{\partial u}{\partial x} + \nu \frac{\partial v}{\partial y} - z \left( \frac{\partial^2 w}{\partial x^2} + \nu \frac{\partial^2 w}{\partial y^2} \right) + \frac{1}{2} \left( \frac{\partial w}{\partial x} \right)^2 + \frac{\nu}{2} \left( \frac{\partial w}{\partial y} \right)^2 \right] \\ \sigma_2 &= \frac{E}{1 - \nu^2} \left[ \frac{\partial v}{\partial y} + \nu \frac{\partial u}{\partial x} - z \left( \frac{\partial^2 w}{\partial y^2} + \nu \frac{\partial^2 w}{\partial x^2} \right) + \frac{1}{2} \left( \frac{\partial w}{\partial y} \right)^2 + \frac{\nu}{2} \left( \frac{\partial w}{\partial x} \right)^2 \right] \\ \sigma_6 &= G \left( \frac{\partial u}{\partial y} + \frac{\partial v}{\partial x} - 2z \frac{\partial^2 w}{\partial x \partial y} + \frac{\partial w}{\partial x} \frac{\partial w}{\partial y} \right) \end{aligned} \quad (2.40)$$

The positive sense of the stress resultants are shown in Figure 2.2. The membrane forces  $N_i$  and the bending and twisting moments  $M_i$  can be written as

$$\begin{aligned}
N_1 &= \frac{Eh}{1-\nu^2} \left[ \frac{\partial u}{\partial x} + \nu \frac{\partial v}{\partial y} + \frac{1}{2} \left( \frac{\partial w}{\partial x} \right)^2 + \frac{\nu}{2} \left( \frac{\partial w}{\partial y} \right)^2 \right] \\
N_2 &= \frac{Eh}{1-\nu^2} \left[ \frac{\partial v}{\partial y} + \nu \frac{\partial u}{\partial x} + \frac{1}{2} \left( \frac{\partial w}{\partial y} \right)^2 + \frac{\nu}{2} \left( \frac{\partial w}{\partial x} \right)^2 \right] \\
N_6 &= Gh \left( \frac{\partial u}{\partial y} + \frac{\partial v}{\partial x} + \frac{\partial w}{\partial x} \frac{\partial w}{\partial y} \right) \\
M_1 &= -D \left( \frac{\partial^2 w}{\partial x^2} + \nu \frac{\partial^2 w}{\partial y^2} \right) \\
M_2 &= -D \left( \frac{\partial^2 w}{\partial y^2} + \nu \frac{\partial^2 w}{\partial x^2} \right) \\
M_6 &= -D(1-\nu) \frac{\partial^2 w}{\partial x \partial y}
\end{aligned} \tag{2.41}$$

Similarly, the generalized inertias  $I_i$  are reduced to

$$I_1 = \rho h, \quad I_3 = \frac{\rho h^3}{12} \tag{2.42}$$

Hamilton's principle is used to derive the equations of motion. These equations in the absence of inplane and rotary inertias can be reduced to

$$\frac{\partial N_1}{\partial x} + \frac{\partial N_6}{\partial y} = 0 \tag{2.43}$$

$$\frac{\partial N_2}{\partial y} + \frac{\partial N_6}{\partial x} = 0 \tag{2.44}$$

$$\frac{\partial^2 M_1}{\partial x^2} + \frac{\partial^2 M_2}{\partial y^2} + 2 \frac{\partial^2 M_6}{\partial x \partial y} + N_1 \frac{\partial^2 w}{\partial x^2} + N_2 \frac{\partial^2 w}{\partial y^2} + 2N_6 \frac{\partial^2 w}{\partial x \partial y} = I_1 \frac{\partial^2 w}{\partial t^2} - q \tag{2.45}$$

Introducing the stress function  $F$  defined by

$$N_1 = \frac{\partial^2 F}{\partial y^2}, \quad N_2 = \frac{\partial^2 F}{\partial x^2}, \quad N_6 = -\frac{\partial^2 F}{\partial x \partial y} \quad (2.46)$$

and the compatibility equation (2.36) results in the following two coupled partial-differential equations in terms of  $w$  and  $F$ :

$$D\nabla^4 w + \rho h \frac{\partial^2 w}{\partial t^2} = \frac{\partial^2 F}{\partial y^2} \frac{\partial^2 w}{\partial x^2} + \frac{\partial^2 F}{\partial x^2} \frac{\partial^2 w}{\partial y^2} - 2 \frac{\partial^2 F}{\partial x \partial y} \frac{\partial^2 w}{\partial x \partial y} + q \quad (2.47)$$

$$\nabla^4 F = Eh \left[ \left( \frac{\partial^2 w}{\partial x \partial y} \right)^2 - \frac{\partial^2 w}{\partial x^2} \frac{\partial^2 w}{\partial y^2} \right] \quad (2.48)$$

where  $\nabla^4$  is the two-dimensional biharmonic operator.

### 2.6.2. Axisymmetric circular plates

In the study of circular plates it is more convenient to use polar rather than rectangular coordinates. Hence the polar coordinates  $(r, \theta)$  are introduced such that they span the  $x$ - $y$  plane, and  $u_r$  and  $u_\theta$  are used to denote the displacements in the  $r$  and  $\theta$  directions, respectively. The relations between the polar coordinate set  $(r, \theta)$  and the rectangular set  $(x, y)$  are

$$\begin{aligned} x &= r \cos \theta, & y &= r \sin \theta \\ r^2 &= x^2 + y^2, & \theta &= \tan^{-1} \frac{y}{x} \end{aligned} \quad (2.49)$$

It follows from equations (2.49) that

$$\begin{aligned}
\frac{\partial r}{\partial x} &= \frac{x}{r} = \cos \theta, & \frac{\partial \theta}{\partial x} &= -\frac{y}{r^2} = -\frac{\sin \theta}{r} \\
\frac{\partial r}{\partial y} &= \frac{y}{r} = \sin \theta, & \frac{\partial \theta}{\partial y} &= \frac{x}{r^2} = \frac{\cos \theta}{r}
\end{aligned}
\tag{2.50}$$

Furthermore, the chain rule of differentiation is used and the following relations are obtained:

$$\begin{aligned}
\frac{\partial}{\partial x} &= \cos \theta \frac{\partial}{\partial r} - \frac{1}{r} \sin \theta \frac{\partial}{\partial \theta} \\
\frac{\partial}{\partial y} &= \sin \theta \frac{\partial}{\partial r} + \frac{1}{r} \cos \theta \frac{\partial}{\partial \theta} \\
\frac{\partial^2}{\partial x^2} &= \cos^2 \theta \frac{\partial^2}{\partial r^2} + \frac{1}{r} \sin^2 \theta \frac{\partial}{\partial r} + \frac{1}{r^2} \sin^2 \theta \frac{\partial^2}{\partial \theta^2} \\
&\quad + \frac{2}{r^2} \sin \theta \cos \theta \frac{\partial}{\partial \theta} - \frac{2}{r} \sin \theta \cos \theta \frac{\partial^2}{\partial r \partial \theta} \\
\frac{\partial^2}{\partial y^2} &= \sin^2 \theta \frac{\partial^2}{\partial r^2} + \frac{1}{r} \cos^2 \theta \frac{\partial}{\partial r} + \frac{1}{r^2} \cos^2 \theta \frac{\partial^2}{\partial \theta^2} \\
&\quad - \frac{2}{r^2} \sin \theta \cos \theta \frac{\partial}{\partial \theta} + \frac{2}{r} \sin \theta \cos \theta \frac{\partial^2}{\partial r \partial \theta} \\
\frac{\partial^2}{\partial x \partial y} &= \sin \theta \cos \theta \frac{\partial^2}{\partial r^2} - \frac{1}{r} \sin \theta \cos \theta \frac{\partial}{\partial r} - \frac{1}{r^2} \sin \theta \cos \theta \frac{\partial^2}{\partial \theta^2} \\
&\quad - \frac{1}{r^2} \cos 2\theta \frac{\partial}{\partial \theta} + \frac{1}{r} \cos 2\theta \frac{\partial^2}{\partial r \partial \theta}
\end{aligned}
\tag{2.51}$$

Here, as in the case of rectangular plates, the stress resultants are defined by

$$\begin{aligned}
(N_r, N_\theta, N_{r\theta}, Q_r, Q_\theta) &= \int_{-h/2}^{h/2} (\sigma_r, \sigma_\theta, \sigma_{r\theta}, \sigma_{rz}, \sigma_{\theta z}) dz \\
(M_r, M_\theta, M_{r\theta}) &= \int_{-h/2}^{h/2} (\sigma_r, \sigma_\theta, \sigma_{r\theta}) z dz
\end{aligned}
\tag{2.52}$$

The positive sense of these stress resultants are shown in Figure 2.3. For axisymmetric circular plates all partial derivatives with respect to  $\theta$  are zero. Then using equations (2.51) one can transform the bending moments for isotropic plates to

$$\begin{aligned} M_r &= -D \left( \frac{\partial^2 w}{\partial r^2} + \frac{\nu}{r} \frac{\partial w}{\partial r} \right) \\ M_\theta &= -D \left( \nu \frac{\partial^2 w}{\partial r^2} + \frac{1}{r} \frac{\partial w}{\partial r} \right) \end{aligned} \quad (2.53)$$

Similarly, it follows from the expressions for  $N_1$  and  $N_2$  in equations (2.41) that the relationships among  $F$ ,  $u_r$ , and the deflections are:

$$Eh \left[ \frac{\partial u_r}{\partial r} + \frac{1}{2} \left( \frac{\partial w}{\partial r} \right)^2 \right] = \frac{1}{r} \frac{\partial F}{\partial r} - \nu \frac{\partial^2 F}{\partial r^2} \quad (2.54)$$

$$Eh \frac{u_r}{r} = \frac{\partial^2 F}{\partial r^2} - \frac{\nu}{r} \frac{\partial w}{\partial r} \quad (2.55)$$

Here, the stress function  $F$  is defined by

$$N_r = \frac{1}{r} \frac{\partial F}{\partial r}, \quad N_\theta = \frac{\partial^2 F}{\partial r^2} \quad (2.56)$$

Finally the governing equations (2.47) and (2.48) are transformed into

$$D \nabla^4 w + \rho h \frac{\partial^2 w}{\partial t^2} = \frac{1}{r} \frac{\partial}{\partial r} \left( \frac{\partial F}{\partial r} \frac{\partial w}{\partial r} \right) + q \quad (2.57)$$

$$\nabla^4 F = - \frac{Eh}{2r} \frac{\partial}{\partial r} \left( \frac{\partial w}{\partial r} \right)^2 \quad (2.58)$$

where

$$\nabla^4 = \left( \frac{\partial^2}{\partial r^2} + \frac{1}{r} \frac{\partial}{\partial r} \right)^2 \quad (2.59)$$

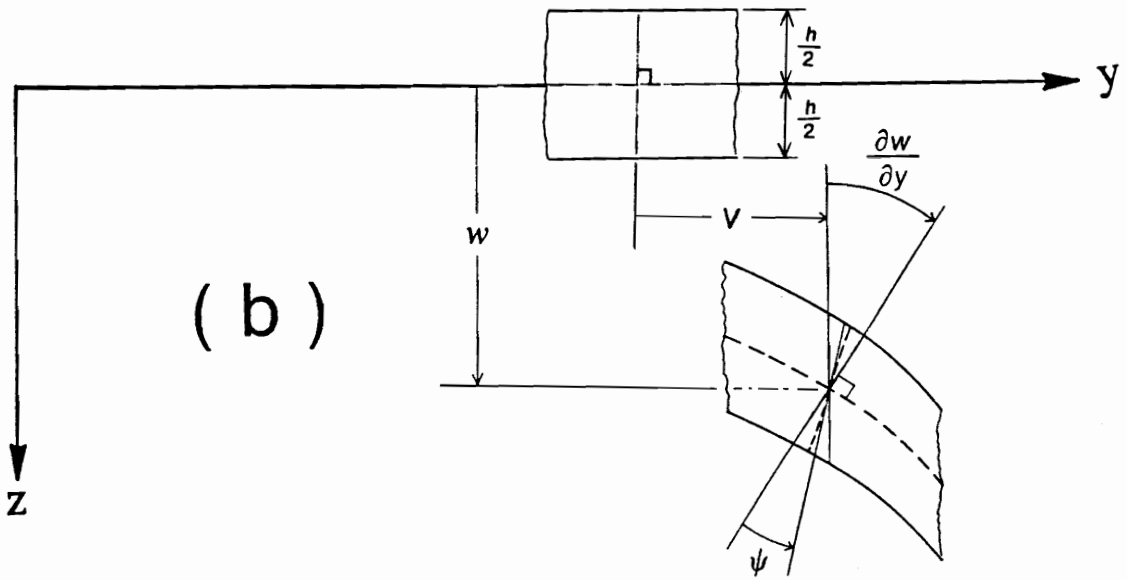
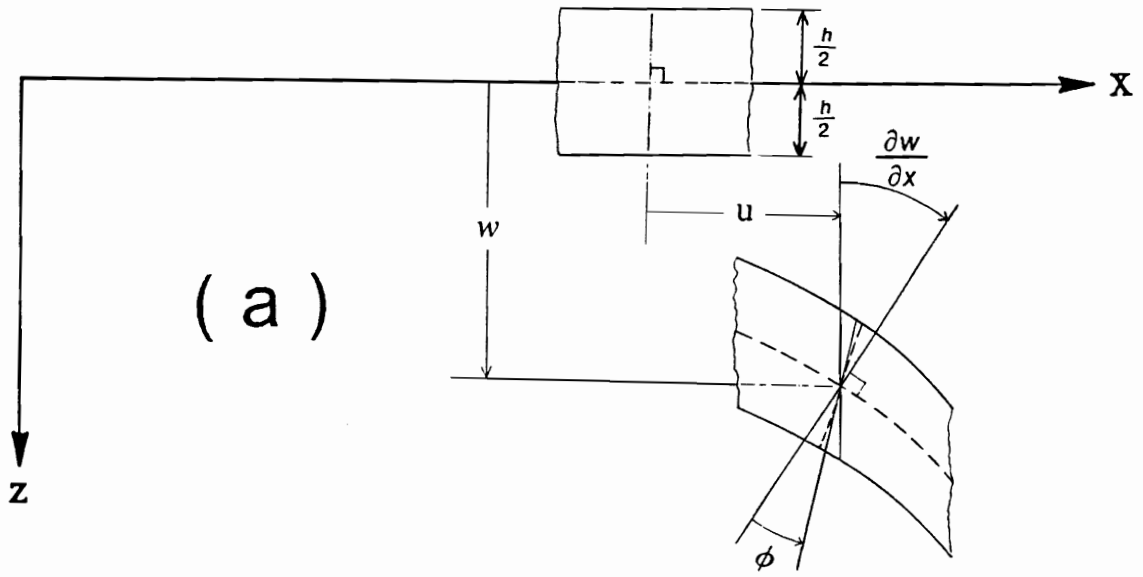


**Figure 2.1.** Geometry of deformation: (a) in the  $x$ - $z$  plane and (b) in the  $y$ - $z$  plane.

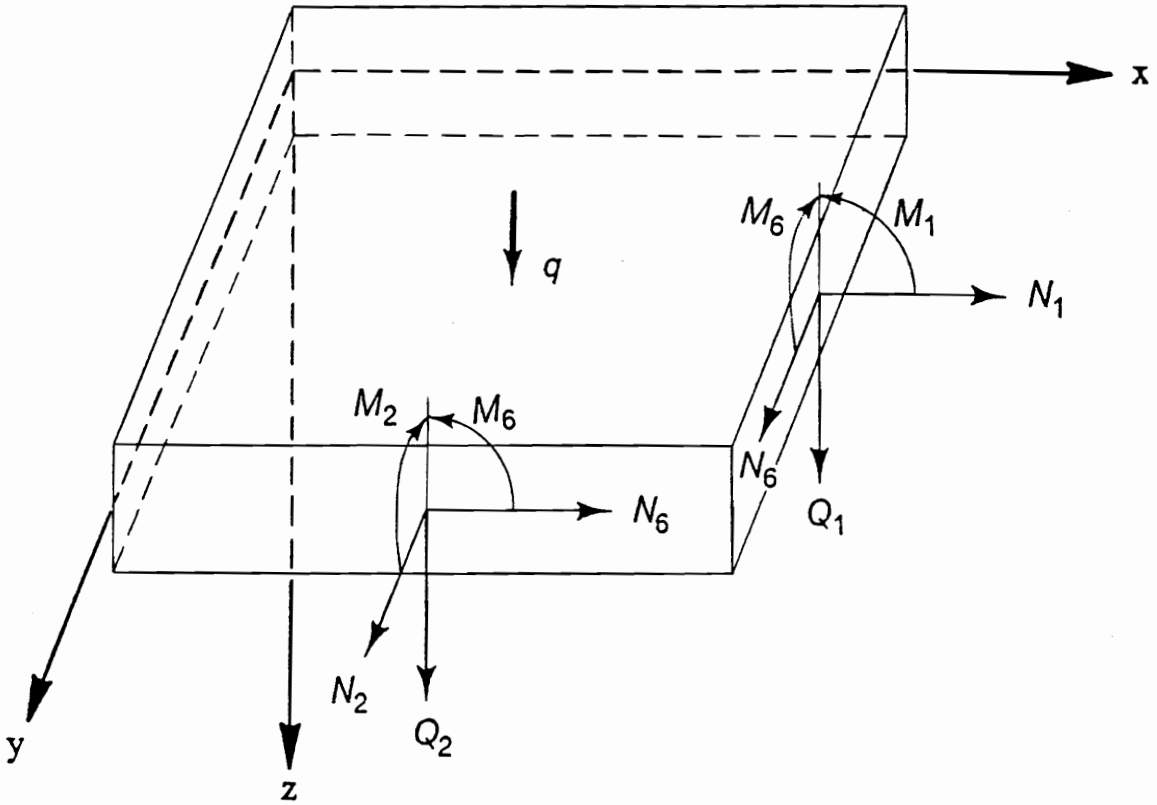


**Figure 2.2.** Inplane forces and moments acting on a rectangular plate element.



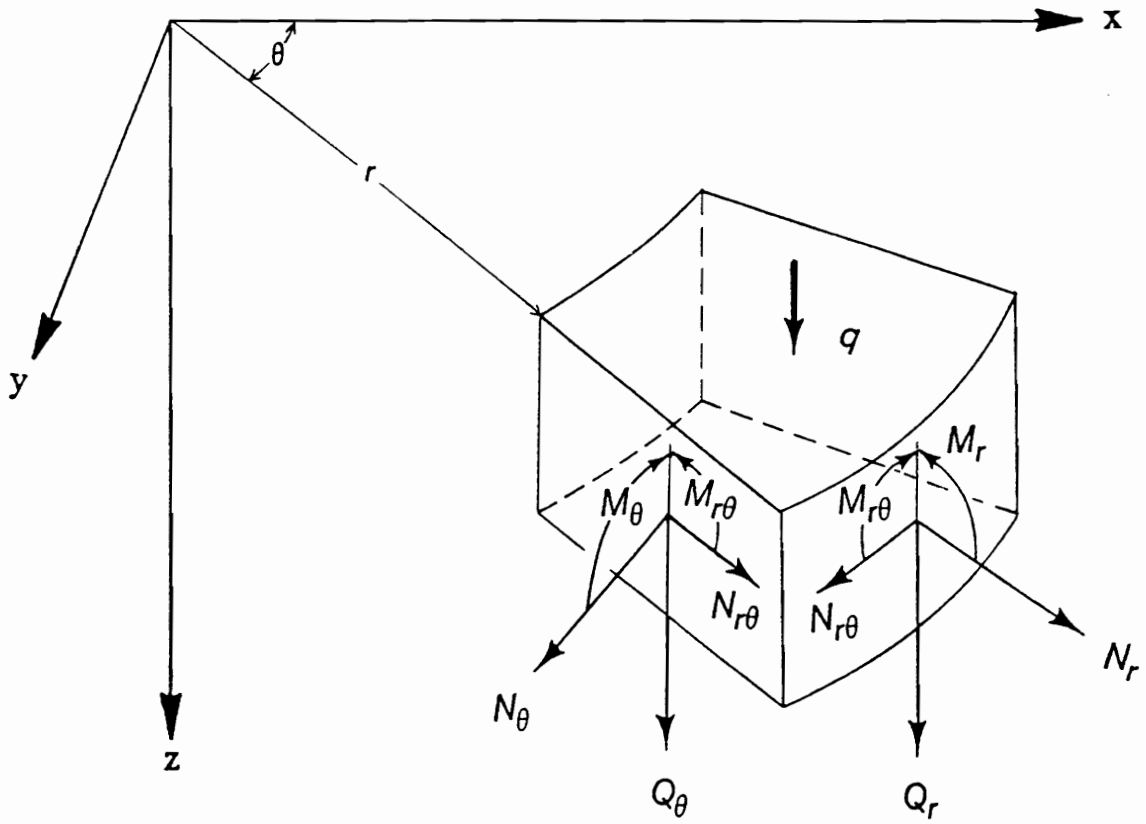


**Figure 2.3.** Inplane forces and moments acting on a polar plate element.

### **3. LINEAR FREE VIBRATIONS AND BUCKLING OF CROSS-PLY LAMINATED PLATES**

Generalized Levy-type solutions are obtained for the problems of linear vibration and stability of cross-ply thin, moderately thick, and thick laminated plates. A review of the buckling of laminated rectangular plate is given by Leissa (1987). Recently, buckling of symmetrically laminated rectangular plates subject to several types of loading conditions is studied by Narita and Leissa (1990). They used the Ritz method and presented numerical results for simply-supported square plates.

Because classical plate theory (CPT) ignores the transverse shear-deformation effects and results in significant errors in the calculated natural frequencies and critical loads of thick laminated plates, we use the higher-order shear-deformation theory (HSDT) of Reddy (1984b), which accounts for quadratic distributions of the transverse shear strains through the thickness.

Khdeir (1988,1989) and Reddy and Khdeir (1989) used the theories developed by Reddy and other researchers to determine Levy-type solutions for the problems of free vibration and buckling of cross-ply laminated plates by using the state-space

concept. Unfortunately, their method of solution is limited to thick and some moderately thick plates because it yields numerically ill-conditioned problems for thin and many moderately thick plates. The loss of accuracy of such an approach was discussed earlier by Kalnins (1964) in connection with the two-point boundary-value problem describing the deformation of shells of revolution subject to symmetrical and nonsymmetrical loads. Kalnins (1964) states that the loss of accuracy does not result from cumulate errors in the integration, but it results from the subtraction of almost equal numbers in the process of satisfaction of the boundary conditions. Consequently, he concluded that for, every set of geometric and material properties of the shell, there is a critical length beyond which the solution loses all accuracy. To overcome this problem, Kalnins (1964) developed a multisegment numerical integration method. The interval of interest is divided into a finite number of subintervals and the two-point boundary-value problem is transformed into initial-value problems over the different segments. Then, the equations of the theory of shells of revolution, characterized in terms of first-order differential equations, are integrated over each segment. After the initial-value problems are integrated over all segments, continuity conditions on all variables are written at the endpoints of the segments, yielding a simultaneous system of linear equations, which is solved by means of Gaussian elimination.

A general approach for solving two-point boundary-value problem is the invariant-imbedding method (Scott, 1974). There are several variations of this method, including the so-called "field method", which is also known as the method of sweeps, the method of factorization, or the method of generalized Riccati transformations. The field method converts the two-point boundary-value problem into two successive numerically stable initial-value problems, which may be solved by standard shooting techniques. Because of its stability, there is no need for

subdividing the interval (Cohen, 1976). Cohen (1982) used the field method to evaluate the effect of transverse shear deformations on anisotropic plate buckling using a first-order shear-deformation theory.

A powerful approach for solving two-point boundary-value problems combines superposition with orthonormalization. Godunov (1961) and Bellman and Kalaba (1965) were the first to propose the use of orthonormalization in implementing the method of superposition. Slightly modified and related procedures were discussed by Conte (1966) and Davey (1973). Gersting and Jankowski (1972) compared Conte's version of the method of orthonormalization with several other numerical schemes for solving the Orr-Sommerfeld problem. Scott and Watts (1977) developed a powerful computer code called SUPORT based on Godunov's version of the method of orthonormalization that uses a variable-step Runge-Kutta-Fehlberg integration scheme. This code has been extensively used by many researchers in hydrodynamic stability. It is robust, easy to use, reliable, and efficient.

In this chapter, a combination of the state-space concept (Brogan, 1974) and the modified method of orthonormalization is used to calculate the natural frequencies and buckling loads of thick, moderately thick, and even thin plates using the higher-order shear-deformation theory of Reddy (1984a-c) and Bhimaraddi and Stevens (1984). Several approaches are discussed and numerical results are obtained and compared with previous results.

### 3.1. Free Vibration

For the case of linear free vibrations of cross-ply laminated plates, equations (2.29)-(2.33) reduce to

$$\begin{aligned} A_{11} \frac{\partial^2 u}{\partial x^2} + A_{66} \frac{\partial^2 u}{\partial y^2} + (A_{12} + A_{66}) \frac{\partial^2 v}{\partial x \partial y} + \hat{B}_{11} \frac{\partial \phi}{\partial x^2} - B_{11} \frac{\partial^3 w}{\partial x^3} \\ = I_1 \frac{\partial^2 u}{\partial t^2} + \bar{I}_2 \frac{\partial^2 \phi}{\partial t^2} - I_2 \frac{\partial^3 w}{\partial x \partial t^2} \end{aligned} \quad (3.1)$$

$$\begin{aligned} A_{66} \frac{\partial^2 v}{\partial x^2} + A_{22} \frac{\partial^2 v}{\partial y^2} + (A_{12} + A_{66}) \frac{\partial^2 u}{\partial x \partial y} + \hat{B}_{22} \frac{\partial^2 \psi}{\partial y^2} - B_{22} \frac{\partial^3 w}{\partial y^3} \\ = I_1 \frac{\partial^2 v}{\partial t^2} + \bar{I}_2 \frac{\partial^2 \psi}{\partial t^2} - I_2 \frac{\partial^3 w}{\partial y \partial t^2} \end{aligned} \quad (3.2)$$

$$\begin{aligned} B_{11} \frac{\partial^3 u}{\partial x^3} + B_{22} \frac{\partial^3 v}{\partial y^3} + \tilde{D}_{11} \frac{\partial^3 \phi}{\partial x^3} + \tilde{D}_{22} \frac{\partial^3 \psi}{\partial y^3} + (\tilde{D}_{12} + 2\tilde{D}_{66}) \left( \frac{\partial^3 \phi}{\partial x \partial y^2} + \frac{\partial^3 \psi}{\partial x^2 \partial y} \right) \\ - D_{11} \frac{\partial^4 w}{\partial x^4} - D_{22} \frac{\partial^4 w}{\partial y^4} - 2(D_{12} + 2D_{66}) \frac{\partial^4 w}{\partial x^2 \partial y^2} \\ = I_1 \frac{\partial^2 w}{\partial t^2} + I_2 \left( \frac{\partial^3 u}{\partial x \partial t^2} + \frac{\partial^3 v}{\partial y \partial t^2} \right) \\ - I_3 \left( \frac{\partial^4 w}{\partial x^2 \partial t^2} + \frac{\partial^4 w}{\partial y^2 \partial t^2} \right) + \bar{I}_0 \left( \frac{\partial^3 \phi}{\partial x \partial t^2} + \frac{\partial^3 \psi}{\partial y \partial t^2} \right) \end{aligned} \quad (3.3)$$

$$\begin{aligned} \hat{B}_{11} \frac{\partial^2 u}{\partial x^2} + \hat{D}_{11} \frac{\partial^2 \phi}{\partial x^2} + \hat{D}_{66} \frac{\partial^2 \phi}{\partial y^2} + (\hat{D}_{12} + \hat{D}_{66}) \frac{\partial^2 \psi}{\partial x \partial y} + D_{55}^* \phi \\ - \tilde{D}_{11} \frac{\partial^3 w}{\partial x^3} - (\tilde{D}_{12} + 2\tilde{D}_{66}) \frac{\partial^3 w}{\partial x \partial y^2} = \bar{I}_2 \frac{\partial^2 u}{\partial t^2} + \bar{I}_3 \frac{\partial^2 \phi}{\partial t^2} - \bar{I}_0 \frac{\partial^3 w}{\partial x \partial t^2} \end{aligned} \quad (3.4)$$

$$\begin{aligned}
& \hat{B}_{22} \frac{\partial^2 v}{\partial y^2} + \hat{D}_{22} \frac{\partial^2 \psi}{\partial y^2} + \hat{D}_{66} \frac{\partial^2 \psi}{\partial x^2} + (\hat{D}_{12} + \hat{D}_{66}) \frac{\partial^2 \phi}{\partial x \partial y} + D_{44}^* \psi \\
& - \tilde{D}_{22} \frac{\partial^3 w}{\partial y^3} - (\tilde{D}_{12} + 2\tilde{D}_{66}) \frac{\partial^3 w}{\partial x^2 \partial y} = \bar{I}_2 \frac{\partial^2 v}{\partial t^2} + \bar{I}_3 \frac{\partial^2 \psi}{\partial t^2} - \bar{I}_0 \frac{\partial^3 w}{\partial y \partial t^2}
\end{aligned} \tag{3.5}$$

We seek Levy-type solutions in which the edges  $x = 0$  and  $x = a$  are assumed to be invariable and simply supported, while the remaining two edges  $y = 0$  and  $y = b$  can have any arbitrary conditions. The boundary conditions at  $y = 0$  and  $y = b$  considered here are

(i) Clamped:

$$u = v = w = \frac{\partial w}{\partial y} = \phi = \psi = 0 \tag{3.6}$$

(ii) Simply supported:

$$u = w = \phi = N_2 = M_2 = \hat{M}_2 = 0 \tag{3.7}$$

(iii) Free:

$$N_2 = N_6 = M_2 = \hat{M}_2 = \hat{M}_6 = 0$$

$$I_2 \frac{\partial^2 v}{\partial t^2} + \bar{I}_0 \frac{\partial^2 \psi}{\partial t^2} - I_3 \frac{\partial^3 w}{\partial y \partial t^2} - N_2 \frac{\partial w}{\partial y} - N_6 \frac{\partial w}{\partial x} - \frac{\partial M_2}{\partial y} - 2 \frac{\partial M_6}{\partial x} = 0 \tag{3.8}$$

Seeking a generalized Levy-type solution, we represent the field variables as

$$\begin{bmatrix} u(x,y,t) \\ v(x,y,t) \\ w(x,y,t) \\ \phi(x,y,t) \\ \psi(x,y,t) \end{bmatrix} = \begin{bmatrix} f_{1m}(y) \cos \alpha_m x \\ f_{2m}(y) \sin \alpha_m x \\ f_{3m}(y) \sin \alpha_m x \\ f_{4m}(y) \cos \alpha_m x \\ f_{5m}(y) \sin \alpha_m x \end{bmatrix} e^{i\omega_m t} \quad (3.9)$$

where  $\alpha_m = m\pi/a$  and  $\omega_m$  denotes the natural frequency of the  $m$ th mode. Substituting equations (3.9) into equations (3.1)-(3.5) and after performing some algebraic manipulations, we obtain

$$\mathbf{q}'(y) = \mathbf{A}(\omega)\mathbf{q}(y) \quad (3.10)$$

where the prime indicates the derivative with respect to  $y$ ,  $\mathbf{A}(\omega)$  is a 12x12 constant matrix whose nonzero elements are listed in Appendix A, and  $\mathbf{q}(y)$  is a vector of length 12 whose elements are

$$\begin{aligned} q_1 &= f_{1m}, & q_2 &= \dot{f}_{1m}, & q_3 &= f_{2m}, & q_4 &= \dot{f}_{2m}, & q_5 &= f_{3m}, & q_6 &= \dot{f}_{3m} \\ q_7 &= \ddot{f}_{3m}, & q_8 &= \dddot{f}_{3m}, & q_9 &= f_{4m}, & q_{10} &= \dot{f}_{4m}, & q_{11} &= f_{5m}, & q_{12} &= \dot{f}_{5m} \end{aligned}$$

Free, clamped, or simply-supported conditions at  $y = 0$  and  $y = b$  yield two disjoint sets of boundary conditions that can be expressed as

$$\mathbf{R}_1 \mathbf{q} = 0 \quad \text{at } y = 0 \quad (3.11a)$$

$$\mathbf{R}_2 \mathbf{q} = 0 \quad \text{at } y = b \quad (3.11b)$$

where  $\mathbf{R}_1$  and  $\mathbf{R}_2$  are 6x12 matrices, which would be frequency dependent only at a free edge; they are given in Appendix B.

### 3.2. Stability

For cross-ply laminated plates subjected to in-plane biaxial loads  $T_{11}$  and  $T_{22}$ , as shown in Figure 3.1, equations (3.1)-(3.11) remain the same except for the following:

- (i) All the inertia terms,  $I_n$ , is dropped.
- (ii) The quantity  $(-T_{11} \frac{\partial^2 w}{\partial x^2} - T_{22} \frac{\partial^2 w}{\partial y^2})$  is added to the left-hand side of equation (3.3).
- (iii) The last equation in (3.8) is reduced to

$$\frac{\partial M_2}{\partial y} + 2 \frac{\partial M_6}{\partial x} - T_{22} \frac{\partial w}{\partial y} = 0$$

- (iv) The coefficient  $e^{i\omega_m t}$  in equations (3.9) is dropped.
- (v) The elements of  $\mathbf{A}$  become functions of  $T_{11}$  and  $T_{22}$  and are listed in Appendix C, where the elements of  $\mathbf{R}$  are listed in Appendix D.

### 3.3. Method of Solution

The general solution (Brogan, 1974) of equation (3.10) can be expressed in the form

$$\mathbf{q}(y) = e^{\mathbf{A}y} \mathbf{k} \quad (3.12)$$

Here, the column vector  $\mathbf{k}$  depends on the boundary conditions while  $e^{\mathbf{A}y}$  can be expressed as



$$e^{A_y} = M e^{J_y} M^{-1} = M \begin{bmatrix} e^{\lambda_{1y}} & & & \\ 0 & e^{\lambda_{2y}} & & \\ & & 0 & \\ & & & e^{\lambda_{11y}} \\ & 0 & & & e^{\lambda_{12y}} \end{bmatrix} M^{-1} \quad (3.13)$$

where the  $\lambda_j$  are the eigenvalues of  $\mathbf{A}$ , which are assumed to be distinct, and the columns of  $\mathbf{M}$  are their corresponding eigenvectors. We note that the proposed method is not limited to the case of distinct eigenvalues. In the general case,  $\mathbf{J}$  is a Jordan form (Franklin, 1968). Substituting equation (3.12) into equations (3.11) yields

$$\mathbf{Q}\mathbf{k} = \mathbf{0} \quad (3.14)$$

where  $\mathbf{Q}$  is 12x12 matrix, which depends on the axial loads and frequencies as well as the type of boundary conditions. For nontrivial solutions, one demands that

$$\det \mathbf{Q} = 0 \quad (3.15)$$

from which the natural frequencies or buckling loads are obtained by a suitable search method, such as a Newton-Raphson procedure.

Unfortunately the above application of the state-space concept breaks down numerically as the ratio  $b/h$  (length to thickness of the plate) is increased. In fact for the majority of structural plates, the length is large enough to cause a numerically ill-conditioned problem because the matrix  $\mathbf{A}$  is real and all of its diagonal elements are zero so that its trace is zero. The complex eigenvalues of  $\mathbf{A}$  occur in conjugate

pairs, and for each real eigenvalue there exists another real eigenvalue of the opposite sign. As  $b$  is increased, the growth rates of the elements of  $e^{Jb}$  that grow exponentially increase while the decay rates of the elements that decay exponentially also increase, hence the calculated solutions lose their numerical independence and the numerical method fails. A shift of the  $x$  coordinate axis by  $b/2$  in the positive  $y$ -direction would improve the accuracy but it is not good enough.

Alternatively, instead of using  $\mathbf{k}$  as the constant vector in equation (3.12), one can combine it with  $\mathbf{M}^{-1}$  and solve for the complex vector  $\hat{\mathbf{k}} = \mathbf{M}^{-1}\mathbf{k}$ . Thus, one can express the solution as

$$\mathbf{q}(y) = \mathbf{M}e^{Jy}\hat{\mathbf{k}} \quad (3.16)$$

Substituting equation (3.16) into the boundary conditions yields

$$\hat{\mathbf{Q}}\hat{\mathbf{k}} = \mathbf{0} \quad (3.17)$$

where  $\hat{\mathbf{Q}}$  is a complex matrix. One may assume a value for  $\omega$ , evaluate  $\det(\hat{\mathbf{Q}})$ , and vary  $\omega$  until the absolute value of  $\det(\hat{\mathbf{Q}})$  becomes smaller than a specified small tolerance. But this does not guarantee that  $\det(\hat{\mathbf{Q}})$  would become zero in a small neighborhood of  $\omega$ . However, if  $\det(\hat{\mathbf{Q}})$  is transformed into a real function of  $\omega$ , one could then apply a search method to locate a frequency. One of these transformations is obtained by separating the real and imaginary parts of both  $\hat{\mathbf{Q}}$  and  $\hat{\mathbf{k}}$  as follows:

$$\hat{\mathbf{Q}} = \hat{\mathbf{Q}}_r + i\hat{\mathbf{Q}}_i, \quad \hat{\mathbf{k}} = \hat{\mathbf{k}}_r + i\hat{\mathbf{k}}_i \quad (3.18)$$

where the subscripts  $r$  and  $i$  denote the real and imaginary parts, respectively. Using equations (3.18), we rewrite equation (3.17) as

$$\begin{bmatrix} \hat{\mathbf{Q}}_r & -\hat{\mathbf{Q}}_i \\ \hat{\mathbf{Q}}_i & \hat{\mathbf{Q}}_r \end{bmatrix} \begin{Bmatrix} \hat{\mathbf{k}}_r \\ \hat{\mathbf{k}}_i \end{Bmatrix} = \mathbf{0} \quad (3.19)$$

For a nontrivial solution

$$\det \begin{bmatrix} \hat{\mathbf{Q}}_r & -\hat{\mathbf{Q}}_i \\ \hat{\mathbf{Q}}_i & \hat{\mathbf{Q}}_r \end{bmatrix} = 0 \quad (3.20)$$

which can be solved numerically. However, this method is limited, and even application of the continuity and transfer-matrix method would not improve the situation at all.

A third alternative is to transform equations (3.10) and (3.11) into a nonhomogeneous system (Asfar et al. 1990). Here, one of the boundary conditions is relaxed (which is later used to test the convergence) and is replaced by fixing a variable, which is nonzero at an edge, to have a fixed value, say unity, at that edge. A value for  $\omega$  is assumed and the new nonhomogeneous system is solved. The solution is substituted into the relaxed boundary condition to check whether it is satisfied. The assumed value of  $\omega$  is varied until the relaxed condition is satisfied. Continuity may also be applied to improve the limitations on the length of the plate. However, there is an undesirable feature. The domains of attraction of many frequencies are too small. One may recover some of these lost frequencies by relaxing a different boundary condition or by fixing another edge variable. All or the first few desired frequencies may be obtained by a particular combination of a relaxed boundary condition and a fixed variable, but as the size of the plate is changed the same choice may not be good any more.

Alternatively, one can find six linearly independent vector solutions of equation (3.11a) and use each of them as an initial condition to determine  $\mathbf{q}$ . This leads to six vector solutions of equation (3.10) denoted by  $\mathbf{z}_1(y), \mathbf{z}_2(y), \dots, \mathbf{z}_6(y)$ . Using superposition, we write the solution of equations (3.10) and (3.11a) as

$$\mathbf{q}(y) = r_1 \mathbf{z}_1(y) + r_2 \mathbf{z}_2(y) + \dots + r_6 \mathbf{z}_6(y) \quad (3.21)$$

or in matrix form as

$$\mathbf{q}(y) = \mathbf{Z}(y) \mathbf{r} \quad (3.22)$$

where the  $r_i$  are constants,

$$\mathbf{r}^T = [r_1 \ r_2 \ r_3 \ r_4 \ r_5 \ r_6] \quad (3.23)$$

and the columns of the matrix  $\mathbf{Z}$  are the  $\mathbf{z}_m$ ; that is,

$$\mathbf{Z}(y) = [\mathbf{z}_1(y) \ \mathbf{z}_2(y) \ \dots \ \mathbf{z}_6(y)] \quad (3.24)$$

Substituting equation (3.22) into equation (3.11b) yields

$$\mathbf{R}_2 \mathbf{Z}(b) \mathbf{r} = 0 \quad (3.25)$$

Equation (3.25) represents a system of six linear homogeneous algebraic equations for the unknown constants  $r_i$ . For a nontrivial solution,  $\det[\mathbf{R}_2 \mathbf{Z}(b)]$  must vanish. Therefore, the natural frequencies or the buckling loads can be obtained by any search method.

Although this superposition procedure is simple and works in many instances, application of this method to thin and many moderately thick plates yields numerically ill-conditioned problems. The problem arises from the presence of

rapidly growing and rapidly decaying elements of  $e^{A_b}$ . This makes the columns of  $Z(y)$  lose their linear independence due the limited computer word length. The problem becomes more serious as the plate becomes thinner. One way that helps to overcome this stiffness problem is to orthonormalize the calculated solution vectors  $z_i(y)$  whenever an impeding loss of independence is detected.

Following the initial-value method in conjunction with continuity, we divide the interval  $y = [0, b]$  into  $n + 1$  nodes at  $y_0, y_1, \dots$ , and  $y_{n+1}$ , where  $y_0 = 0$  and  $y_{n+1} = b$ . From equation (3.11a), one can find six orthonormal vectors at  $y = 0$  and express the initial value of  $q$  as a linear combination of these vectors:

$$q(0) = c_1 q^{(1)}(0) + c_2 q^{(2)}(0) + \dots + c_6 q^{(6)}(0) \quad (3.26)$$

The general solution of equation (3.10) that satisfies equation (3.11a) can be expressed as

$$q(y) = c_1 q^{(1)}(y) + c_2 q^{(2)}(y) + \dots + c_6 q^{(6)}(y) \quad (3.27a)$$

where

$$q^{(k)}(y) = M e^{Jy} M^{-1} q^{(k)}(0) \quad (3.27b)$$

These six linearly independent vectors  $q^{(k)}$  are then evaluated at  $y_1$  and orthonormalized by the modified Gram-Schmidt procedure (Noble and Daniel, 1977). These orthonormalized vectors are used as initial conditions for the second interval  $[y_1, y_2]$  and six linearly independent solution vectors are evaluated at  $y_2$ . The process is then continued until six linearly independent vectors  $\hat{q}^{(k)}$  at  $y_{n+1}$  are found. The solution at  $y = b$  is expressed as a linear combination of these vectors in the form

$$q(b) = \hat{c}_1 \hat{q}^{(1)}(b) + \hat{c}_2 \hat{q}^{(2)}(b) + \dots + \hat{c}_6 \hat{q}^{(6)}(b) \quad (3.28)$$

Substitution of equation (3.28) into equation (3.11b) yields

$$\mathbf{R}_2 \hat{\mathbf{Q}} \hat{\mathbf{c}} = 0 \quad (3.29)$$

where  $\hat{\mathbf{Q}}$  is a 12x6 real matrix whose columns are the  $\hat{\mathbf{q}}^{(k)}(b)$  and  $\hat{\mathbf{c}}$  is a constant column vector of length six. For a nontrivial solution,

$$\det(\mathbf{R}_2 \hat{\mathbf{Q}}) = 0 \quad (3.30)$$

from which all the natural frequencies or buckling loads are determined. This method takes a little more computer time due to the orthonormalization process but it yields all the desired natural frequencies or buckling loads. The total computation time is reduced greatly by increasing the number of nodes even though the number of orthonormalizations is increased, because the absolute value of the exponent  $\mathbf{Jy}$  in equation (3.13) is decreased and hence the computer carries smaller numbers.

### 3.4. Numerical Results

Numerical results are obtained by applying the continuity condition in conjunction with orthonormalization to the system described by equations (3.10) and (3.11). Cross-ply laminated plates whose geometrical and material properties are the same for all layers are considered. These properties are as follows:

$$G_{12} = G_{13} = 0.6E_2, G_{23} = 0.5E_2, \nu_{12} = 0.25$$

The effect of the plate thickness and number of elements on the convergence of the dimensionless fundamental frequency of symmetric and antisymmetric square plates for various boundary conditions are investigated. The results are compared with the Levy-type solutions obtained by Khdeir (1988) and Reddy and Khdeir (1989), which are available for only thick plates, and are listed in Tables 3.1 and 3.2 along with the results of the classical plate theory (CPT). The converged results for the uniaxial buckling load ( $T_{11} \neq 0$ ) of these plates with similar comparisons are listed in Tables 3.3 and 3.4. The procedure described in this paper converges faster than that used by Khdeir and Reddy and yields results that are in good agreement with their results. As shown in Tables 3.1-3.4, the present procedure overcomes the difficulties involved in the numerical calculation of both the natural frequencies and buckling loads of moderately thick and thin plates. Continuity is not used in CPT because the problem is not stiff. We note that CPT overestimates the fundamental frequencies in all cases, especially as the plate thickness increases. For example, in the case of free vibration of a simply-supported two-layered antisymmetric plate, the error obtained by using CPT for the case  $a/h = 5$  is about 18% whereas for the case  $a/h = 100$  the error decreases to less than 0.07%. The corresponding error obtained in calculating the buckling load for the case  $a/h = 5$  is more than 45% whereas for the case  $a/h = 100$  the error decreases to 0.12%.

In Table 3.5, we compare the dimensionless critical loads for square cross-ply laminated plates using the third-order shear-deformation theory with the results obtained by Cohen (1982) using the first-order shear-deformation theory, the results obtained using classical plate theory, and the results obtained by Noor (1975) using the theory of elasticity. The plate properties are  $E_1/E_2 = 30$ ,  $G_{12}/E_2 = 0.6$ ,  $G_{23}/E_2 = 0.5$ , and  $\nu_{ij} = 0.25$ . Again, the accuracy of the classical plate theory deteriorates as  $a/h$  decreases and as the number of layers increase. The higher-order

shear-deformation theory produces results that are closer to the three-dimensional elasticity solutions than the first-order shear-deformation theory when the number of layers is 9 and 10. When the number of layers is 2 or 3, the results of the first-order theory are closer to the three-dimensional elasticity solutions than the higher-order theory.

The effect of the degree of orthotropy on the fundamental frequencies and critical loads obtained by using the present procedure for various simply-supported plates is compared with the three-dimensional elasticity solutions of Noor (1973, 1975) in Figures 3.2 and 3.3. The results obtained by HSDT are in excellent agreement with those of Noor. These results are overestimated by CPT. The overestimation error in CPT increases as the ratio  $E_1/E_2$  increases. However, HSDT yields results that remain very close to the results obtained by Noor.

In Figures 3.4 and 3.5, we compare variation of the fundamental frequencies and uniaxial buckling loads of thin and thick clamped plates with  $E_1/E_2$  obtained by using HSDT with those obtained by using CPT. In Figure 3.5, the critical loads when  $E_1/E_2$  is less than 17.3, between 17.3 and 45.3, and more than 45.3 belong to modes 2,3, and 4, respectively. The critical loads of Figures 3.5b-d correspond to the second mode ( $m = 2$ ). Clearly, the overestimation error in the results obtained by CPT not only increases as the degree of orthotropy increases, but it is also magnified as the plate thickness increases.

The effect of the plate thickness on the frequencies and critical loads calculated by using HSDT and CPT is shown in Figures 3.6 and 3.7. Again the overestimation errors obtained with CPT increase as either the thickness or the degree of orthotropy of the plate increases. These results verify that CPT may be used to predict the fundamental frequencies of thin plates. This prediction becomes more accurate as the orthotropy ratio is reduced. For example, CPT is expected to lead to very



accurate results for thin isotropic plates which have an orthotropy ratio of unity. The fundamental frequencies of even a moderately thick plate with a low orthotropy ratio may be estimated by using CPT. As discussed above, these estimates are not good for either thick plates or laminated plates with a high orthotropy ratio. For thick laminated plates, a HSDT is needed to produce accurate results.

The results of biaxial compressions of symmetric and antisymmetric plates are shown in Figures 3.8a and 3.8b, respectively. Clearly as one load decreases the other one increases. The curves corresponding to the HSDT results are broken. When  $T_{22}$  is small, the plates buckle in the second mode. But when  $T_{22}$  is increased beyond the broken point the plates buckle in the first mode. In either case the buckling loads are overestimated by using CPT.

We emphasize that with the present procedure one can calculate the natural frequency of any mode. The first ten dimensionless frequencies of a thin square plate for various mode numbers  $m$  and boundary conditions are listed in Tables 3.6 and 3.7. For each mode the clamped-clamped plate has the highest frequency whereas the free-free plate has the lowest frequency. These higher frequencies are very important in the study of modal interactions.

**Table 3.1.** Comparison of the converged dimensionless fundamental frequency  $\bar{\omega} = \omega a^2 \sqrt{\rho/E_2} / h$  with the HSDT results of Khdeir (1988), denoted by (K), and CPT for thick, moderately thick, and thin symmetric plates (3-layers;  $E_1/E_2 = 40$ ).  $\&$  is the number of elements per unit of dimensionless length  $a/h$ . The boundary conditions at the edges are any combination of simply-supported (S), clamped (C), and free (F) conditions.

B.C.	Theory	a/h=5	a/h=10	a/h=20	a/h=50	a/h=100
SS	HSDT(&=0.4)	10.264	14.702	17.483	18.641	18.828
	HSDT(&=0.6)	10.263	14.702	17.483	18.641	18.828
	HSDT(&=1.0)	10.263	14.702	17.483	18.641	18.828
	HSDT(&=2.0)	10.263	14.702	17.483	18.641	18.828
	HSDT( K )	10.263	14.702	NA	NA	NA
	CPT	18.297	18.738	18.853	18.885	18.890
CC	HSDT(&=0.4)	12.332	20.320	30.210	38.228	40.065
	HSDT(&=0.6)	12.333	20.315	30.207	38.231	40.063
	HSDT(&=1.0)	12.333	20.315	30.208	38.231	40.063
	HSDT(&=2.0)	12.333	20.315	30.208	38.231	40.063
	HSDT( K )	NA	20.315	NA	NA	NA
	CPT	39.316	40.372	40.650	40.728	40.740
FF	HSDT(&=0.4)	3.987	4.322	4.422	4.451	4.455
	HSDT(&=0.6)	3.987	4.322	4.422	4.451	4.455
	HSDT(&=1.0)	3.987	4.322	4.422	4.451	4.455
	HSDT(&=2.0)	3.987	4.322	4.422	4.451	4.455
	HSDT( K )	NA	4.322	NA	NA	NA
	CPT	4.385	4.438	4.452	4.456	4.162
SC	HSDT(&=0.4)	11.156	17.426	23.652	27.496	28.237
	HSDT(&=0.6)	11.156	17.427	23.652	27.496	28.238
	HSDT(&=1.0)	11.156	17.427	23.652	27.496	28.238
	HSDT(&=2.0)	11.156	17.427	23.652	27.496	28.238
	HSDT( K )	NA	17.427	NA	NA	NA
	CPT	27.537	28.251	28.438	28.491	28.498
CF	HSDT(&=0.4)	5.976	7.335	7.980	8.216	8.255
	HSDT(&=0.6)	5.975	7.335	7.980	8.216	8.254
	HSDT(&=1.0)	5.975	7.335	7.980	8.216	8.254
	HSDT(&=2.0)	5.975	7.335	7.980	8.216	8.254
	HSDT( K )	NA	7.334	NA	NA	NA
	CPT	8.077	8.220	8.256	8.267	8.268
SF	HSDT(&=0.4)	4.482	4.895	5.024	5.065	5.073
	HSDT(&=0.6)	4.483	4.895	5.024	5.065	5.072
	HSDT(&=1.0)	4.483	4.895	5.024	5.065	5.072
	HSDT(&=2.0)	4.483	4.895	5.024	5.065	5.072
	HSDT( K )	NA	4.892	NA	NA	NA
	CPT	4.971	5.049	5.069	5.075	5.076

**Table 3.2.** Comparison of the converged dimensionless fundamental frequency  $\bar{\omega} = \omega a^2 \sqrt{\rho/E_2}/h$  with the HSDT results of Reddy and Khdeir (1989), denoted by (R&K), and CPT for thick, moderately thick, and thin antisymmetric plates (2-layers;  $E_1/E_2 = 40$ ).  $\&$  is the number of elements per unit of dimensionless length  $a/h$ .

B.C.	Theory	a/h=5	a/h=10	a/h=20	a/h=50	a/h=100
SS	HSDT(&=0.4)	9.122	10.582	11.102	11.279	11.293
	HSDT(&=0.6)	9.087	10.568	11.105	11.275	11.300
	HSDT(&=1.0)	9.087	10.568	11.105	11.275	11.300
	HSDT(&=2.0)	9.087	10.568	11.105	11.275	11.300
	HSDT( R&K )	9.087	10.568	NA	NA	NA
	CPT	10.721	11.154	11.269	11.302	11.307
CC	HSDT(&=0.4)	11.765	15.626	17.720	18.584	18.840
	HSDT(&=0.6)	11.891	15.712	17.821	18.652	18.786
	HSDT(&=1.0)	11.890	15.712	17.821	18.653	18.786
	HSDT(&=2.0)	11.890	15.712	17.821	18.653	18.786
	HSDT( R&K )	11.890	15.709	NA	NA	NA
	CPT	17.741	18.543	18.758	18.819	18.828
FF	HSDT(&=0.4)	6.127	6.940	7.219	7.301	7.321
	HSDT(&=0.6)	6.128	6.944	7.217	7.301	7.313
	HSDT(&=1.0)	6.128	6.944	7.217	7.301	7.313
	HSDT(&=2.0)	6.128	6.944	7.217	7.301	7.313
	HSDT( R&K )	6.128	6.943	NA	NA	NA
	CPT	7.122	7.267	7.305	7.315	7.317
SC	HSDT(&=0.4)	10.334	12.857	13.921	14.309	14.428
	HSDT(&=0.6)	10.393	12.871	13.972	14.358	14.417
	HSDT(&=1.0)	10.393	12.871	13.973	14.358	14.416
	HSDT(&=2.0)	10.393	12.871	13.973	14.358	14.416
	HSDT( R&K )	10.393	12.870	NA	NA	NA
	CPT	13.627	14.223	14.382	14.428	14.434
CF	HSDT(&=0.4)	6.863	7.843	8.146	8.269	8.264
	HSDT(&=0.6)	6.831	7.810	8.157	8.268	8.286
	HSDT(&=1.0)	6.831	7.811	8.157	8.268	8.286
	HSDT(&=2.0)	6.831	7.811	8.157	8.268	8.286
	HSDT( R&K )	6.836	7.810	NA	NA	NA
	CPT	7.986	8.214	8.273	8.290	8.292
SF	HSDT(&=0.4)	6.350	7.273	7.580	7.689	7.689
	HSDT(&=0.6)	6.384	7.277	7.582	7.677	7.692
	HSDT(&=1.0)	6.385	7.277	7.582	7.677	7.692
	HSDT(&=2.0)	6.385	7.277	7.582	7.677	7.692
	HSDT( R&K )	6.387	7.277	NA	NA	NA
	CPT	7.422	7.629	7.680	7.694	7.696

**Table 3.3.** Comparison of the dimensionless critical load  $\bar{T}_{11} = T_{11}a^2/E_2h^3$  of 2-layered antisymmetric square plates with the HSDT results of Reddy and Khdeir (1989) (denoted by R&K) and CPT ( $E_1/E_2 = 40$ ). The arbitrary boundary conditions are any combination of simply supported (S), clamped (C), and free (F) conditions.

B.C.	Theory	a/h=5	a/h=10	a/h=25	a/h=100
SS	present	8.769	11.563	12.711	12.942
	R&K	8.769	11.562	NA	NA
	CPT	12.957	12.957	12.957	12.957
SC	present	10.754	17.133	20.327	21.064
	R&K	10.754	17.133	NA	NA
	CPT	21.116	21.116	21.116	21.116
SF	present	4.285	5.445	5.902	5.995
	R&K	4.283	5.442	NA	NA
	CPT	6.003	6.003	6.003	6.003
CC	present	11.490	21.464	29.079	31.131
	R&K	11.490	21.464	NA	NA
	CPT	31.280	31.280	31.280	31.280
CF	present	4.912	6.279	6.839	6.958
	R&K	4.908	6.274	NA	NA
	CPT	6.968	6.968	6.968	6.968
FF	present	3.905	4.940	5.341	5.420
	R&K	3.905	4.940	NA	NA
	CPT	5.425	5.425	5.425	5.425

**Table 3.4.** Comparison of the dimensionless critical load  $\bar{T}_{11} = T_{11}a^2/E_2h^3$  of 10-layered antisymmetric square plates with the HSDT results of Reddy and Khdeir (1989) (denoted by R&K) and CPT subjected to various combinations of boundary conditions ( $E_1/E_2 = 40$ ).

B.C.	Theory	a/h=5	a/h=10	a/h=25	a/h=100
SS	present	12.109	25.422	33.176	35.096
	R&K	12.109	25.423	NA	NA
	CPT	35.232	35.232	35.232	35.232
SC	present	12.607	32.885	52.432	58.795
	R&K	12.607	32.885	NA	NA
	CPT	59.288	59.288	59.288	59.288
SF	present	7.053	12.509	16.085	16.960
	R&K	7.050	12.506	NA	NA
	CPT	17.023	17.023	17.023	17.023
CC	present	13.254	35.376	71.621	88.354
	R&K	13.254	35.376	NA	NA
	CPT	89.770	89.770	89.770	89.770
CF	present	8.224	14.356	18.337	19.316
	R&K	8.221	14.351	NA	NA
	CPT	19.389	19.389	19.389	19.389
FF	present	6.780	12.077	15.529	16.367
	R&K	6.780	12.077	NA	NA
	CPT	16.426	16.426	16.426	16.426

**Table 3.5.** Variation of dimensionless critical load  $\bar{T}_{11} = T_{11}a^2/E_1h^3$  of square cross-ply laminated plates with number of layers (NL) and length to thickness ratio ( $a/h$ ). Classical stands for results calculated using CPT, Noor stands for the theory of elasticity solution of Noor (1975), and Cohen stands for the results obtained by Cohen (1982) using first-order shear deformation theory.  $E_1/T_2 = 30$ ,  $G_{12}/E_2 = 0.6$ ,  $G_{23}/E_2 = 0.5$ , and  $\nu_{ij} = 0.25$ .

<u><math>a/h</math></u>	<u>NL</u>	<u>Classical</u>	<u>Noor</u>	<u>Cohen</u>	<u>Present</u>
10	2	10.891	9.375	9.754	9.869
	3	27.936	19.304	19.097	18.878
	9	27.936	20.961	21.560	21.178
	10	27.254	20.635	21.254	20.986
5	2	10.891	6.664	7.452	7.721
	3	27.936	10.383	10.236	10.078
	9	27.936	12.138	12.953	12.413
	10	27.254	12.070	12.799	12.488

**Table 3.6.** Dimensionless frequencies  $\bar{\omega} = \omega a^2 \sqrt{\rho/E_2} / h$  of ten-layered antisymmetric square plates ( $a/h = 50$ ) for various modes obtained by using CPT and the present procedure ( $E_1/E_2 = 40$ ).

	CC	SC	SS	CF	SF	FF
m=1	32.0	24.2	18.6	13.8	13.0	12.7
	81.2	66.4	53.3	32.2	24.8	13.6
	157.0	135.7	116.0	81.5	66.8	33.1
	258.1	230.5	121.7	157.1	118.3	81.8
	384.4	350.5	204.5	258.1	135.9	114.8
	535.4	375.8	318.1	373.3	230.5	157.3
	710.9	495.3	456.6	384.2	350.3	258.1
	717.5	664.6	619.8	534.9	494.8	383.9
	721.9	721.9	707.4	709.9	663.7	534.3
m=2	756.2	751.4	736.5	714.2	707.4	706.6
	59.5	55.6	53.3	51.4	51.1	50.9
	96.6	84.5	74.5	60.6	56.7	51.8
	166.5	146.6	128.4	97.9	85.7	61.8
	265.0	238.0	212.8	167.4	147.5	99.0
	389.7	356.3	243.3	265.5	238.7	168.3
	539.9	430.9	324.4	390.0	240.0	236.5
	714.7	500.0	461.8	426.9	356.6	266.1
	751.5	668.6	624.1	539.7	500.0	390.2
m=3	913.9	861.6	751.4	714.1	668.1	539.5
	1136.9	1078.5	810.9	912.7	749.0	713.4
	119.1	117.2	116.0	114.8	114.6	114.4
	142.7	134.6	128.4	120.4	118.3	115.3
	198.3	181.7	167.3	144.5	136.4	121.7
	287.3	262.6	239.9	200.1	183.6	146.3
	406.4	374.3	344.1	288.8	264.1	201.9
	552.9	509.6	365.0	407.4	361.6	290.2
	725.4	514.0	476.9	504.6	375.5	358.2
m=4	799.3	680.0	636.3	553.5	514.7	408.4
	922.9	871.2	799.3	725.4	680.1	554.0
	1144.6	1086.7	821.0	922.3	796.1	725.3
	206.3	205.2	204.5	203.5	203.4	203.2
	221.9	216.7	212.8	207.6	206.3	204.1
	262.7	250.3	239.9	224.0	218.6	208.9
	336.5	315.5	296.8	265.1	252.6	226.0
	443.9	414.7	387.5	338.8	317.9	267.4
	582.3	545.4	486.7	445.8	416.7	341.0
m=4	749.0	602.7	510.4	583.6	483.3	447.7
	861.7	705.1	663.0	597.3	546.9	479.9
	942.4	891.8	842.9	749.8	706.0	585.0
	1161.0	1104.0	861.7	942.4	857.8	750.5

**Table 3.7.** Dimensionless frequencies  $\bar{\omega} = \omega a^2 \sqrt{\rho/E_2} / h$  of ten-layered antisymmetric square plates ( $a/h = 50$ ) for various modes obtained by using HSDT and the present procedure ( $E_1/E_2 = 40$ ).

	CC	SC	SS	CF	SF	FF
m=1	31.0	23.8	18.5	13.7	12.9	12.6
	75.6	63.3	51.9	31.5	24.6	13.5
	139.6	124.3	109.2	77.4	64.8	32.8
	218.1	201.4	121.7	143.2	118.3	79.2
	307.7	290.7	184.5	224.4	127.5	114.8
	405.4	375.8	273.4	317.1	207.2	147.1
	509.1	388.9	372.0	373.3	299.7	231.2
	617.2	493.5	477.5	418.2	401.4	327.2
	717.5	602.6	587.7	525.1	509.3	431.7
	721.8	714.8	701.0	636.2	621.4	542.0
m=2	57.7	54.1	51.9	50.0	49.7	49.5
	90.9	80.9	72.3	58.8	55.2	50.4
	149.2	135.0	121.4	93.2	83.0	60.3
	225.0	208.9	192.7	153.3	138.7	95.6
	313.1	296.4	243.3	231.7	215.1	157.7
	409.8	393.6	279.5	322.8	239.9	236.4
	512.9	430.9	377.0	422.8	305.8	238.9
	620.6	497.5	481.7	427.0	406.3	333.2
	731.5	606.1	591.3	529.1	513.5	436.6
	751.4	717.9	704.2	639.7	625.1	546.2
m=3	112.2	110.3	109.2	108.1	107.9	107.7
	133.3	126.7	121.4	113.4	111.4	108.5
	179.3	167.7	156.9	135.8	128.9	114.7
	246.8	232.2	217.9	183.6	171.6	138.3
	329.7	314.0	298.2	253.6	238.7	188.0
	423.2	407.5	365.0	339.6	323.6	260.9
	524.0	509.0	391.6	436.3	361.6	350.1
	630.1	509.6	493.7	504.6	420.4	358.2
	739.8	615.9	601.4	540.3	525.1	450.2
	799.2	726.5	712.9	649.3	635.0	557.5
m=4	186.3	185.2	184.5	183.6	183.5	183.3
	200.5	196.2	192.7	187.5	186.2	184.1
	234.5	225.8	217.9	202.9	198.2	188.7
	290.2	278.0	266.2	238.5	229.4	205.2
	364.0	350.0	336.0	296.8	284.2	242.8
	451.0	436.4	421.7	373.7	359.3	303.8
	547.1	532.9	486.7	463.9	449.0	383.9
	649.7	602.7	518.3	563.2	483.3	477.4
	756.8	636.1	622.2	597.2	548.8	480.1
	861.6	743.9	730.8	668.8	655.0	580.2



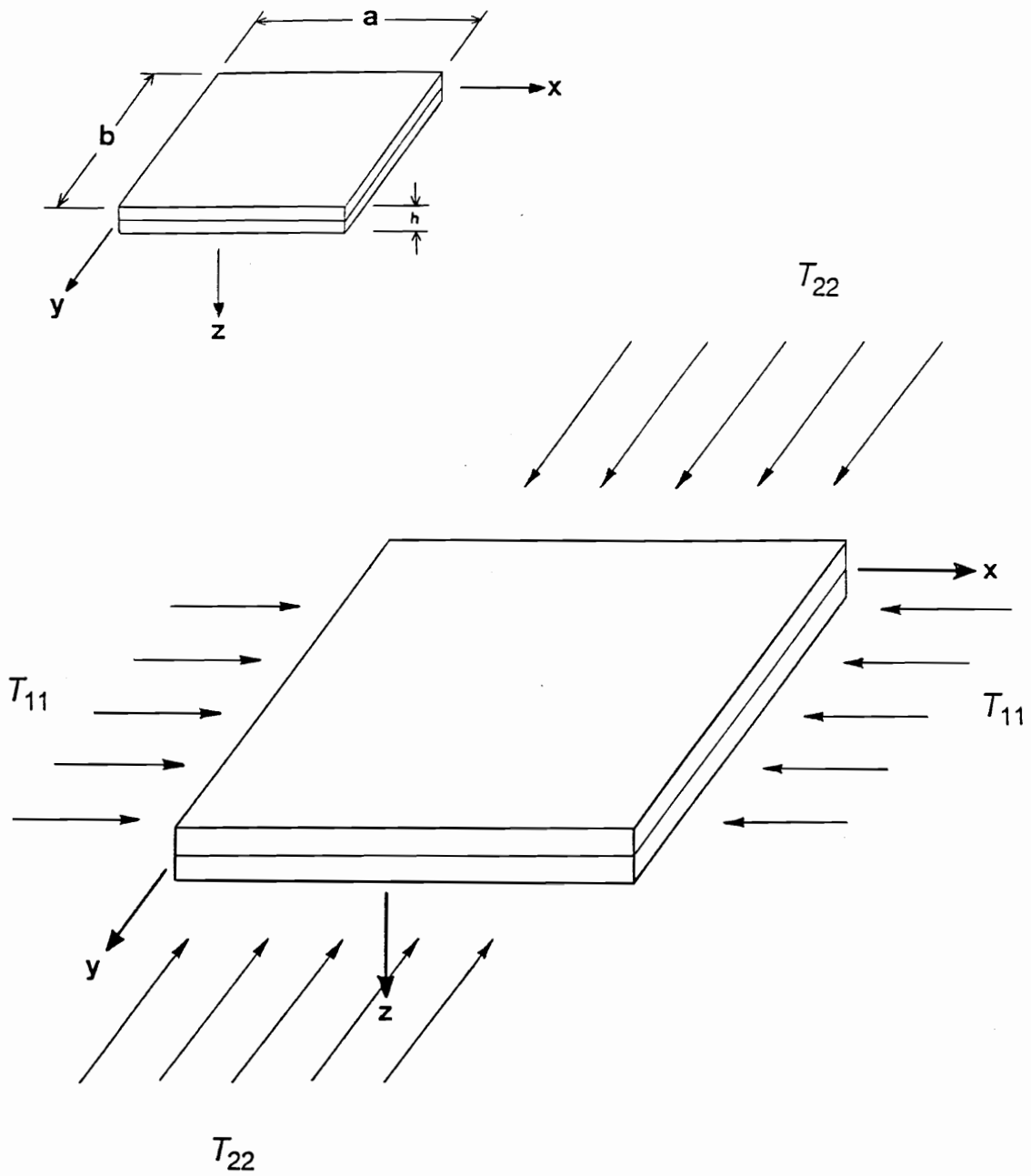


**Figure 3.1.** Plates subjected to in-plane compressive loadings.

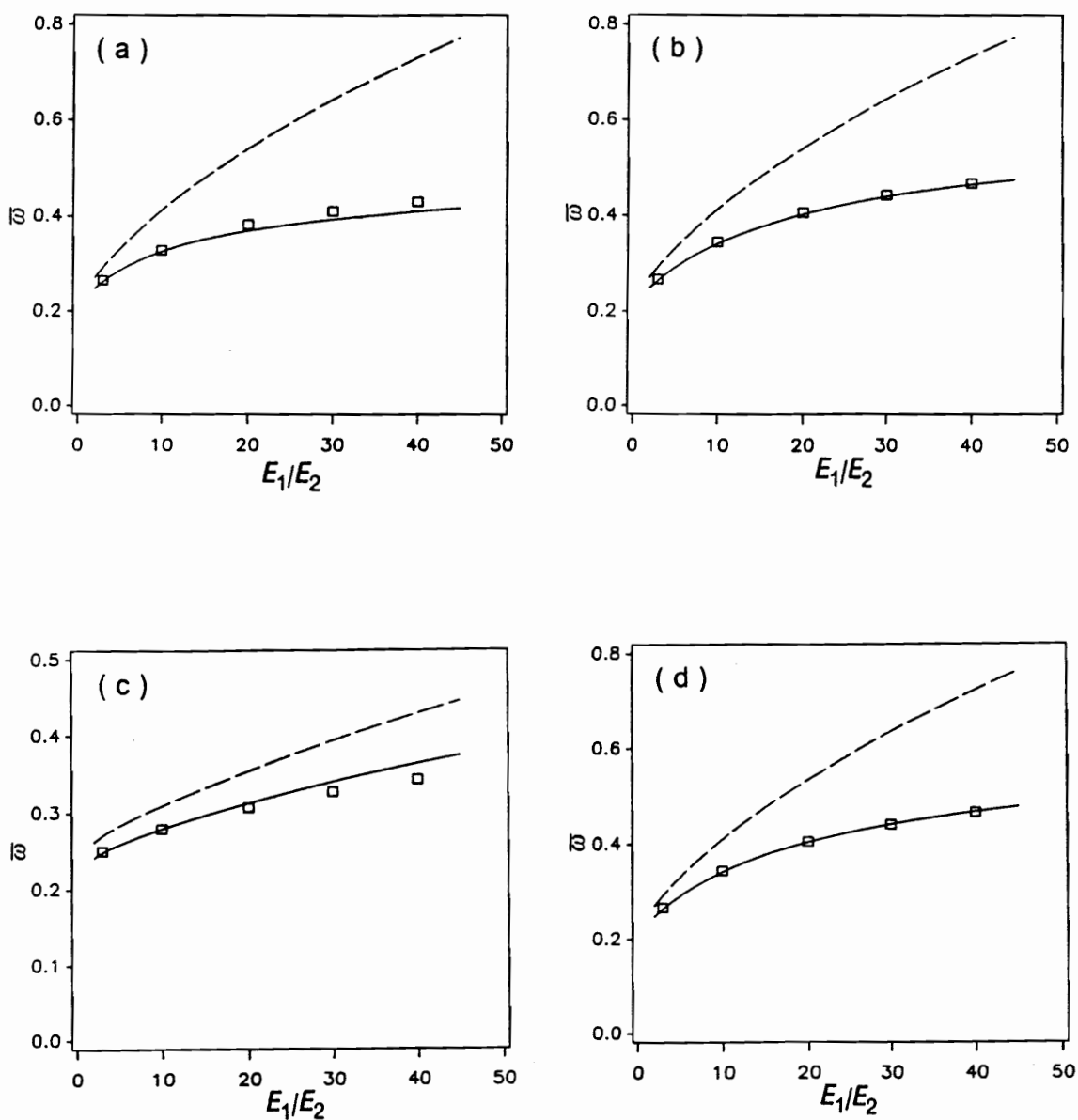


**Figure 3.2.** Comparison of the dimensionless natural frequency  $\bar{\omega} = \omega h \sqrt{\rho/E_2}$  of simply-supported square plates ( $a/h = 5$ ) obtained by the (—) present procedure with those obtained using the CPT (---) and those obtained by Noor using the three-dimensional theory of elasticity ( $\square$ ): (a) 3-layered symmetric, (b) 9-layered symmetric, (c) 2-layered antisymmetric, and (d) 10-layered antisymmetric plates.

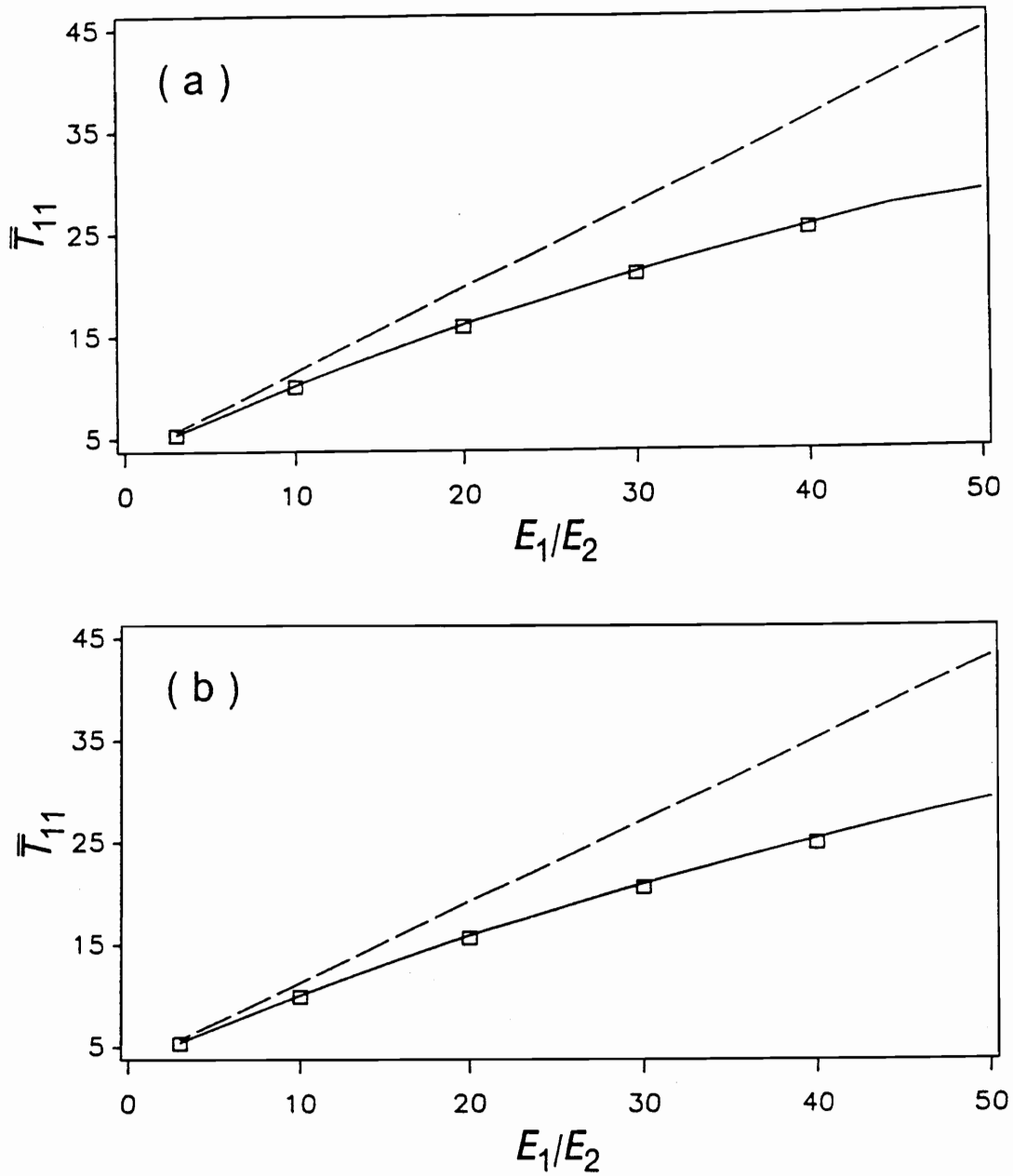


**Figure 3.3.** Comparison of the dimensionless critical load  $\bar{T}_{11} = T_{11}a^2/E_2h^3$  of simply supported square plates ( $a/h = 10$ ) obtained by the present procedure (—) with those obtained using CPT (---) and those obtained by Noor (1973) using the three-dimensional theory of elasticity (□): (a) 9-layered symmetric and (b) 10-layered antisymmetric plates.

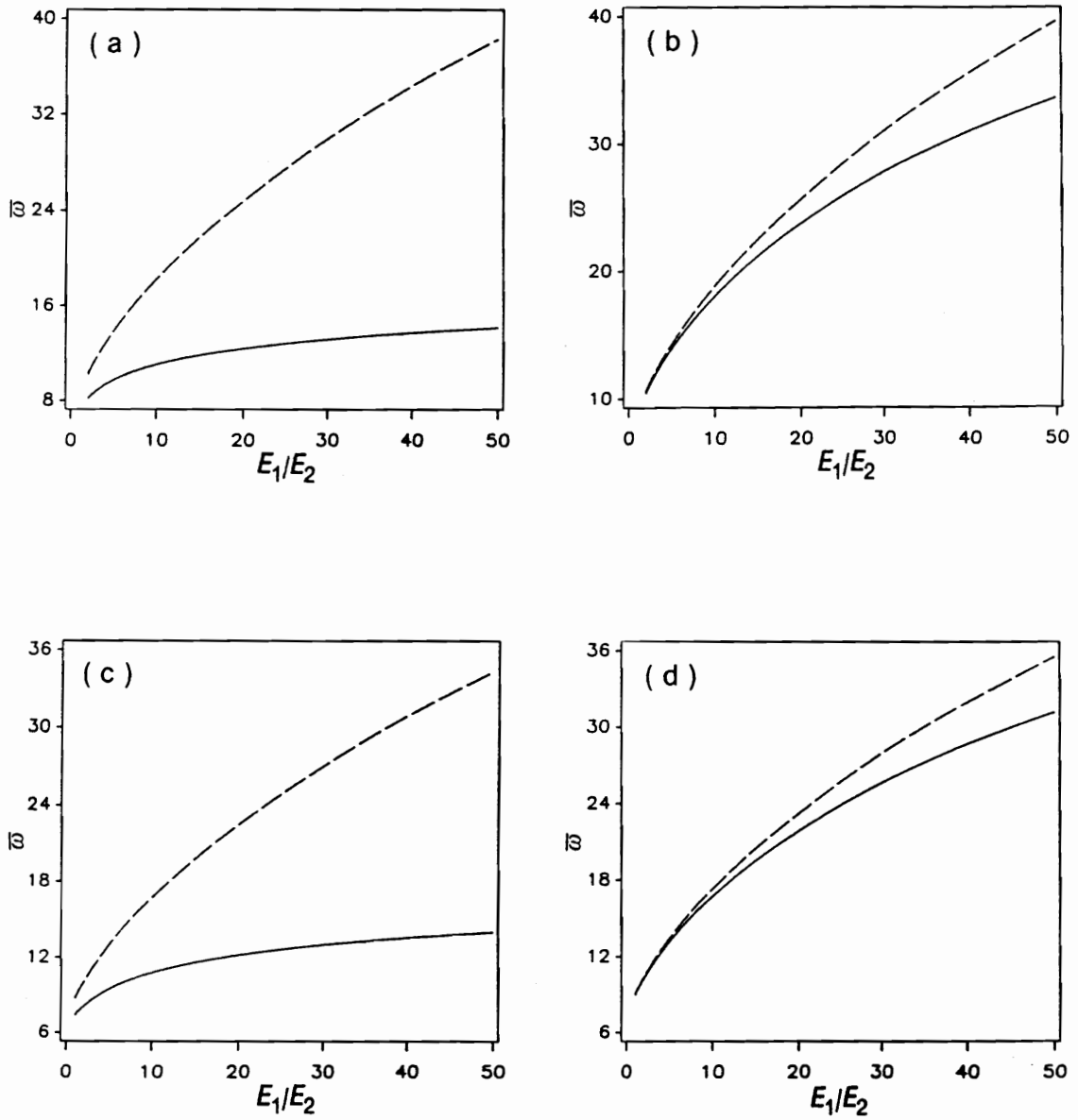


**Figure 3.4.** The effect of the degree of orthotropy on the dimensionless natural frequency  $\bar{\omega} = \omega a^2 \sqrt{\rho/E_2}/h$  for CC square plates obtained by using HSDT (—) CPT (---): (a) 9-layered symmetric ( $a/h = 5$ ), (b) 9-layered symmetric ( $a/h = 25$ ), (c) 10-layered antisymmetric ( $a/h = 5$ ), and (d) 10-layered antisymmetric ( $a/h = 25$ ) plates.

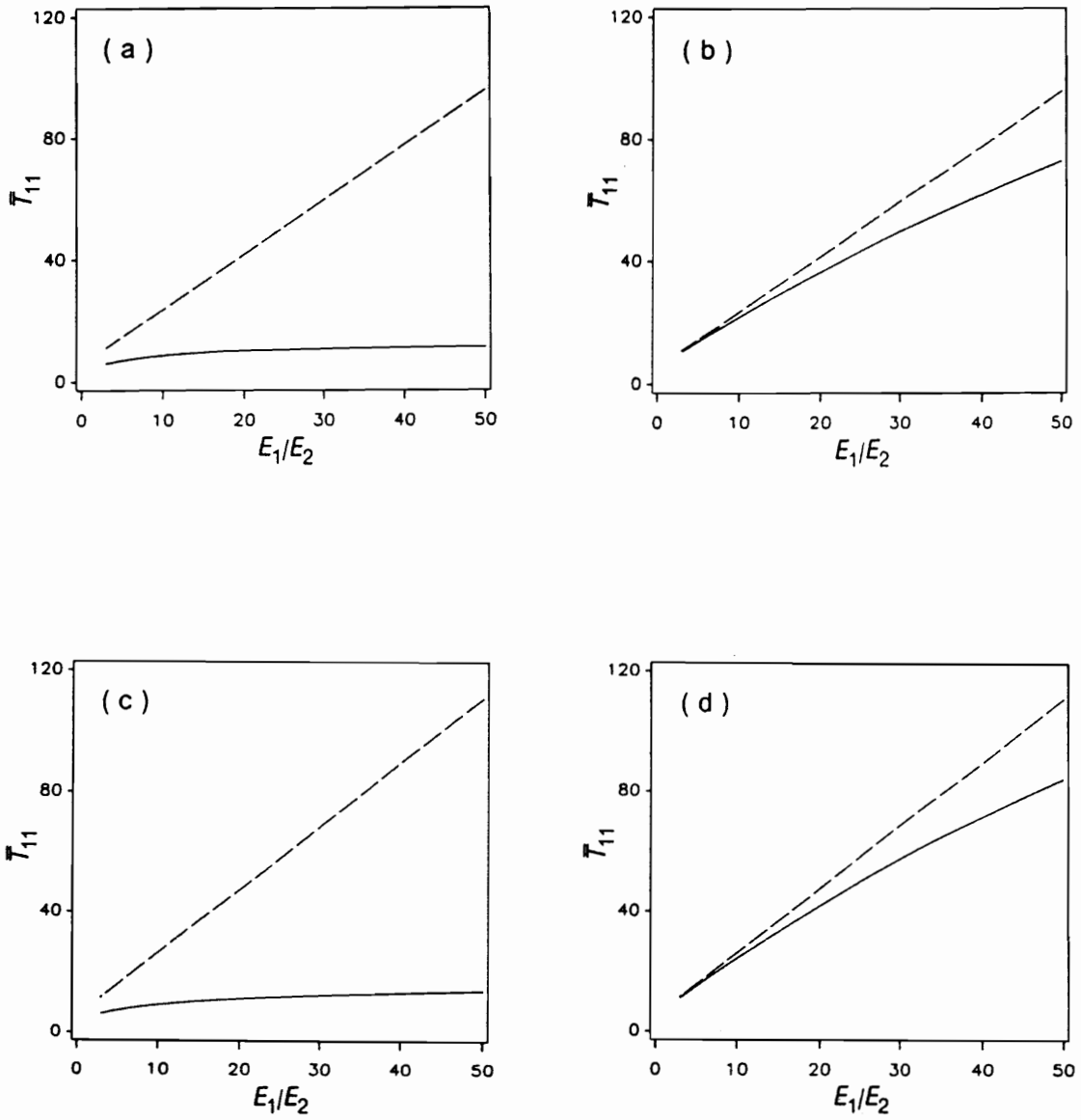


**Figure 3.5.** The effect of the degree of orthotropy on the dimensionless critical load  $\bar{T}_{11} = T_{11}a^2/E_2h^3$  for CC square plates obtained by using HSDT (—) and CPT (---): (a) 9-layered symmetric ( $a/h = 5$ ), (b) 9-layered symmetric ( $a/h = 25$ ), (c) 10-layered antisymmetric ( $a/h = 5$ ), and (d) 10-layered antisymmetric ( $a/h = 25$ ) plates.

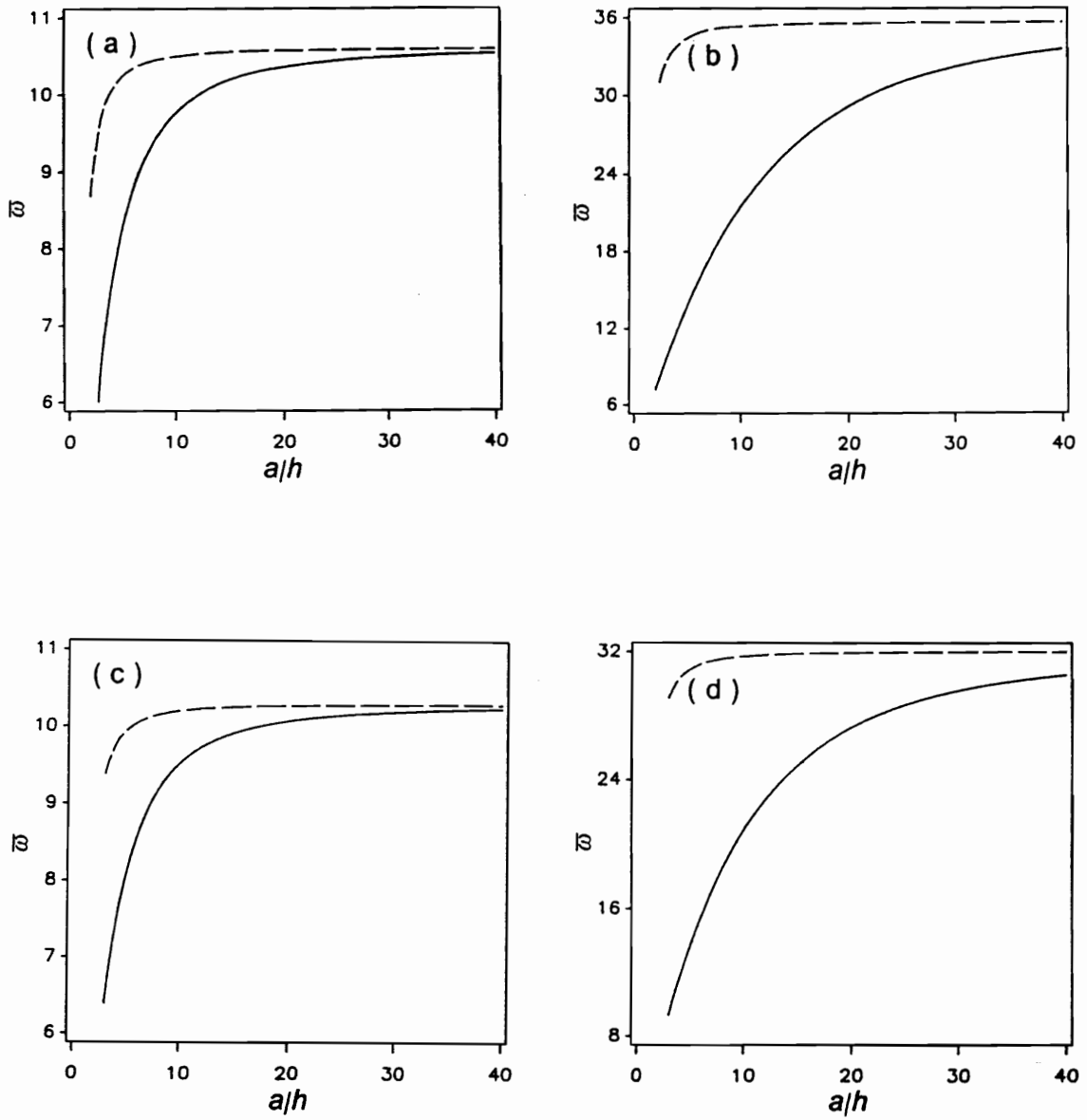


**Figure 3.6.** The effect of the dimensionless plate length ( $a/h$ ) on the dimensionless natural frequency  $\bar{\omega} = \omega a^2 \sqrt{\rho/E_2}/h$  for CC square plates obtained by using HSDT (—) and CPT (---): (a) 9-layered symmetric ( $E_1/E_2 = 2$ ), (b) 9-layered symmetric ( $E_1/E_2 = 40$ ), (c) 10-layered antisymmetric ( $E_1/E_2 = 2$ ), and (d) 10-layered antisymmetric ( $E_1/E_2 = 40$ ) plates.

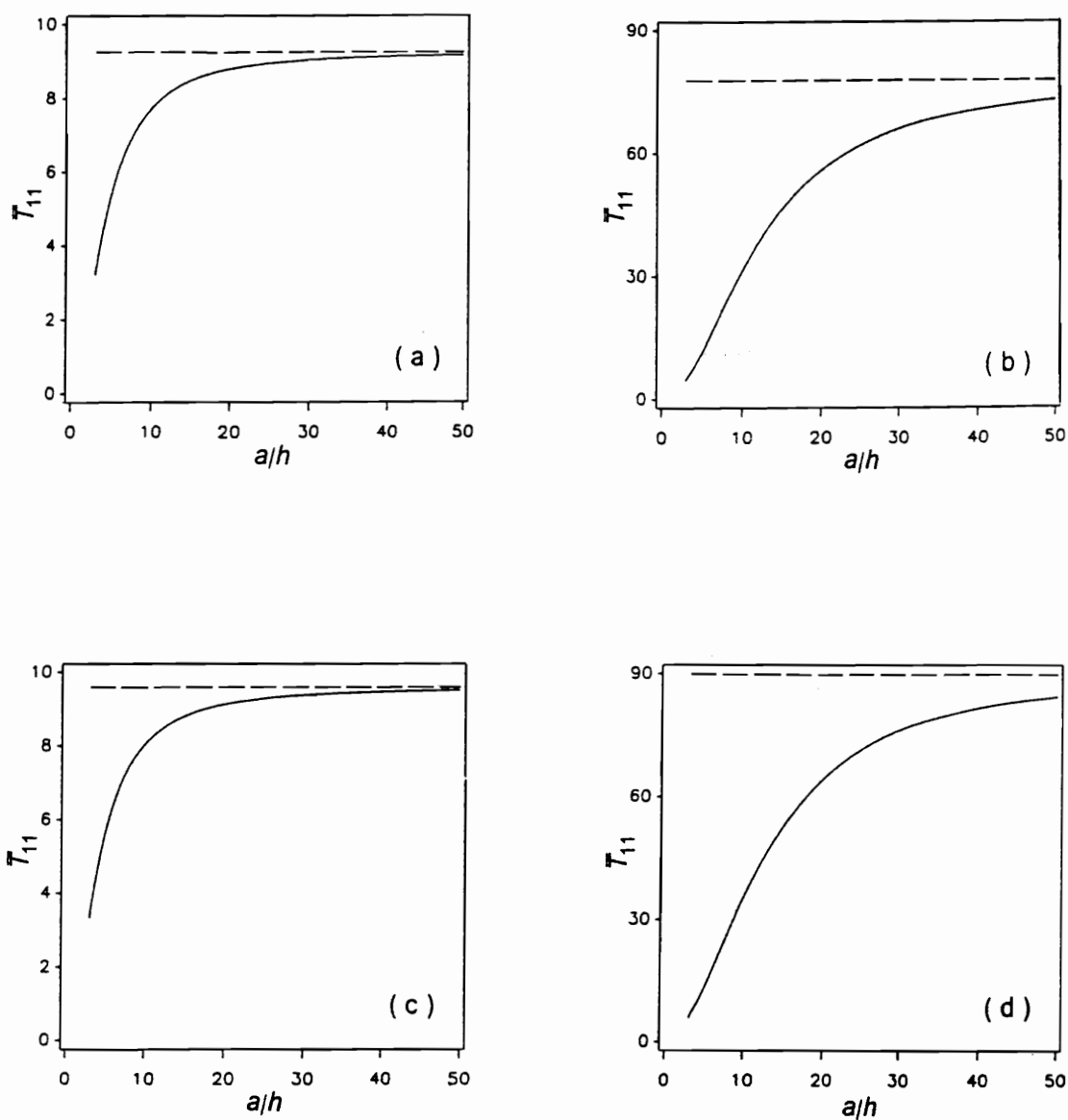


**Figure 3.7.** The effect of the dimensionless plate length ( $a/h$ ) on the dimensionless critical load  $\bar{T}_{11} = T_{11}a^2/E_2h^3$  for CC square plates obtained by using HSDT (—) and CPT (---): (a) 9-layered symmetric ( $E_1/E_2 = 2$ ), (b) 9-layered symmetric ( $E_1/E_2 = 40$ ), (c) 10-layered antisymmetric ( $E_1/E_2 = 2$ ), and (d) 10-layered antisymmetric ( $E_1/E_2 = 40$ ) plates.

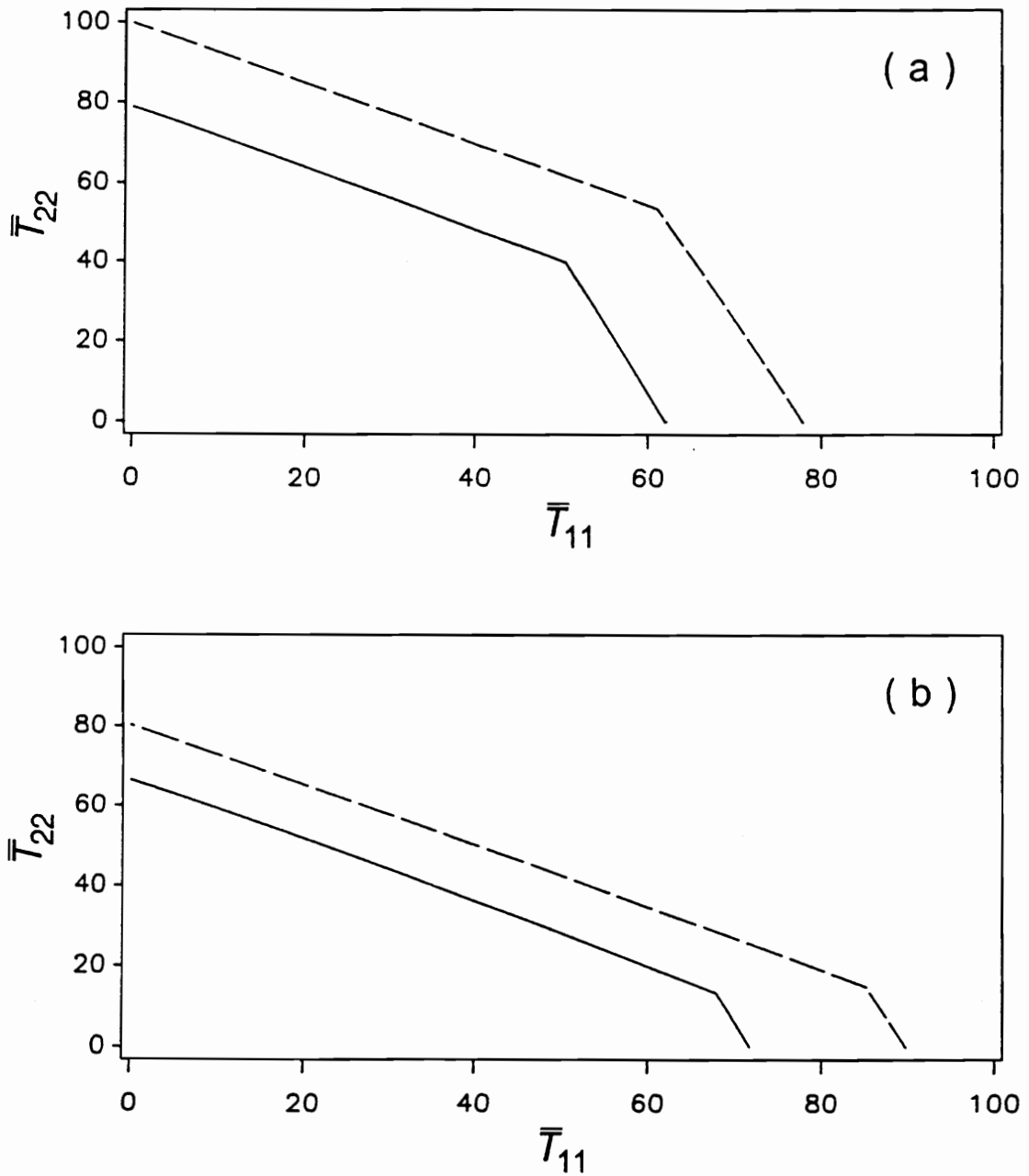


**Figure 3.8.** The relationship between the dimensionless critical loads  $\bar{T}_{ii} = T_{ii}a^2/E_2h^3$  in biaxial compressed CC square plates ( $a/h = 25, E_1/E_2 = 40$ ) obtained by using HSDT (—) and CPT (---): (a) 9-layered symmetric and (b) 10-layered antisymmetric plates.



## **4. MODAL INTERACTION IN THE RESPONSE OF COMPOSITE RECTANGULAR PLATES**

A composite plate whose elastic modulus is much larger than its shear modulus is weak in shear. The plate under transverse periodic loadings may encounter deflections the order of, or higher than, its thickness. Therefore, the use of linear classical plate theory to analyze the response of such plates might lead to serious errors, especially for thick laminated plates.

In this chapter, interaction of modes in composite plates is investigated by using the higher-order shear-deformation theory of Reddy and Bhimaraddi and Stevens. Rather than attacking the nonlinear partial-differential equations and nonlinear boundary conditions, we apply the method of multiple scales directly to the Lagrangian and derive nonlinear autonomous first-order ordinary-differential equations governing the modulation of the amplitudes and phases of the interacting modes. The fixed points of these equations are calculated and their stability is determined. Besides the one-mode solution, which is the directly excited mode,

multi-mode solutions are possible. In the latter case, the indirectly excited modes may dominate the response. For certain plate and excitation parameter values, Hopf bifurcations are possible. Near these bifurcations, limit-cycle solutions of the modulation equations are found. These limit-cycle solutions undergo a sequence of period-doubling bifurcations, leading to chaos. Consequently, the response of the composite plate to a harmonic load may be (a) a nonlinear single-mode periodic motion, (b) a nonlinear two-mode periodic motion (phase locking), (c) an amplitude- and phase-modulated (two-period quasi-periodic) motion (two torus), or (d) a chaotically modulated motion.

## 4.1. Solution Procedure

Using equations (2.29)-(2.34), one can express the linearized equations of motion in terms of the five original variables  $u, v, w, \phi$ , and  $\psi$  as

$$\begin{aligned}
 & A_{11} \frac{\partial^2 u}{\partial x^2} + 2A_{16} \frac{\partial^2 u}{\partial x \partial y} + A_{66} \frac{\partial^2 u}{\partial y^2} + A_{16} \frac{\partial^2 v}{\partial x^2} + (A_{12} + A_{66}) \frac{\partial^2 v}{\partial x \partial y} + A_{26} \frac{\partial^2 v}{\partial y^2} \\
 & + \hat{B}_{11} \frac{\partial^2 \phi}{\partial x^2} + 2\hat{B}_{16} \frac{\partial^2 \phi}{\partial x \partial y} + \hat{B}_{66} \frac{\partial^2 \phi}{\partial y^2} + \hat{B}_{16} \frac{\partial^2 \psi}{\partial x^2} + (\hat{B}_{12} + \hat{B}_{66}) \frac{\partial^2 \psi}{\partial x \partial y} + \hat{B}_{26} \frac{\partial^2 \psi}{\partial y^2} \\
 & - B_{11} \frac{\partial^3 w}{\partial x^3} - 3B_{16} \frac{\partial^3 w}{\partial x^2 \partial y} - (B_{12} + 2B_{66}) \frac{\partial^3 w}{\partial x \partial y^2} - B_{26} \frac{\partial^3 w}{\partial y^3} \\
 & = I_1 \frac{\partial^2 u}{\partial t^2} + \bar{I}_2 \frac{\partial^2 \phi}{\partial t^2} - I_2 \frac{\partial^3 w}{\partial x \partial t^2}
 \end{aligned} \tag{4.1}$$

$$\begin{aligned}
& A_{16} \frac{\partial^2 u}{\partial x^2} + (A_{12} + A_{66}) \frac{\partial^2 u}{\partial x \partial y} + A_{26} \frac{\partial^2 u}{\partial y^2} + A_{66} \frac{\partial^2 v}{\partial x^2} + 2A_{26} \frac{\partial^2 v}{\partial x \partial y} + A_{22} \frac{\partial^2 v}{\partial y^2} \\
& + \hat{B}_{16} \frac{\partial^2 \phi}{\partial x^2} + (\hat{B}_{12} + \hat{B}_{66}) \frac{\partial^2 \phi}{\partial x \partial y} + \hat{B}_{26} \frac{\partial^2 \phi}{\partial y^2} + \hat{B}_{66} \frac{\partial^2 \psi}{\partial x^2} + 2\hat{B}_{26} \frac{\partial^2 \psi}{\partial x \partial y} + \hat{B}_{22} \frac{\partial^2 \psi}{\partial y^2} \\
& - B_{16} \frac{\partial^3 w}{\partial x^3} - (B_{12} + 2B_{66}) \frac{\partial^3 w}{\partial x^2 \partial y} - 3B_{26} \frac{\partial^3 w}{\partial x \partial y^2} - B_{22} \frac{\partial^3 w}{\partial y^3} \\
& = I_1 \frac{\partial^2 v}{\partial t^2} + \bar{I}_2 \frac{\partial^2 \psi}{\partial t^2} - I_2 \frac{\partial^3 w}{\partial y \partial t^2}
\end{aligned} \tag{4.2}$$

$$\begin{aligned}
& B_{11} \frac{\partial^3 u}{\partial x^3} + 3B_{16} \frac{\partial^3 u}{\partial x^2 \partial y} + (B_{12} + 2B_{66}) \frac{\partial^3 u}{\partial x \partial y^2} + B_{26} \frac{\partial^3 u}{\partial y^3} + B_{16} \frac{\partial^3 v}{\partial x^3} + (B_{12} + 2B_{66}) \frac{\partial^3 v}{\partial x^2 \partial y} \\
& + 3B_{26} \frac{\partial^3 v}{\partial x \partial y^2} + B_{22} \frac{\partial^3 v}{\partial y^3} + \tilde{D}_{11} \frac{\partial^3 \phi}{\partial x^3} + 3\tilde{D}_{16} \frac{\partial^3 \phi}{\partial x^2 \partial y} + (\tilde{D}_{12} + 2\tilde{D}_{66}) \frac{\partial^3 \phi}{\partial x \partial y^2} + \tilde{D}_{26} \frac{\partial^3 \phi}{\partial y^3} \\
& + \tilde{D}_{16} \frac{\partial^3 \psi}{\partial x^3} + (\tilde{D}_{12} + 2\tilde{D}_{66}) \frac{\partial^3 \psi}{\partial x^2 \partial y} + 3\tilde{D}_{26} \frac{\partial^3 \psi}{\partial x \partial y^2} + \tilde{D}_{22} \frac{\partial^3 \psi}{\partial y^3} \\
& - D_{11} \frac{\partial^4 w}{\partial x^4} - 4D_{16} \frac{\partial^4 w}{\partial x^3 \partial y} - 2(D_{12} + 2D_{66}) \frac{\partial^4 w}{\partial x^2 \partial y^2} - 4D_{26} \frac{\partial^4 w}{\partial x \partial y^3} - D_{22} \frac{\partial^4 w}{\partial y^4} \\
& = -q + I_1 \frac{\partial^2 w}{\partial t^2} + I_2 \left( \frac{\partial^3 u}{\partial x \partial t^2} + \frac{\partial^3 v}{\partial y \partial t^2} \right) - I_3 \left( \frac{\partial^4 w}{\partial x^2 \partial t^2} + \frac{\partial^4 w}{\partial y^2 \partial t^2} \right) + \bar{I}_0 \left( \frac{\partial^3 \phi}{\partial x \partial t^2} + \frac{\partial^3 \psi}{\partial y \partial t^2} \right)
\end{aligned} \tag{4.3}$$

$$\begin{aligned}
& \hat{B}_{11} \frac{\partial^2 u}{\partial x^2} + 2\hat{B}_{16} \frac{\partial^2 u}{\partial x \partial y} + \hat{B}_{66} \frac{\partial^2 u}{\partial y^2} + \hat{B}_{16} \frac{\partial^2 v}{\partial x^2} + (\hat{B}_{12} + \hat{B}_{66}) \frac{\partial^2 v}{\partial x \partial y} + \hat{B}_{26} \frac{\partial^2 v}{\partial y^2} \\
& + \hat{D}_{11} \frac{\partial^2 \phi}{\partial x^2} + 2\hat{D}_{16} \frac{\partial^2 \phi}{\partial x \partial y} + \hat{D}_{66} \frac{\partial^2 \phi}{\partial y^2} + D_{45}^* \psi + \hat{D}_{16} \frac{\partial^2 \psi}{\partial x^2} + (\hat{D}_{12} + \hat{D}_{66}) \frac{\partial^2 \psi}{\partial x \partial y} + \hat{D}_{26} \frac{\partial^2 \psi}{\partial y^2} + D_{55}^* \phi \\
& - \tilde{D}_{11} \frac{\partial^3 w}{\partial x^3} - 3\tilde{D}_{16} \frac{\partial^3 w}{\partial x^2 \partial y} - (\tilde{D}_{12} + 2\tilde{D}_{66}) \frac{\partial^3 w}{\partial x \partial y^2} - \tilde{D}_{26} \frac{\partial^3 w}{\partial y^3} \\
& = \bar{I}_2 \frac{\partial^2 u}{\partial t^2} + \bar{I}_3 \frac{\partial^2 \phi}{\partial t^2} - \bar{I}_0 \frac{\partial^3 w}{\partial x \partial t^2}
\end{aligned} \tag{4.4}$$

$$\begin{aligned}
& \hat{B}_{16} \frac{\partial^2 u}{\partial x^2} + (\hat{B}_{12} + \hat{B}_{33}) \frac{\partial^2 u}{\partial x \partial y} + \hat{B}_{26} \frac{\partial^2 u}{\partial y^2} + \hat{B}_{66} \frac{\partial^2 v}{\partial x^2} + 2\hat{B}_{26} \frac{\partial^2 v}{\partial x \partial y} + \hat{B}_{22} \frac{\partial^2 v}{\partial y^2} \\
& + \hat{D}_{16} \frac{\partial^2 \phi}{\partial x^2} + (\hat{D}_{12} + \hat{D}_{66}) \frac{\partial^2 \phi}{\partial x \partial y} + \hat{D}_{26} \frac{\partial^2 \phi}{\partial y^2} + D_{45}^* \phi + \hat{D}_{66} \frac{\partial \psi}{\partial x^2} + 2\hat{D}_{26} \frac{\partial^2 \psi}{\partial x \partial y} + \hat{D}_{22} \frac{\partial^2 \psi}{\partial y^2} + D_{44}^* \psi \\
& - \tilde{D}_{16} \frac{\partial^3 w}{\partial x^3} - (\tilde{D}_{12} + 2\tilde{D}_{66}) \frac{\partial^3 w}{\partial x^2 \partial y} - 3\tilde{D}_{26} \frac{\partial^3 w}{\partial x \partial y^2} - \tilde{D}_{22} \frac{\partial^3 w}{\partial y^3} \\
& = \bar{I}_2 \frac{\partial^2 v}{\partial t^2} + \bar{I}_3 \frac{\partial^2 \psi}{\partial t^2} - \bar{I}_0 \frac{\partial^3 w}{\partial y \partial t^2}
\end{aligned} \tag{4.5}$$

The general solution of equations (4.1)-(4.5) can be expressed in the form

$$u = \sum_{m=1}^{\infty} \sum_{n=1}^{\infty} \hat{C}_{mn}(T_1) \hat{g}_{1mn}(x, y) e^{i\bar{\omega}_{mn}T_0} + cc \tag{4.6a}$$

$$v = \sum_{m=1}^{\infty} \sum_{n=1}^{\infty} \hat{C}_{mn}(T_1) \hat{g}_{2mn}(x, y) e^{i\bar{\omega}_{mn}T_0} + cc \tag{4.6b}$$

$$w = \sum_{m=1}^{\infty} \sum_{n=1}^{\infty} \hat{C}_{mn}(T_1) \hat{g}_{3mn}(x, y) e^{i\bar{\omega}_{mn}T_0} + cc \tag{4.6c}$$

$$\phi = \sum_{m=1}^{\infty} \sum_{n=1}^{\infty} \hat{C}_{mn}(T_1) \hat{g}_{4mn}(x, y) e^{i\bar{\omega}_{mn}T_0} + cc \tag{4.6d}$$

$$\psi = \sum_{m=1}^{\infty} \sum_{n=1}^{\infty} \hat{C}_{mn}(T_1) \hat{g}_{5mn}(x, y) e^{i\bar{\omega}_{mn}T_0} + cc \tag{4.6e}$$

where  $T_0$  and  $T_1$  are fast and slow time scales, respectively, the  $\bar{\omega}_{mn}$  are the natural frequencies, the  $\hat{C}_{mn}(T_1)$  are complex functions of  $T_1$ , and cc stands for the complex conjugate of the preceding terms.

Using equations (2.1), (2.4), (2.11), (2.12), and (2.15), we can rewrite the Lagrangian (2.19) as

$$\begin{aligned}
 L = & \frac{1}{2} \int_0^b \int_0^a \left\{ I_1 \left[ \left( \frac{\partial u}{\partial t} \right)^2 + \left( \frac{\partial v}{\partial t} \right)^2 + \left( \frac{\partial w}{\partial t} \right)^2 \right] \right. \\
 & + I_3 \left[ \left( \frac{\partial^2 w}{\partial x \partial t} \right)^2 + \left( \frac{\partial^2 w}{\partial y \partial t} \right)^2 \right] + \bar{I}_3 \left[ \left( \frac{\partial^2 \phi}{\partial x \partial t} \right)^2 + \left( \frac{\partial^2 \psi}{\partial y \partial t} \right)^2 \right] \\
 & + 2\bar{I}_2 \left[ \frac{\partial u}{\partial t} \frac{\partial \phi}{\partial t} + \frac{\partial v}{\partial t} \frac{\partial \psi}{\partial t} \right] - 2\bar{I}_0 \left[ \frac{\partial^2 w}{\partial x \partial t} \frac{\partial \phi}{\partial t} + \frac{\partial^2 w}{\partial y \partial t} \frac{\partial \psi}{\partial t} \right] \\
 & \left. - 2I_2 \left[ \frac{\partial^2 w}{\partial x \partial t} \frac{\partial u}{\partial t} + \frac{\partial^2 w}{\partial y \partial t} \frac{\partial v}{\partial t} \right] \right\} dx dy \\
 & - \frac{1}{2} \int_0^b \int_0^a \{ N_1 \varepsilon_1^0 + N_2 \varepsilon_2^0 + N_6 \varepsilon_6^0 + M_1 \kappa_1^0 + M_2 \kappa_2^0 + M_6 \kappa_6^0 \\
 & + P_1 \kappa_1^2 + P_2 \kappa_2^2 + P_6 \kappa_6^2 + Q_1 \varepsilon_5^0 + Q_2 \varepsilon_4^0 + R_1 \kappa_5^2 + R_2 \kappa_4^2 \} dx dy \\
 & + \int_0^b \int_0^a q w dx dy
 \end{aligned} \tag{4.7}$$

The Lagrangian can be further expressed in terms of the five original variables  $u, v, w, \phi$ , and  $\psi$  by using equations (2.4), (2.16), and (2.17). We substitute equations (4.6) into the Lagrangian (4.7), integrate over the domain, average the result over the fast time scale, and obtain the averaged Lagrangian (Nayfeh, 1973). Writing down the Euler-Lagrange equations yields the desired modulation equations. Miles (1984a) and Balachandran and Nayfeh (1990) have also used this procedure to obtain a first-order approximation.

## 4.2. Autoparametric Resonance

A two-to-one autoparametric resonance may occur when one linear natural frequency of the plate is approximately twice another. As an example, we consider a simply-supported 9.45" x 15.75" antisymmetric cross-ply plate made of eight identical orthotropic layers with a total thickness of one inch. The properties of each layer are

$$\begin{aligned} E_1 &= 19.2 \times 10^6 \text{ psi}, & E_2 &= 1.56 \times 10^6 \text{ psi}, & G_{12} &= G_{13} = 0.82 \times 10^6 \text{ psi}, \\ G_{23} &= 0.523 \times 10^6 \text{ psi}, & \nu_{12} &= \nu_{13} = 0.24, & \rho &= 1.2 \times 10^{-4} \text{ lb} - \text{s}^2/\text{in}^4 \end{aligned}$$

The stacking sequence is  $[90^\circ/0/90^\circ/0/90^\circ/0/90^\circ/0]$ . Because of this special stacking sequence, some of plate inertias and stiffness coefficients vanish, namely,

$$I_2 = I_4 = \bar{I}_2 = 0$$

$$\begin{aligned} A_{16} &= A_{26} = A_{45} = B_{12} = B_{16} = B_{26} = B_{66} = D_{16} = D_{26} = D_{45} \\ &= E_{12} = E_{16} = E_{26} = E_{66} = F_{16} = F_{26} = F_{45} = H_{16} = H_{26} = 0 \end{aligned}$$

In this case, the  $\hat{g}_{kmn}(x,y)$  in equations (4.6) become

$$\hat{g}_{1mn}(x,y) = \Gamma_{1mn} \cos \frac{m\pi x}{a} \sin \frac{n\pi y}{b} \quad (4.8a)$$

$$\hat{g}_{2mn}(x,y) = \Gamma_{2mn} \sin \frac{m\pi x}{a} \cos \frac{n\pi y}{b} \quad (4.8b)$$

$$\hat{g}_{3mn}(x,y) = \Gamma_{3mn} \sin \frac{m\pi x}{a} \sin \frac{n\pi y}{b} \quad (4.8c)$$

$$\hat{g}_{4mn}(x,y) = \Gamma_{4mn} \cos \frac{m\pi x}{a} \sin \frac{n\pi y}{b} \quad (4.8d)$$

$$\hat{g}_{5mn}(x,y) = \Gamma_{5mn} \sin \frac{m\pi x}{a} \cos \frac{n\pi y}{b} \quad (4.8e)$$

where the  $\Gamma_{kmn}$  are real constants. Equations (4.6) and (4.8) satisfy all the boundary conditions. Substituting equations (4.6) and (4.8) into the linearized equations of motion yields

$$\begin{aligned} & (\hat{\alpha}_m^2 A_{11} + \hat{\beta}_n^2 A_{66}) \Gamma_{1mn} + \hat{\alpha}_m \hat{\beta}_n (A_{12} + A_{66}) \Gamma_{2mn} - \hat{\alpha}_m^3 B_{11} \Gamma_{3mn} + \hat{\alpha}_m^2 \hat{B}_{11} \Gamma_{4mn} \\ & = \bar{\omega}_{mn}^2 I_1 \Gamma_{1mn} \end{aligned} \quad (4.9)$$

$$\begin{aligned} & \hat{\alpha}_m \hat{\beta}_n (A_{12} + A_{66}) \Gamma_{1mn} + (\hat{\alpha}_m^2 A_{66} + \hat{\beta}_n^2 A_{22}) \Gamma_{2mn} - \hat{\beta}_n^3 B_{22} \Gamma_{3mn} + \hat{\beta}_n^2 \hat{B}_{22} \Gamma_{5mn} \\ & = \bar{\omega}_{mn}^2 I_1 \Gamma_{2mn} \end{aligned} \quad (4.10)$$

$$\begin{aligned} & \hat{\alpha}_m^3 B_{11} \Gamma_{1mn} + \hat{\beta}_n^3 B_{22} \Gamma_{2mn} - [\hat{\alpha}_m^4 D_{11} + \hat{\beta}_n^4 D_{22} + 2\hat{\alpha}_m^2 \hat{\beta}_n^2 (D_{12} + 2D_{66})] \Gamma_{3mn} \\ & + [\hat{\alpha}_m^3 \tilde{D}_{11} + \hat{\alpha}_m \hat{\beta}_n^2 (\tilde{D}_{12} + 2\tilde{D}_{66})] \Gamma_{4mn} + [\hat{\beta}_n^3 \tilde{D}_{22} + \hat{\alpha}_m^2 \hat{\beta}_n (\tilde{D}_{12} + 2\tilde{D}_{66})] \Gamma_{5mn} \\ & = \bar{\omega}_{mn}^2 \left\{ - [I_1 + (\hat{\alpha}_m^2 + \hat{\beta}_n^2) I_3] \Gamma_{3mn} \right. \\ & \quad \left. + \hat{\alpha}_m \bar{I}_0 \Gamma_{4mn} + \hat{\beta}_n \bar{I}_0 \Gamma_{5mn} \right\} \end{aligned} \quad (4.11)$$

$$\begin{aligned} & \hat{\alpha}_m^2 \hat{B}_{11} \Gamma_{1mn} - [\hat{\alpha}_m^3 \tilde{D}_{11} + \hat{\alpha}_m \hat{\beta}_n^2 (\tilde{D}_{12} + 2\tilde{D}_{66})] \Gamma_{3mn} \\ & + (\hat{\alpha}_m^2 \hat{D}_{11} + \hat{\beta}_n^2 \hat{D}_{66} - D_{55}^*) \Gamma_{4mn} + \hat{\alpha}_m \hat{\beta}_n (\hat{D}_{12} + \hat{D}_{66}) \Gamma_{5mn} \\ & = \bar{\omega}_{mn}^2 (-\hat{\alpha}_m \bar{I}_0 \Gamma_{3mn} + \bar{I}_3 \Gamma_{4mn}) \end{aligned} \quad (4.12)$$

$$\begin{aligned} & \hat{\beta}_n^2 \hat{B}_{22} \Gamma_{2mn} - [\hat{\beta}_n^3 \tilde{D}_{22} + \hat{\alpha}_m^2 \hat{\beta}_n (\tilde{D}_{12} + 2\tilde{D}_{66})] \Gamma_{3mn} \\ & + \hat{\alpha}_m \hat{\beta}_n (\hat{D}_{12} + \hat{D}_{66}) \Gamma_{4mn} + (\hat{\alpha}_m^2 \hat{D}_{66} + \hat{\beta}_n^2 \hat{D}_{22} - D_{44}^*) \Gamma_{5mn} \\ & = \bar{\omega}_{mn}^2 (-\hat{\beta}_n \bar{I}_0 \Gamma_{3mn} + \bar{I}_3 \Gamma_{5mn}) \end{aligned} \quad (4.13)$$

where

$$\hat{\alpha}_m = \frac{m\pi}{a} \quad \text{and} \quad \hat{\beta}_n = \frac{n\pi}{b}$$

Requiring the  $\Gamma_{kmn}$  to be nontrivial yields the frequencies  $\bar{\omega}_{mn}$ . They are listed in Table 4.1.

For the plate under investigation, we note that  $\bar{\omega}_{13} \approx 2\bar{\omega}_{31}$ . In this study, we consider a uniform periodic external transverse load  $q = F \cos(\Omega t)$  with constant amplitude  $F$  when the excitation frequency  $\Omega$  is near  $\bar{\omega}_{13}$ .

Because all of the modes which are not directly excited by the load or indirectly excited by the internal resonance decay with time owing to the presence of damping, the plate response consists of only the two modes that are involved in the internal resonance. To simplify the notation, we denote the modes 31 and 13 by modes 1 and 2, respectively. Hence, we express the displacement field as

$$\begin{bmatrix} u \\ v \\ w \\ \phi \\ \psi \end{bmatrix} = \begin{bmatrix} g_{11} \\ g_{21} \\ g_{31} \\ g_{41} \\ g_{51} \end{bmatrix} C_1(T_1) e^{i\omega_1 T_0} + \begin{bmatrix} g_{12} \\ g_{22} \\ g_{32} \\ g_{42} \\ g_{52} \end{bmatrix} C_2(T_1) e^{i\omega_2 T_0} + cc \quad (4.14)$$

where

$$g_{k1} = \hat{g}_{k31}, \quad g_{k2} = \hat{g}_{k13}, \quad C_1 = \hat{C}_{31}, \quad C_2 = \hat{C}_{13}, \quad \omega_1 = \bar{\omega}_{31}, \quad \omega_2 = \bar{\omega}_{13}$$

Next, we introduce the detuning parameters  $\sigma_1$  and  $\sigma_2$  defined according to

$$\sigma_1 = \omega_2 - 2\omega_1 \quad \text{and} \quad \sigma_2 = \Omega - \omega_2 \quad (4.15)$$



Plugging equations (4.14) into the Lagrangian and averaging the result yields

$$\begin{aligned} \langle L \rangle = & -2i\alpha_3\bar{C}_1C_1' - 2i\alpha_4\bar{C}_2C_2' + \alpha_1C_1\bar{C}_1 + \alpha_2C_2\bar{C}_2 - \alpha_6C_1^2\bar{C}_1^2 \\ & - \alpha_7C_2^2\bar{C}_2^2 - \alpha_8C_1\bar{C}_1C_2\bar{C}_2 - \alpha_5C_1^2\bar{C}_2e^{-i\sigma_1T_1} + F\alpha_0\bar{C}_2e^{i\sigma_2T_1} + cc \end{aligned} \quad (4.16)$$

where the expressions for the  $\alpha_i$  are greatly reduced for antisymmetric cross-ply laminated plates and are given in Appendix E. Next, we express the  $C_k$  in polar and cartesian forms and derive the modulation equations in both forms.

#### 4.2.1. Polar form

The expression for the  $C_k$  in polar form is

$$C_k = \frac{1}{2} a_k e^{i\beta_k} \quad (k = 1, 2) \quad (4.17)$$

where the  $a_k$  and  $\beta_k$  are real function of  $T_1$ . Substituting equation (4.17) into equation (4.16), one obtains

$$\begin{aligned} \langle L \rangle = & \alpha_3 a_1^2 \beta_1' + \alpha_4 a_2^2 \beta_2' - \frac{1}{8} (\alpha_6 a_1^4 + \alpha_7 a_2^4 + \alpha_8 a_1^2 a_2^2) \\ & - \frac{1}{4} \alpha_5 a_1^2 a_2 \cos(\sigma_1 T_1 + \beta_2 - 2\beta_1) + \alpha_0 F a_2 \cos(\sigma_2 T_1 - \beta_2) \end{aligned} \quad (4.18)$$

Writing the Euler-Lagrange equations corresponding to the averaged Lagrangian (4.18) and adding linear viscous damping terms, we obtain

$$a_1' = -\mu_1 a_1 - \Lambda_1 a_1 a_2 \sin \gamma_1 \quad (4.19a)$$

$$a_2' = -\mu_2 a_2 + \Lambda_2 a_1^2 \sin \gamma_1 + F \Lambda_0 \sin \gamma_2 \quad (4.19b)$$

$$a_1 \beta_1' = \Lambda_3 a_1^3 + \Lambda_5 a_1 a_2^2 + \Lambda_1 a_1 a_2 \cos \gamma_1 \quad (4.19c)$$

$$a_2 \beta_2' = \Lambda_4 a_2^3 + \Lambda_6 a_1^2 a_2 + \Lambda_2 a_1^2 \cos \gamma_1 - F \Lambda_0 \cos \gamma_2 \quad (4.19d)$$

where  $\mu_1$  and  $\mu_2$  are the damping coefficients of the first and second modes, respectively, the  $\Lambda_k$  are real constants defined by

$$\begin{aligned} \Lambda_0 &= \frac{\alpha_0}{2\alpha_4}, \quad \Lambda_1 = \frac{\alpha_5}{4\alpha_3}, \quad \Lambda_2 = \frac{\alpha_5}{8\alpha_4}, \quad \Lambda_3 = \frac{\alpha_6}{4\alpha_3} \\ \Lambda_4 &= \frac{\alpha_7}{4\alpha_4}, \quad \Lambda_5 = \frac{\alpha_8}{8\alpha_3}, \quad \Lambda_6 = \frac{\alpha_8}{8\alpha_4} \end{aligned} \quad (4.20)$$

and

$$\gamma_1 = \sigma_1 T_1 + \beta_2 - 2\beta_1 \quad \text{and} \quad \gamma_2 = \sigma_2 T_1 - \beta_2 \quad (4.21)$$

It is convenient to rewrite equations (4.19) in terms of scaled variables. The scaled variables, denoted by overhats, are defined as follows:

$$\begin{aligned} \hat{\omega}_j &= \omega_j \tau, \quad \hat{\sigma}_j = \sigma_j \tau, \quad \hat{\mu}_j = \mu_j \tau, \quad \hat{a}_j = a_j / \ell, \quad (j = 1, 2) \\ \hat{T}_1 &= T_1 / \tau, \quad \hat{F} = F \Lambda_0 \tau / \ell \\ \hat{\Lambda}_j &= \Lambda_j \tau \ell, \quad (j = 1, 2) \\ \hat{\Lambda}_j &= \Lambda_j \tau \ell^2, \quad (j = 3, 4, 5, 6) \end{aligned} \quad (4.22)$$

where  $\tau = a(b/h)\sqrt{\rho/E_2}$  and  $\ell = h^3/ab$ . Substituting these definitions into equations (4.19) and dropping the overhats in the final result, we obtain

$$a_1' = -\mu_1 a_1 - \Lambda_1 a_1 a_2 \sin \gamma_1 \quad (4.23a)$$

$$a_2' = -\mu_2 a_2 + \Lambda_2 a_1^2 \sin \gamma_1 + F \sin \gamma_2 \quad (4.23b)$$

$$a_1 \beta_1' = \Lambda_1 a_1 a_2 \cos \gamma_1 + \Lambda_3 a_1^3 + \Lambda_5 a_1 a_2^2 \quad (4.23c)$$

$$a_2 \beta_2' = \Lambda_2 a_1^2 \cos \gamma_1 + \Lambda_4 a_2^3 + \Lambda_6 a_1^2 a_2 - F \cos \gamma_2 \quad (4.23d)$$

where the prime denotes the derivative with respect to the scaled  $T_1$ .

#### 4.2.2. Cartesian form

The expression for the  $C_k$  in cartesian form is

$$C_k = \frac{1}{2} (p_k + i q_k) e^{i \theta_k} \quad (k = 1, 2) \quad (4.24)$$

where the  $p_k$  and  $q_k$  are real function of  $T_1$  and

$$\theta_1 = \frac{1}{2} (\sigma_1 + \sigma_2) T_1 \quad (4.25a)$$

$$\theta_2 = \sigma_2 T_1 \quad (4.25b)$$

Substituting equations (4.24) and (4.25) into equation (4.16), one obtains

$$\begin{aligned} \langle L \rangle = & \alpha_3 [p_1 q_1' - p_1' q_1 + (p_1^2 + q_1^2) \theta_1'] + \alpha_4 [p_2 q_2' - p_2' q_2 + (p_2^2 + q_2^2) \theta_2'] \\ & - \frac{\alpha_5}{4} [p_2 (p_1^2 - q_1^2) + 2 p_1 q_1 q_2] - \frac{\alpha_6}{8} (p_1^2 + q_1^2)^2 - \frac{\alpha_7}{8} (p_2^2 + q_2^2)^2 \\ & - \frac{\alpha_8}{8} (p_1^2 + q_1^2) (p_2^2 + q_2^2) + \alpha_0 F p_2 \end{aligned} \quad (4.26)$$

Writing the Euler-Lagrange equations corresponding to the averaged Lagrangian (4.26), and adding linear viscous damping terms, we obtain

$$\begin{aligned} \dot{p}_1 = & -\mu_1 p_1 + \frac{1}{2}(\sigma_1 + \sigma_2)q_1 - \Lambda_1(p_1 q_2 - p_2 q_1) \\ & - \Lambda_3 q_1(p_1^2 + q_1^2) - \Lambda_5 q_1(p_2^2 + q_2^2) \end{aligned} \quad (4.27a)$$

$$\begin{aligned} \dot{q}_1 = & -\mu_1 q_1 - \frac{1}{2}(\sigma_1 + \sigma_2)p_1 + \Lambda_1(p_1 p_2 + q_1 q_2) \\ & + \Lambda_3 p_1(p_1^2 + q_1^2) + \Lambda_5 p_1(p_2^2 + q_2^2) \end{aligned} \quad (4.27b)$$

$$\begin{aligned} \dot{p}_2 = & -\mu_2 p_2 + \sigma_2 q_2 - 2\Lambda_2 p_1 q_1 - \Lambda_4 q_2(p_2^2 + q_2^2) \\ & - \Lambda_6 q_2(p_1^2 + q_1^2) \end{aligned} \quad (4.27c)$$

$$\begin{aligned} \dot{q}_2 = & -\mu_2 q_2 - \sigma_2 p_2 + \Lambda_2(p_1^2 - q_1^2) + \Lambda_4 p_2(p_2^2 + q_2^2) \\ & + \Lambda_6 p_2(p_1^2 + q_1^2) - \Lambda_0 F \end{aligned} \quad (4.27d)$$

These autonomous equations could have been also obtained from equations (4.19) by the following transformation

$$p_k = a_k \cos(\beta_k - \theta_k) \quad (k = 1, 2) \quad (4.28a)$$

$$q_k = a_k \sin(\beta_k - \theta_k) \quad (k = 1, 2) \quad (4.28b)$$

The new scaled variables  $\hat{p}_k$  and  $\hat{q}_k$  defined by

$$\hat{p}_k = p_k/\ell, \quad \hat{q}_k = q_k/\ell \quad (k = 1, 2) \quad (4.29)$$

and equations (4.22) are used to scale equations (4.27). Dropping the overhats in the scaled equations, we obtain

$$\begin{aligned} \dot{p}_1 = & -\mu_1 p_1 + \frac{1}{2}(\sigma_1 + \sigma_2)q_1 - \Lambda_1(p_1 q_2 - p_2 q_1) \\ & - \Lambda_3 q_1(p_1^2 + q_1^2) - \Lambda_5 q_1(p_2^2 + q_2^2) \end{aligned} \quad (4.30a)$$

$$\begin{aligned} q_1' = & -\mu_1 q_1 - \frac{1}{2}(\sigma_1 + \sigma_2)p_1 + \Lambda_1(p_1 p_2 + q_1 q_2) \\ & + \Lambda_3 p_1(p_1^2 + q_1^2) + \Lambda_5 p_1(p_2^2 + q_2^2) \end{aligned} \quad (4.30b)$$

$$\begin{aligned} p_2' = & -\mu_2 p_2 + \sigma_2 q_2 - 2\Lambda_2 p_1 q_1 - \Lambda_4 q_2(p_2^2 + q_2^2) \\ & - \Lambda_6 q_2(p_1^2 + q_1^2) \end{aligned} \quad (4.30c)$$

$$\begin{aligned} q_2' = & -\mu_2 q_2 - \sigma_2 p_2 + \Lambda_2(p_1^2 - q_1^2) + \Lambda_4 p_2(p_2^2 + q_2^2) \\ & + \Lambda_6 p_2(p_1^2 + q_1^2) - F \end{aligned} \quad (4.30d)$$

### 4.3. Numerical Results

Here, we consider the simply-supported antisymmetric cross-ply laminated plate whose material properties and geometric configurations are given in Section 4.2. The corresponding scaled values of  $\Lambda_k$ ,  $\omega_j$ , and  $\sigma_1$  are calculated and the results are

$$\begin{aligned} \Lambda_1 &= 2.876192 \times 10^{-4}, \quad \Lambda_2 = 7.219099 \times 10^{-5}, \quad \Lambda_3 = 2.843552 \times 10^{-3}, \\ \Lambda_4 &= 9.96887 \times 10^{-3}, \quad \Lambda_5 = 2.621421 \times 10^{-3}, \quad \Lambda_6 = 1.315927 \times 10^{-3}, \\ \omega_1 &= 34.585, \quad \omega_2 = 69.001, \quad \sigma_1 = -0.169 \end{aligned}$$

The value of  $0.969 \times 10^{-3}$  is used for the scaled values of both  $\mu_1$  and  $\mu_2$ . The fixed-points of equations (4.30) represent periodic solutions of equations (2.22)-(2.26). The nonlinear algebraic equations governing the fixed-points can be obtained from equations (4.30) by setting their right-hand sides equal to zero. Setting the  $p_k'$  and  $q_k'$  equal to zero we obtain the following set of four algebraic equations governing the fixed-points

$$\begin{aligned}
& -\mu_1 p_1 + \frac{1}{2}(\sigma_1 + \sigma_2)q_1 - \Lambda_1(p_1 q_2 - p_2 q_1) - \Lambda_3 q_1(p_1^2 + q_1^2) \\
& - \Lambda_5 q_1(p_2^2 + q_2^2) = 0
\end{aligned} \tag{4.31a}$$

$$\begin{aligned}
& -\mu_1 q_1 - \frac{1}{2}(\sigma_1 + \sigma_2)p_1 + \Lambda_1(p_1 p_2 + q_1 q_2) + \Lambda_3 p_1(p_1^2 + q_1^2) \\
& + \Lambda_5 p_1(p_2^2 + q_2^2) = 0
\end{aligned} \tag{4.31b}$$

$$-\mu_2 p_2 + \sigma_2 q_2 - 2\Lambda_2 p_1 q_1 - \Lambda_4 q_2(p_2^2 + q_2^2) - \Lambda_6 q_2(p_1^2 + q_1^2) = 0 \tag{4.31c}$$

$$-\mu_2 q_2 - \sigma_2 p_2 + \Lambda_2(p_1^2 - q_1^2) + \Lambda_4 p_2(p_2^2 + q_2^2) + \Lambda_6 p_2(p_1^2 + q_1^2) - F = 0 \tag{4.31d}$$

The stability of a fixed-point of equations (4.30) is determined by investigating the behavior of small perturbation to it. Expanding equations (4.30) in Taylor series about the fixed-point solution and linearizing the results yields the associated Jacobian matrix  $\mathbf{J}_1$ . The elements of  $\mathbf{J}_1$  are listed in Appendix F. The fixed-point is asymptotically stable if the real part of every eigenvalue of the Jacobian matrix is negative and it is unstable if the real part of at least one eigenvalue is positive. All the other cases are degenerate and the Jacobian matrix alone is inconclusive in the stability analysis. In a degenerate case more terms in the Taylor series expansions of equations (4.30) should be retained.

By inspection we note that  $p_1 = q_1 = 0$  is a solution of equations (4.31). Therefore, a single-mode solution is possible and is treated separately.

### 4.3.1. Single-mode solutions

In a single-mode solution ( $p_1 = q_1 = 0$ ), equations (4.31) can be reduced to

$$-\mu_2(p_2^2 + q_2^2) - Fq_2 = 0 \quad (4.32a)$$

$$\sigma_2(p_2^2 + q_2^2) - \Lambda_4(p_2^2 + q_2^2)^2 + Fp_2 = 0 \quad (4.32b)$$

Using equations (4.21), (4.25), and (4.28), one can transform equations (4.32) into

$$-\mu_2 a_2 + F \sin \gamma_2 = 0 \quad (4.33a)$$

$$a_2 \sigma_2 - \Lambda_4 a_2^3 + F \cos \gamma_2 = 0 \quad (4.33b)$$

Eliminating  $\gamma_2$  from equations (4.33), we obtain the force- and frequency-response equations

$$F^2 = (a_2 \mu_2)^2 + a_2^2 (\sigma_2 - \Lambda_4 a_2^2)^2 \quad (4.34a)$$

$$\sigma_2 = \Lambda_4 a_2^2 \pm [(F/a_2)^2 - \mu_2^2]^{1/2} \quad (4.34b)$$

The eigenvalues  $\lambda$  of the Jacobian matrix  $\mathbf{J}_1$  in the single-mode case  $p_1 = q_1 = 0$  are the roots of the following algebraic equation

$$\left\{ (\mu_1 + \lambda)^2 - \Lambda_1^2 (p_2^2 + q_2^2) + \left[ \frac{1}{2} (\sigma_1 + \sigma_2) - \Lambda_5 (p_2^2 + q_2^2) \right]^2 \right\} [(\mu_2 + \lambda)^2 + \sigma_2^2 - 4\sigma_2 \Lambda_4 (p_2^2 + q_2^2) + 3\Lambda_4^2 (p_2^2 + q_2^2)^2] = 0 \quad (4.35)$$

The necessary and sufficient conditions for the real parts of all four eigenvalues to be negative are

$$\mu_1^2 - \Lambda_1^2(p_2^2 + q_2^2) + \left[ \frac{1}{2}(\sigma_1 + \sigma_2) - \Lambda_5(p_2^2 + q_2^2) \right]^2 > 0 \quad (4.36a)$$

$$\mu_2^2 + \sigma_2^2 + 3\Lambda_4^2(p_2^2 + q_2^2)^2 - 4\sigma_2\Lambda_4(p_2^2 + q_2^2) > 0 \quad (4.36b)$$

Inequalities (4.36) can be transformed into polar form as

$$\mu_1^2 - \Lambda_1^2 a_2^2 + \left[ \frac{1}{2}(\sigma_1 + \sigma_2) - \Lambda_5 a_2^2 \right]^2 > 0 \quad (4.37a)$$

$$\mu_2^2 + (\sigma_2 - \Lambda_4 a_2^2)(\sigma_2 - 3\Lambda_4 a_2^2) > 0 \quad (4.37b)$$

Therefore a fixed-point solution is stable if and only if inequalities (4.37) are satisfied.

A typical frequency-response curve is shown in Figure 4.1a. This curve resembles the frequency-response curve of a hardening spring. The solid lines represent stable solutions and the broken lines represent unstable solutions. A typical force-response curve is shown in Figure 4.1b. Here only the upper and lower branches are stable and there are two turning points: one at  $F = 0.0096$  and the other at  $F = 3.6771$ . There is only one unstable solution branch. In both Figures 4.1a and 4.1b the stable branches lose stability at turning points. At each turning point one of the real eigenvalues of the Jacobian matrix  $\mathbf{J}$ , crosses the imaginary axis to the right half of the complex plane. These turning points are clearly saddle-node bifurcation points. Here, the only way that the one-mode response can go from one stable branch to the other stable branch is through a jump (Nayfeh and Mook, 1979).



### 4.3.2. Two-modes solutions

#### 4.3.2.1. Fixed point solutions of the averaged equations and their stability

When  $a_1 \neq 0$  we solve equations (4.21) in scaled form for the  $\beta_k'$ , substitute them into equations (4.23), and rewrite the results in the following autonomous form:

$$a_1' = -\mu_1 a_1 - \Lambda_1 a_1 a_2 \sin \gamma_1 \quad (4.38a)$$

$$a_2' = -\mu_2 a_2 + \Lambda_2 a_1^2 \sin \gamma_1 + F \sin \gamma_2 \quad (4.38b)$$

$$\gamma_1' = \sigma_1 - F \frac{\cos \gamma_2}{a_2} + \Lambda_2 a_1^2 \frac{\cos \gamma_1}{a_2} - 2\Lambda_1 a_2 \cos \gamma_1 + (\Lambda_6 - 2\Lambda_3) a_1^2 + (\Lambda_4 - 2\Lambda_5) a_2^2 \quad (4.38c)$$

$$\gamma_2' = \sigma_2 + F \frac{\cos \gamma_2}{a_2} - \Lambda_2 a_1^2 \frac{\cos \gamma_1}{a_2} - \Lambda_4 a_2^2 - \Lambda_6 a_1^2 \quad (4.38d)$$

Setting the right hand side of equations (4.38) equal to zero, we obtain a set of four nonlinear algebraic equations governing the fixed-points as follows

$$-\mu_1 a_1 - \Lambda_1 a_1 a_2 \sin \gamma_1 = 0 \quad (4.39a)$$

$$-\mu_2 a_2 + \Lambda_2 a_1^2 \sin \gamma_1 + F \sin \gamma_2 = 0 \quad (4.39b)$$

$$\sigma_1 - F \frac{\cos \gamma_2}{a_2} + (\Lambda_2 a_1^2 - 2\Lambda_1 a_2^2) \frac{\cos \gamma_1}{a_2} + (\Lambda_6 - 2\Lambda_3) a_1^2 + (\Lambda_4 - 2\Lambda_5) a_2^2 = 0 \quad (4.39c)$$

$$\sigma_2 + F \frac{\cos \gamma_2}{a_2} - \Lambda_2 a_1^2 \frac{\cos \gamma_1}{a_2} - \Lambda_4 a_2^2 - \Lambda_6 a_1^2 = 0 \quad (4.39d)$$

Unfortunately, unlike equations (4.33), equations (4.39) can not be solved in closed form and we resort to numerical techniques. A Newton-Raphson method is used but the method is found to be extremely sensitive to the initial guesses. As an alternative, a homotopy based routine in Hompack (Watson et al., 1987) is used. For several pairs of values of  $\sigma_2$  and  $F$  the homotopy technique is applied until a set of zeros of equations (4.39) is obtained. Since homotopy alone is expensive, once the roots of equations (4.39) for a particular pair of  $\sigma_2$  and  $F$  are found, the roots for other values of  $\sigma_2$  and  $F$  can be obtained by integrating equations (4.39) along either  $\sigma_2$  or  $F$  or both.

The frequency-response curves are shown in Figures 4.2 and 4.3. First a set of real solutions (with  $a_1 > 0$  and  $a_2 > 0$ ) of equations (4.39) are obtained by using homotopy. Then these solutions are used as initial conditions for the integration of equations (4.39) along  $\sigma_2$ . The homotopy is applied periodically to check the accuracy of integration and the possibility of evolution of new branches. This check is done repeatedly near a turning point. However, the homotopy based routine is expected to fail at a turning point. Therefore, continuation techniques are used to avoid failure at turning points.

Expanding equations (4.38) in Taylor series about the fixed-point solution and linearizing the results yields the associated Jacobian matrix  $\mathbf{J}_2$ . The elements of  $\mathbf{J}_2$  are listed in Appendix F.

The stability of each branch is determined from the eigenvalues of the Jacobian matrix  $\mathbf{J}_2$ . A fixed-point is asymptotically stable if the corresponding real parts of all eigenvalues of the Jacobian matrix  $\mathbf{J}_2$  are negative. In the frequency-response curves of Figures 4.2 and 4.3, besides the stable branch which begins at  $\sigma_2 = 0.67$ , there is another stable branch between the two turning points at  $\sigma_2 = 0.97$  and  $\sigma_2 = 1.15$ , connecting two unstable branches. As  $\sigma_2$  is increased, there remain only

one stable and three unstable branches, which are shown for only  $\sigma_2 < 5$  due to the fact that when the detuning parameter becomes large the perturbation solution loses its accuracy.

The amplitudes  $a_1$  and  $a_2$  of the steady-state response for the two-mode solution as functions of  $F$  are shown in Figures 4.4 and 4.5, respectively. Two-mode solutions exist only when  $0.01 < F < 7.01$ . There are exactly two stable branches. One of them starts from a turning point at  $F = 0.01$  and continues to the point  $F = 7.01$  at which  $a_1$  decays to zero while  $a_2$  increases to its corresponding one-mode solution. The other stable branch starts from a turning point at  $F = 2.307$  and continues until  $F$  exceeds the critical value  $F = 2.8424$ . Beyond this value, a pair of complex eigenvalues of the Jacobian of equations (4.38) transversely crosses the imaginary axis to the right-hand side of the complex plane. Thus, the solutions undergo a Hopf bifurcation (Seydel, 1988) at  $F = 2.8424$ . Near this Hopf bifurcation point, limit-cycle solutions of the modulation equations are expected.

#### **4.3.2.2. Periodic solutions of the averaged equations and their stability**

The stability of the periodic solutions of equations (4.38) is determined by using Floquet theory (Nayfeh and Mook, 1979). If we define  $\vec{\chi} = \{a_1, a_2, \gamma_1, \gamma_2\}^T$ , then we can write equations (4.38) as

$$\vec{\chi}' = \vec{G}[\vec{\chi}(T_1); F] \quad (4.40)$$

In the above representation, the amplitude of the external excitation  $F$  is the only control parameter that can be varied in studying the periodic solutions. To determine

the stability of a T-periodic limit cycle  $\vec{\chi}^*(T_1) = \vec{\chi}^*(T_1 + T)$ , we superimpose on it a small disturbance  $\vec{\theta}(T_1)$  and obtain the perturbed equation

$$\vec{\chi}^{**} + \vec{\theta}' = \vec{G}[\vec{\chi}^*(T_1) + \vec{\theta}(T_1)] \quad (4.41)$$

Expanding equation (4.41) in a Taylor series for small  $\vec{\theta}(T_1)$  and linearizing the flow of the vector field in (4.40) about the periodic orbit, we obtain the linear variational equation

$$\vec{\theta}' = A(T_1)\vec{\theta} \quad (4.42)$$

where

$$A(T_1) = \frac{\partial \vec{G}}{\partial \vec{\chi}} [\vec{\chi}^*(T_1)] \quad (4.43)$$

is a square 4x4 variational matrix with T-periodic elements. We let  $\Theta(T_1)$  be the fundamental-matrix solution satisfying

$$\Theta' = A(T_1)\Theta, \quad \Theta(0) = I \quad (4.44)$$

Then, the Floquet multipliers are the eigenvalues of the monodromy matrix  $\Theta(T)$ . As the control parameter F is varied, the positions of the multipliers relative to the unit circle in the complex plane determine the stability of the orbit. Because equations (4.38) are autonomous, one of the multipliers is always +1, corresponding to  $\vec{\theta}(T_1)$  along the trajectory  $\vec{\chi}^*(T_1)$ , while the others describe what happens perpendicular to it. If all the other multipliers lie inside the unit circle, then the orbit is asymptotically stable. If one of the multipliers leaves the unit circle, then the orbit is unstable. The type of the resulting bifurcation depends on the way a multiplier leaves the unit circle.

There are three generic ways in which this happens. First, a multiplier leaves the unit circle through  $+1$ , resulting in either a cyclic-fold (tangent) or pitchfork (symmetry-breaking) bifurcation. Second, a multiplier leaves the unit circle through  $-1$ , resulting in a flip or period-doubling bifurcation. Third, two complex conjugate multipliers leave the unit circle, resulting in a Hopf bifurcation. In our computer simulations, we observe period-doubling bifurcations associated with one of the three multipliers crossing the unit circle at  $-1$  on the real axis while the other two remain inside the unit circle.

To describe the dynamics of the system (4.38), we need to determine the steady-state periodic waveforms (attractors). It is computationally inefficient to determine these solutions by conventional numerical-integration methods. Therefore, we use an algorithm originally proposed by Aprille and Trick (1972) to eliminate transient responses, thereby latching onto a limit cycle and calculating its period. The algorithm uses a combination of a numerical integration scheme and a Newton-Raphson iteration procedure. This algorithm proved to be efficient in reducing the computation time but it is sensitive to the initial guesses and the step size of the integration.

Spectral analysis techniques are used to look for cyclical patterns or periodicities in signals. The algorithm developed by Cooley and Tukey (1965) and implemented by Singleton (1969) is used to compute the fast Fourier transform (FFT).

Next, we investigate local bifurcations of the periodic solutions of the modulation equations and the existence of chaotic attractors using the amplitude of the external excitation  $F$  as a control parameter. Below the Hopf bifurcation value  $F = 2.8424$ , the modulation equations possess only fixed-point solutions. As  $F$  is increased beyond  $F = 2.8424$ , the modulation equations possess a sequence of period-doubling solutions. In Figure 4.6a, we show a two-dimensional projection onto the  $a_1 - a_2$  plane

of a typical period-1 attractor at  $F = 2.84286$ . The time evolution of the amplitude  $a_1$  is shown in Figure 4.6b. The power spectrum of this attractor shown in Figure 4.6c is made up of a major peak at the fundamental frequency  $1/T$  and smaller peaks at its harmonics. As  $F$  is increased further, the period one attractor evolves smoothly. At  $F = 2.84296$ , the period one attractor loses its stability and undergoes a period-doubling bifurcation with one of its Floquet multipliers leaving the unit circle through -1. As a result, a period-2 attractor is born. Figures 4.7a-c depict this attractor. As  $F$  is increased further, a cascade of period-doubling bifurcations take place culminating into chaos at  $F = 2.843006$ .

The projections of period-2, 4, 8, and 16 attractors onto the  $a_1 - a_2$  plane along with their corresponding time evolutions and power spectra are shown in Figures 4.7, 4.8, 4.9, and 4.10, respectively.

The phase portrait displayed in Figure 4.11a demonstrates two important characteristics of the chaotic attractor: its irregular nature and the sensitive dependence on the initial conditions. The trajectories, therefore, converge toward some well-defined geometrical structure in the state space. The waveform in Figure 11b shows that the attractor is never periodic, nor almost periodic. In terms of the frequency content, the Fourier transform of the  $a_1$  signal in Figure 4.11c has a broadband component. The values of the  $F_k$  corresponding to the  $k$ th period-doubling bifurcation and the ratio of their successive differences,  $\Delta_k = \frac{F_{k+1} - F_k}{F_{k+2} - F_{k+1}}$  are calculated as follows:

$$F_1 = 2.842959564 \quad F_2 = 2.843000385 \quad F_3 = 2.843005118 \quad F_4 = 2.843005696$$

$$F_5 = 2.843005779 \quad F_6 = 2.843005794 \quad F_7 = 2.843005747$$

$$\Delta_1 = 8.63 \quad \Delta_2 = 8.18 \quad \Delta_3 = 7.01$$

$$\Delta_4 = 5.46 \quad \Delta_5 = 4.73$$

It is obvious that  $\Delta_k$  is approaching the Feigenbaum number 4.66920 as it is expected to be for any road to chaos through period-doubling bifurcations.

The algorithm for the determination of the limit cycle solutions and their stability shows that each new limit cycle stays stable over a range of the amplitude of external excitation  $F$  smaller than the range of stability of the preceding limit cycle. Consequently, there is a limit to the sequence of period-doubling bifurcations after which the system becomes chaotic (irregular). This leads us to check the compatibility of our results with the Feigenbaum number (1979).

The Lyapunov exponents are computed and used to quantify the expansion and contraction occurring in the chaotic attractor. The algorithm proposed by Wolf et al. (1985) is used to calculate the Lyapunov exponents. They are found to be 0.0018, 0.0000, -0.0032, and -0.0044. The positive exponent indicates an exponential divergence of neighboring trajectories and thus confirms the chaotic nature of the attractor. The Lyapunov dimension  $d_L$  of the attractor is also calculated using the relation proposed by Frederickson et al. (1983). Accordingly the Lyapunov dimension is  $d_L = 2.5572$ .

**Table 4.1.** The nondimensional frequencies  $\hat{\omega}_{mn} = \bar{\omega}_{mn} \frac{ab}{h} \sqrt{\rho/E_2}$ .

	n=1	n=2	n=3	n=4	n=5	n=6	n=7
m=1	12.553	37.945	69.001	101.512	134.486	167.852	201.761
m=2	20.439	41.962	71.619	103.479	136.084	169.213	202.956
m=3	34.585	51.036	77.608	107.882	139.571	172.111	205.445
m=4	51.824	64.425	87.239	115.136	145.339	176.890	209.523
m=5	70.424	80.437	99.817	125.032	153.366	183.600	215.271
m=6	89.624	97.882	114.461	137.082	163.397	192.111	222.626
m=7	109.114	116.134	130.505	150.799	175.118	202.228	231.466
m=8	128.783	134.894	147.523	165.804	188.247	213.752	241.657
m=9	148.610	154.028	165.268	181.827	202.557	226.514	253.077
m=10	168.614	173.487	183.600	198.690	217.876	240.372	265.618
m=11	188.826	193.260	202.444	216.275	234.082	255.217	279.193
m=12	209.283	213.355	221.762	234.509	251.084	270.963	293.729
m=13	230.023	233.790	241.539	253.345	268.821	287.543	309.166
m=14	251.082	254.589	261.771	272.756	287.248	304.911	325.458
m=15	272.493	275.774	282.466	292.727	306.337	323.027	342.568
m=16	294.288	297.370	303.631	313.252	326.067	341.867	360.467
m=17	316.495	319.399	325.281	334.330	346.428	361.410	379.133
m=18	339.140	341.885	347.427	355.964	367.412	381.643	398.547
m=19	362.247	364.847	370.085	378.161	389.017	402.556	418.697
m=20	385.838	388.304	393.267	400.925	411.242	424.142	439.571



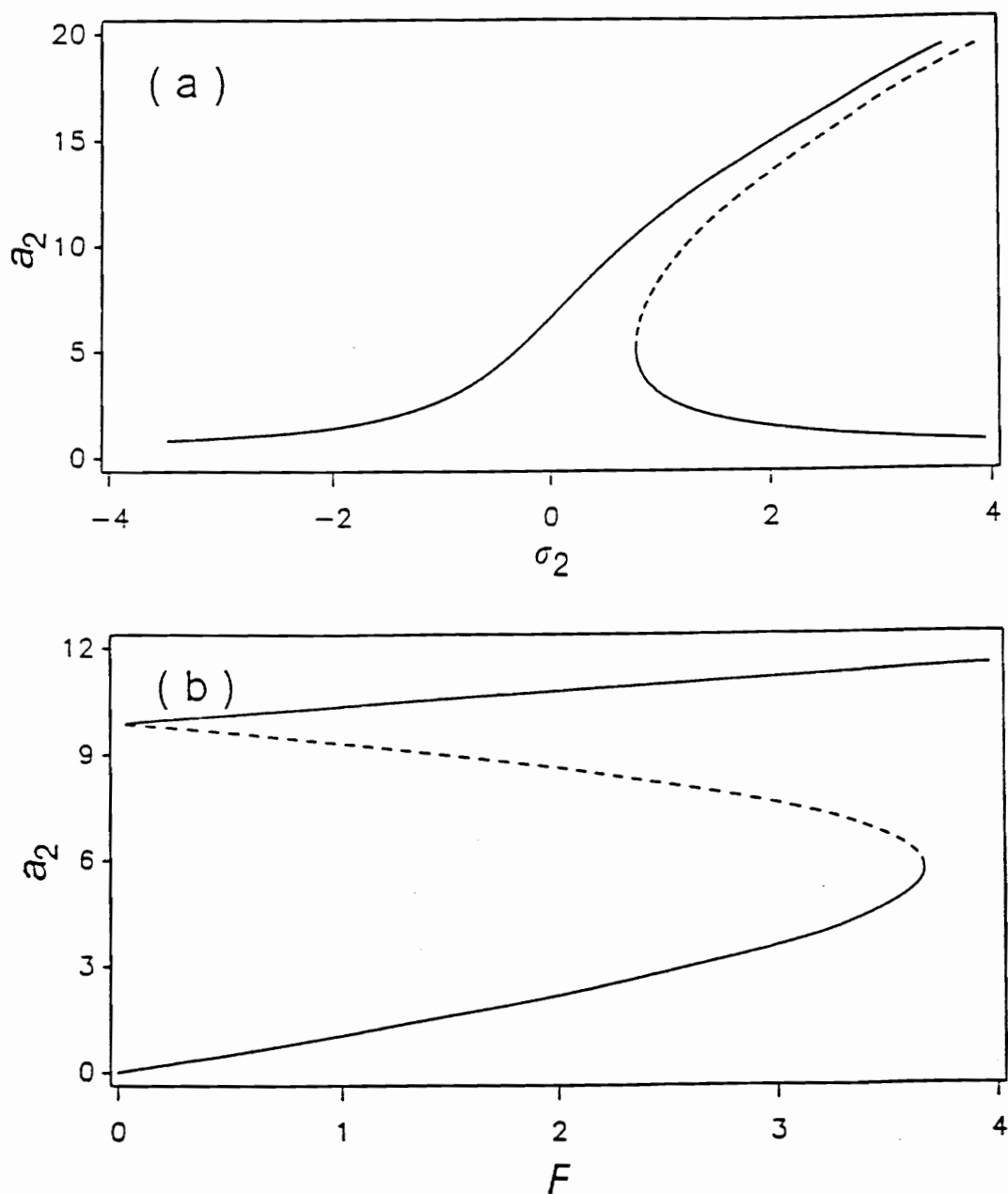


**Figure 4.1.** Variation of the steady-state amplitude for the case of one-mode solution when  $\Omega \approx \omega_2$  and  $\mu = 0.969 \times 10^{-3}$  with (a) the detuning of the excitation for  $F = 2.843$  and (b) the amplitude of the excitation for  $\sigma_2 = 0.969$ : —, stable; - - -, unstable.

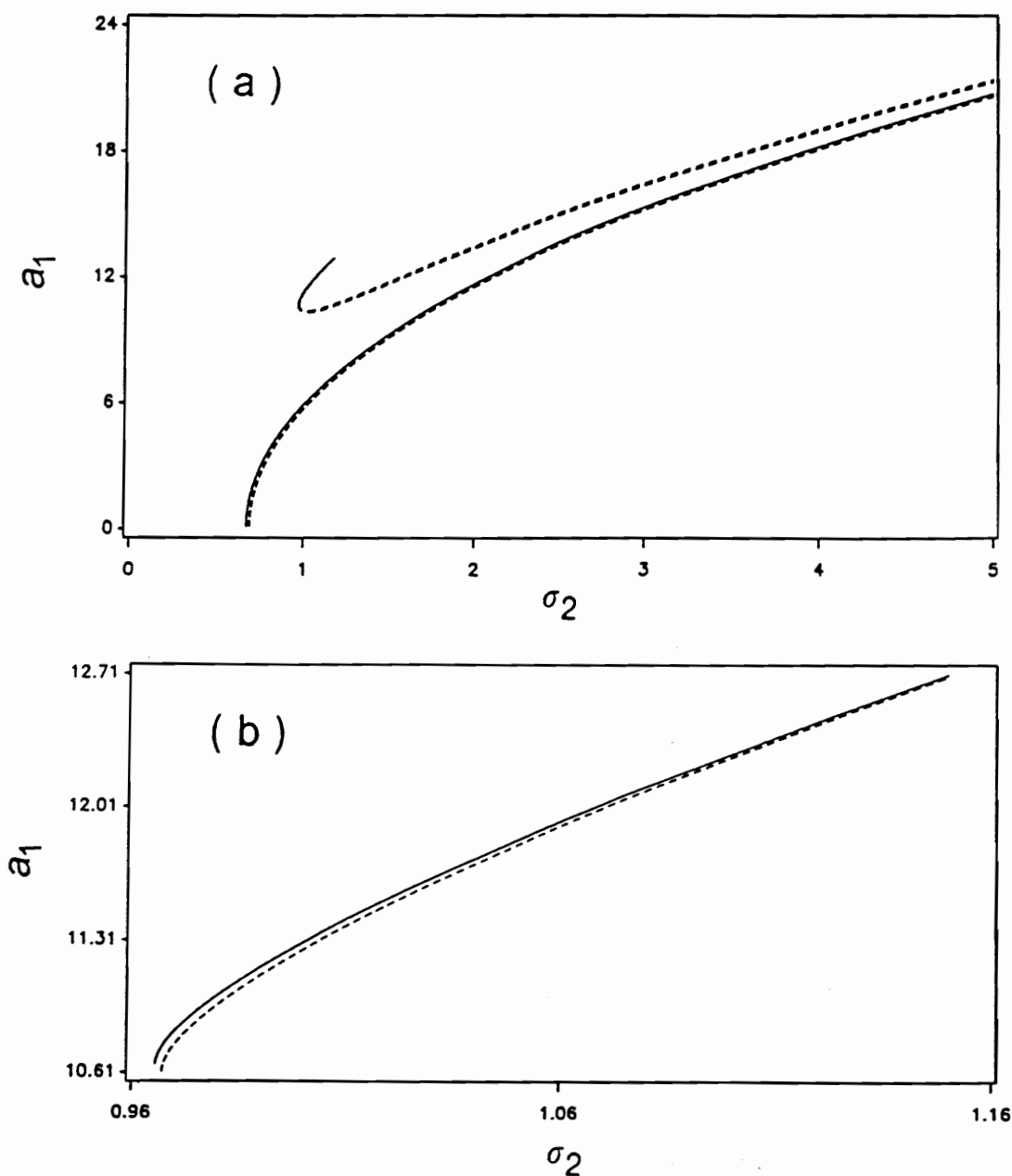


**Figure 4.2.** (a) The amplitude  $a_1$  of the steady-state response for the two-mode solution as a function of the detuning of the excitation for  $F = 2.843$ ; (b) an enlargement of the upper branches in (a) —, stable; - - -, unstable:  $\mu = 0.969 \times 10^{-3}$ .

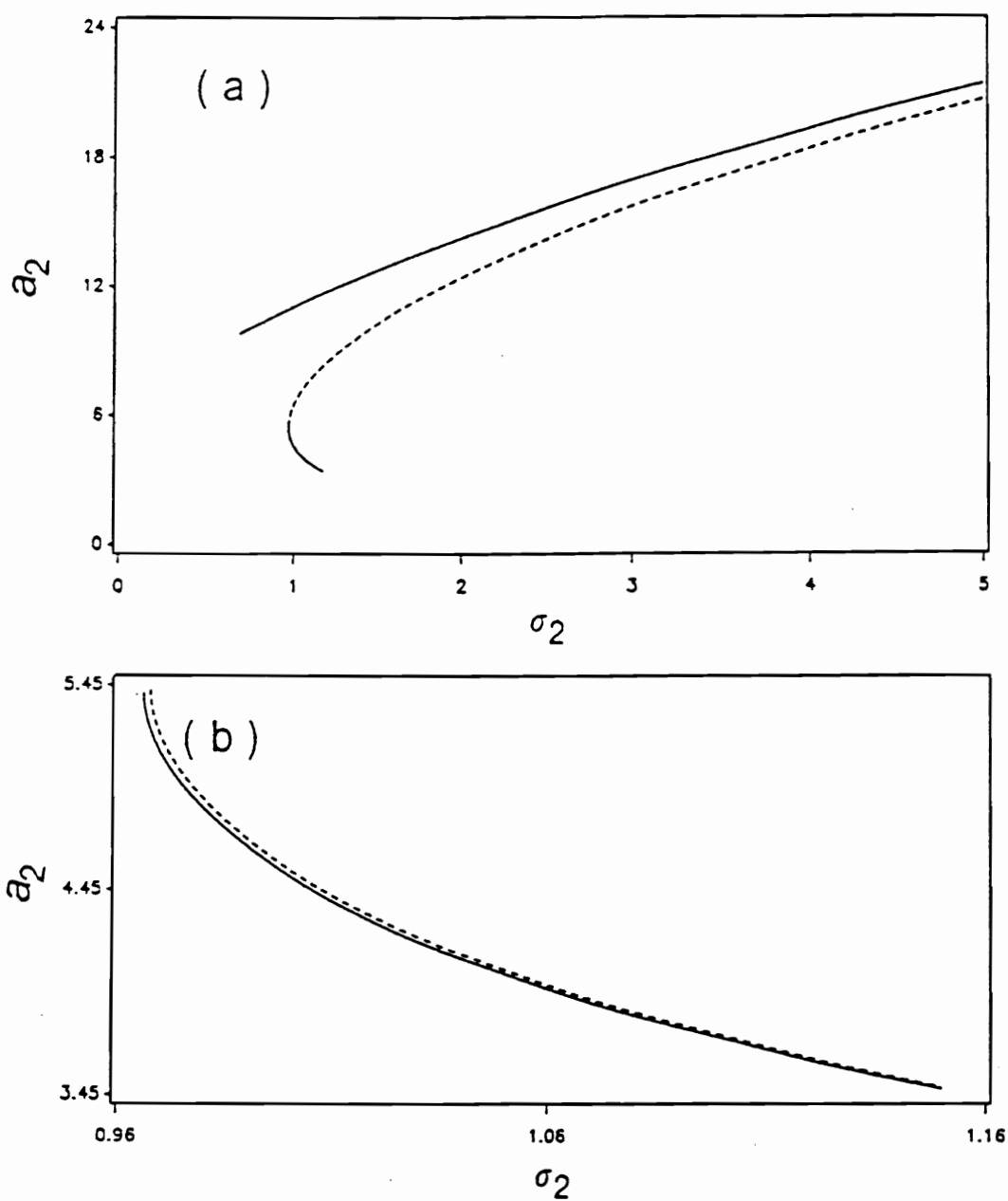


**Figure 4.3.** (a) The amplitude  $a_2$  of the steady-state response for the two-mode solution as a function of the detuning of the excitation for  $F = 2.843$ ; (b) an enlargement of the lower branches in (a) —, stable; - - -, unstable:  $\mu = 0.969 \times 10^{-3}$ .

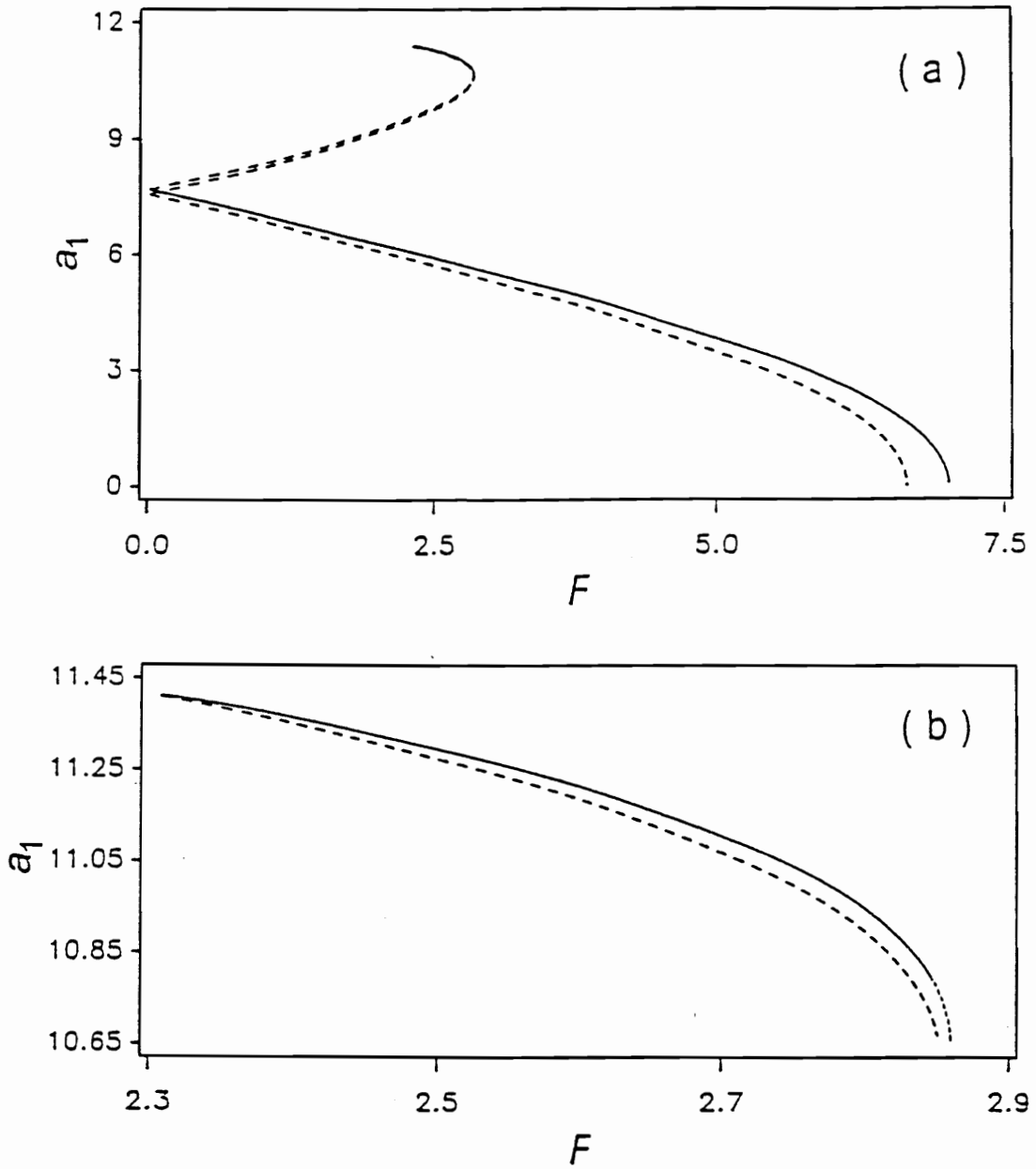


**Figure 4.4.** (a) The amplitude  $a_1$  of the steady-state response for the two-mode solution as a function of the amplitude of the excitation for  $\sigma_2 = 0.969$ ; (b) an enlargement of the upper branches in (a) —, stable; ---, unstable with real eigenvalues; ....., unstable with the real part of a complex conjugate pair of eigenvalues being positive:  $\mu = 0.969 \times 10^{-3}$ .

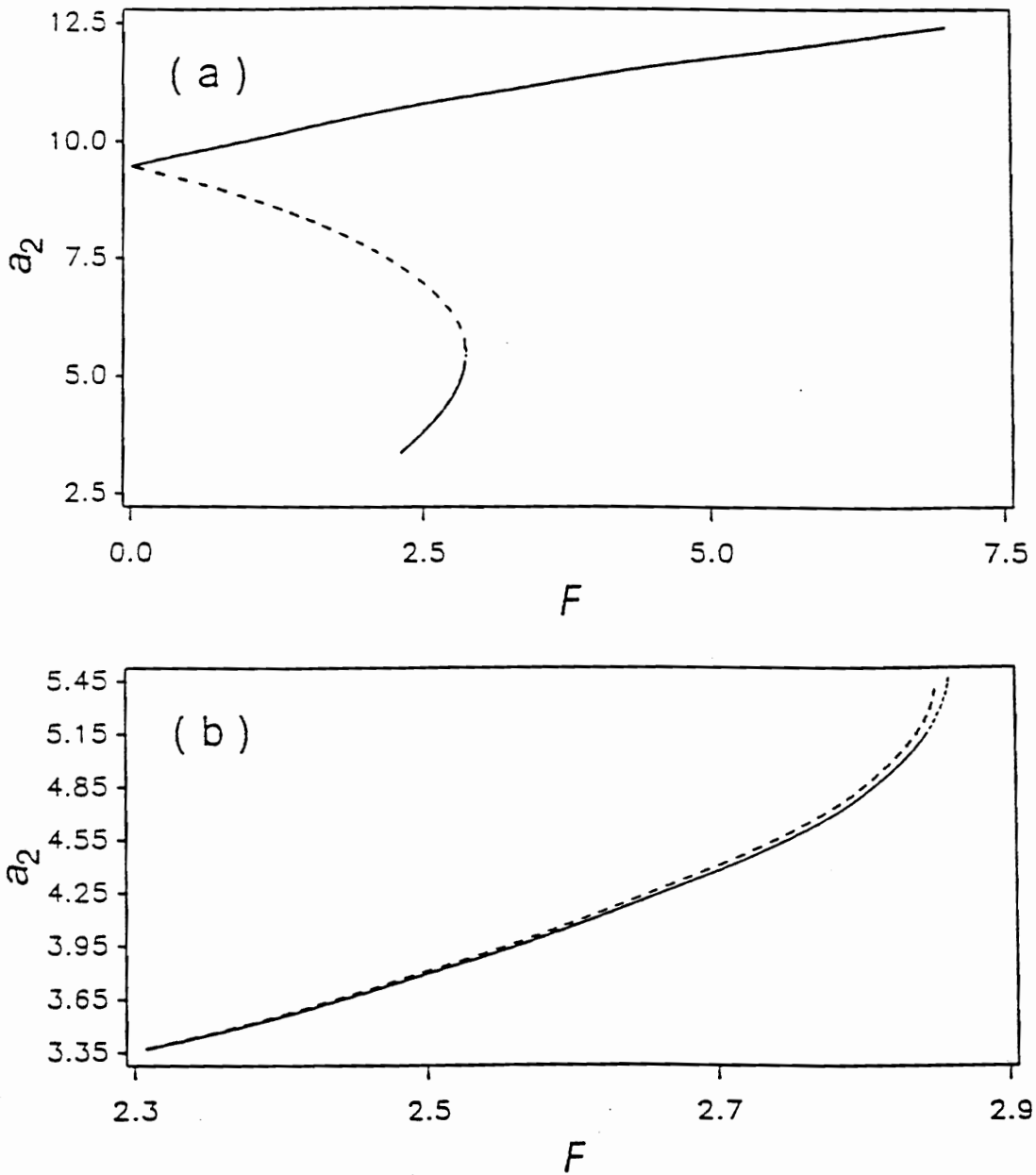


**Figure 4.5.** (a) The amplitude  $a_2$  of the steady-state response for the two-mode solution as a function of the amplitude of excitation for  $\sigma_2 = 0.969$ ; (b) an enlargement of the lower branches in (a) —, stable; ---, unstable with real eigenvalues; ....., unstable with the real part of a complex conjugate pair of eigenvalues being positive:  $\mu = 0.969 \times 10^{-3}$ .

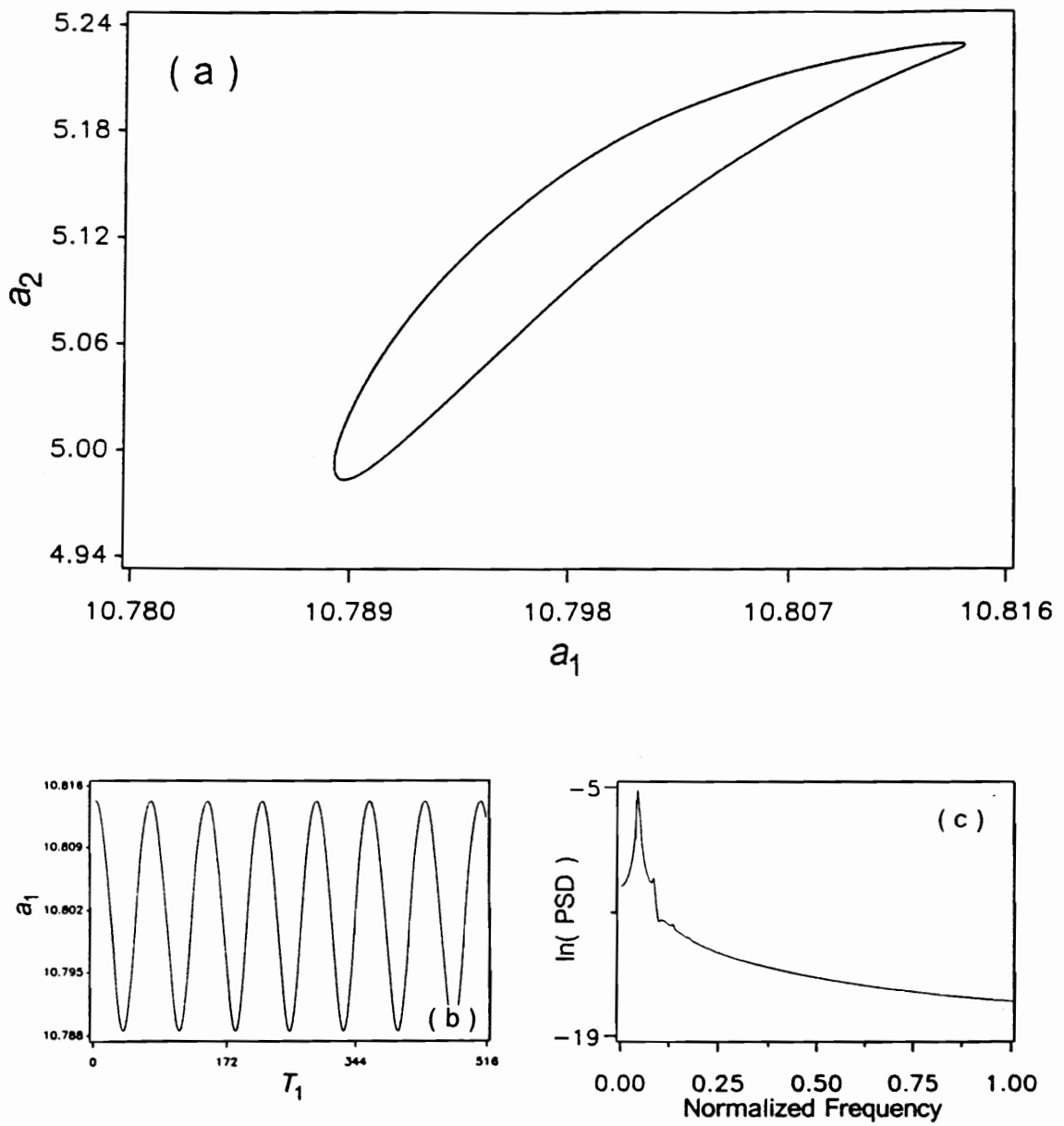


**Figure 4.6.** (a) Projection of the period-one limit-cycle on the  $a_1 - a_2$  plane; (b) the time evolution of  $a_1$ ; (c) FFT of the response:  $\mu = 0.969 \times 10^{-3}$ ;  $\sigma_2 = 0.969$ ;  $F = 2.84286$ .

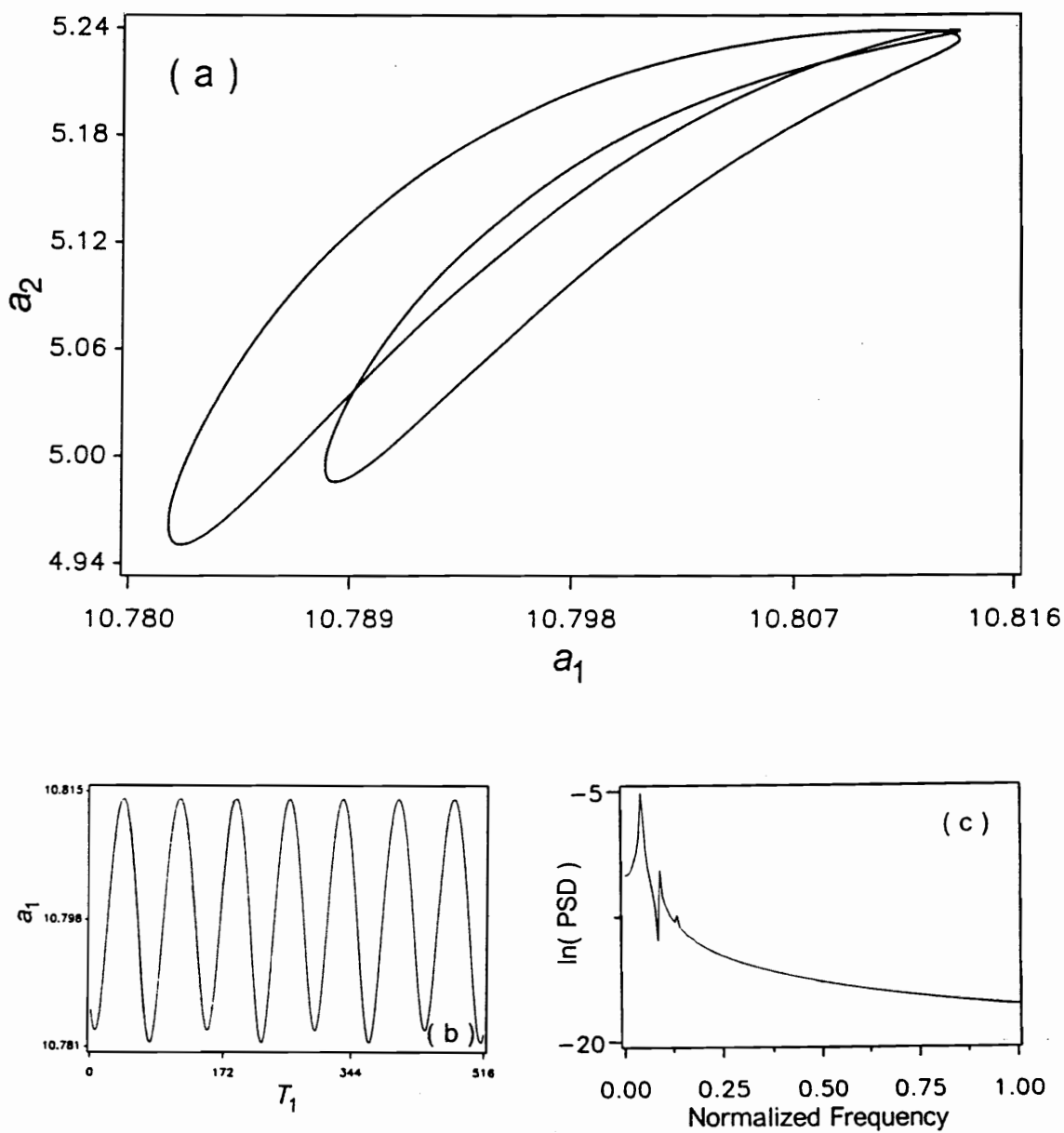


**Figure 4.7.** (a) Projection of the period-two limit-cycle on the  $a_1 - a_2$  plane; (b) the time evolution of  $a_1$ ; (c) FFT of the response:  $\mu = 0.969 \times 10^{-3}$ ;  $\sigma_2 = 0.969$ ;  $F = 2.842989$ .

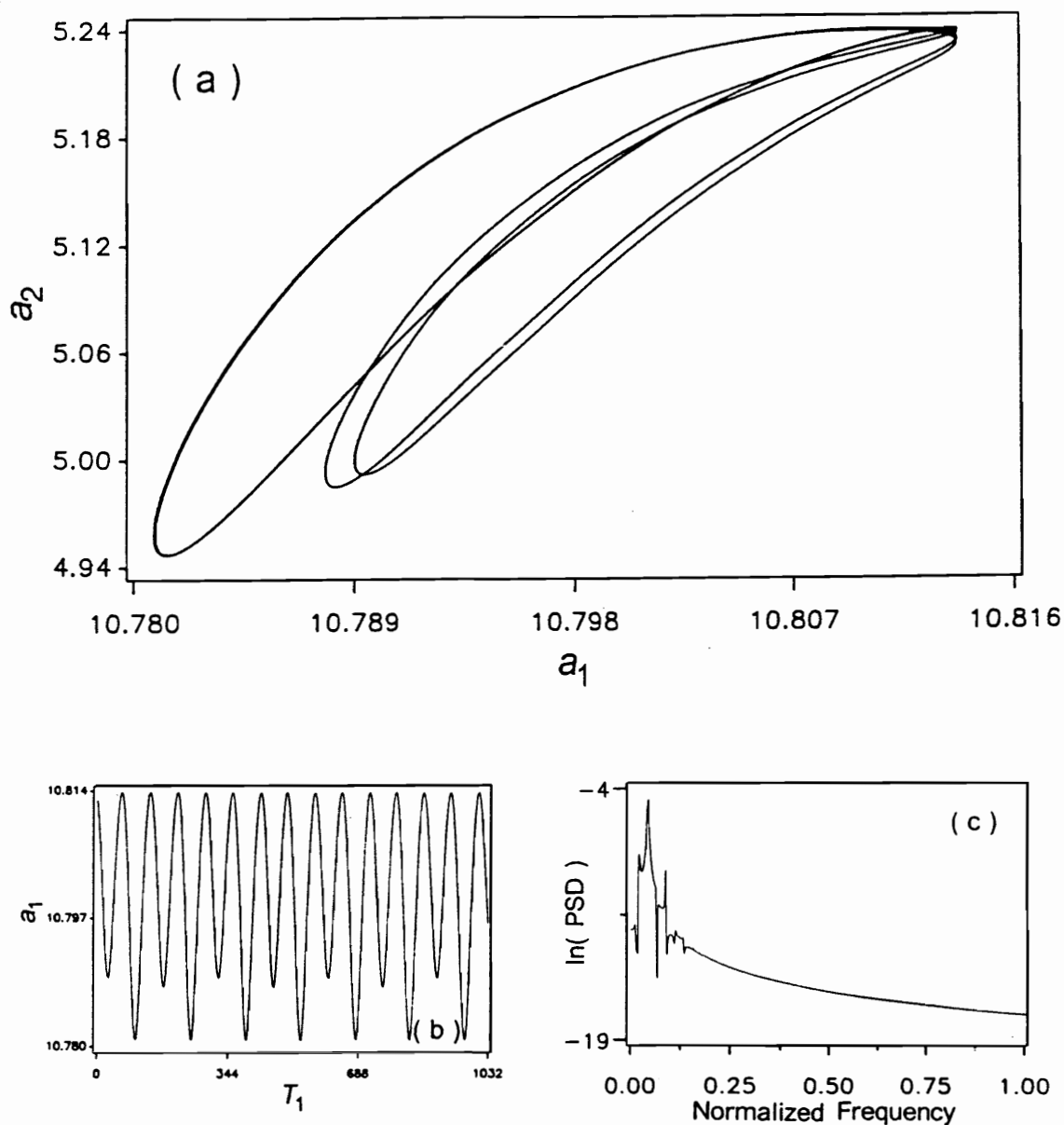


**Figure 4.8.** (a) Projection of the period-four limit cycle on the  $a_1 - a_2$  plane; (b) the time evolution of  $a_1$ ; (c) FFT of the response:  $\mu = 0.969 \times 10^{-3}$ ;  $\sigma_2 = 0.969$ ;  $F = 2.84300244$ .



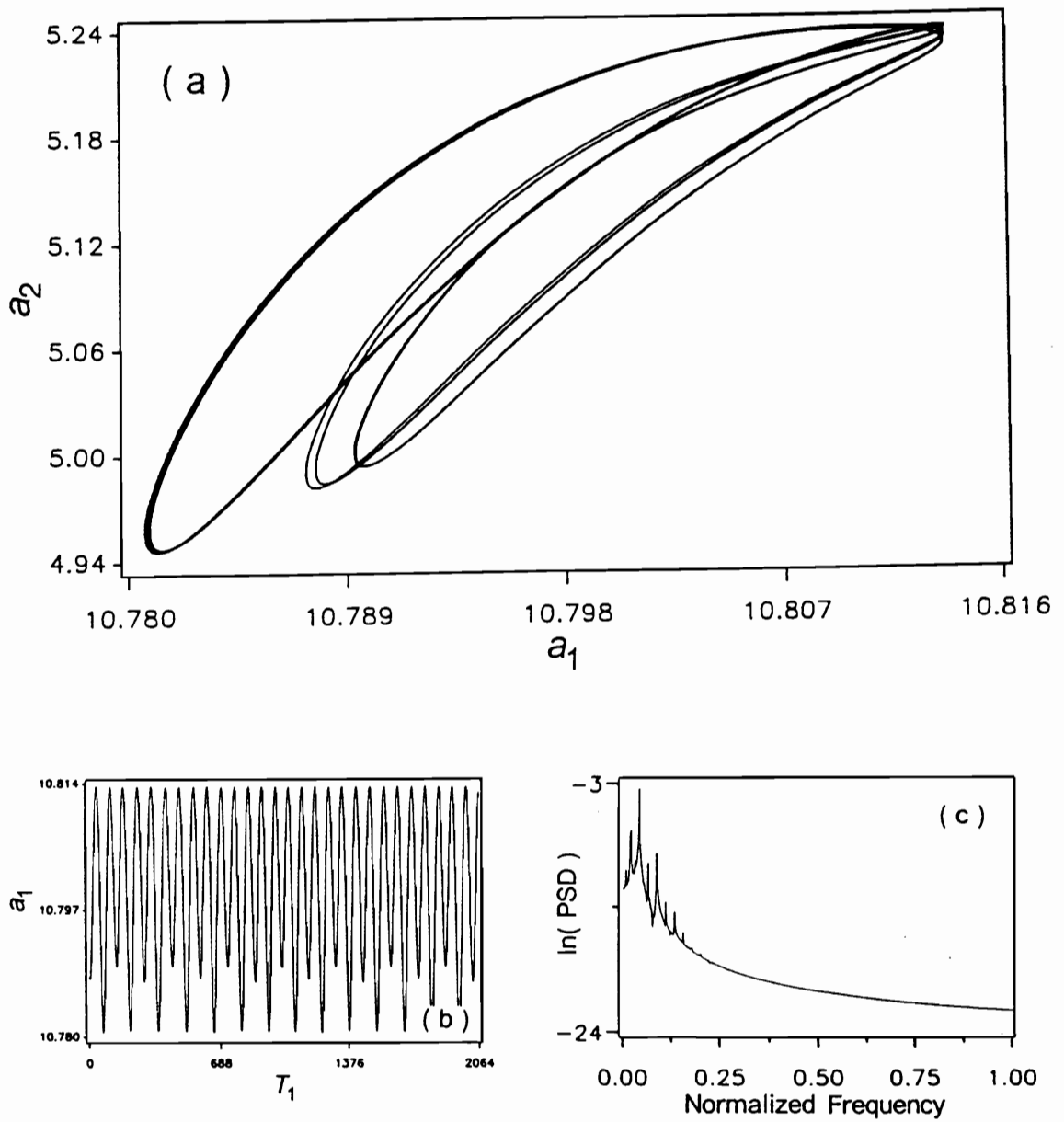


**Figure 4.9.** (a) Projection of the period-eight limit-cycle on the  $a_1 - a_2$  plane; (b) the time evolution of  $a_1$ ; (c) FFT of the response:  $\mu = 0.969 \times 10^{-3}$ ;  $\sigma_2 = 0.969$ ;  $F = 2.84300554$ .

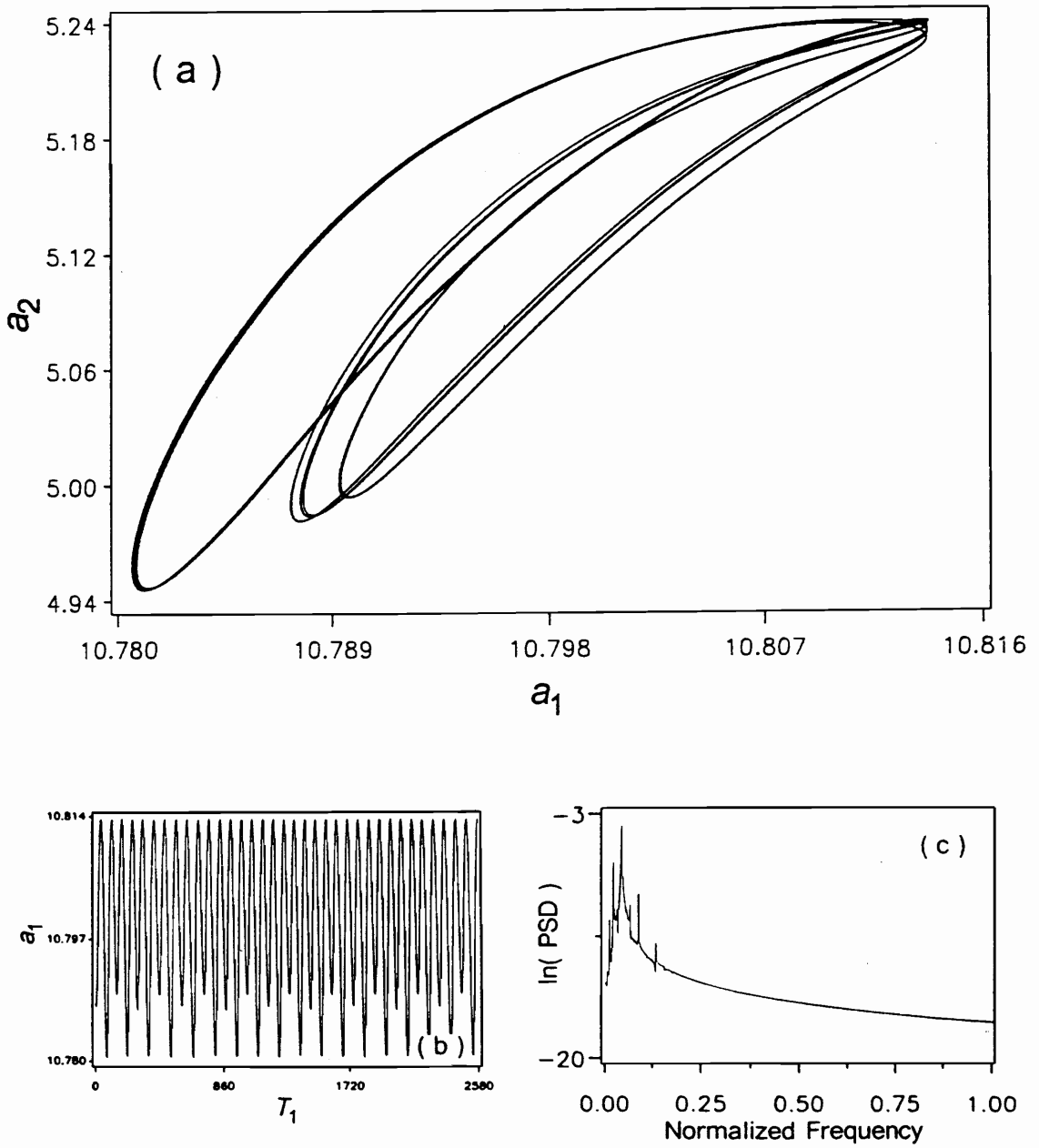


**Figure 4.10.** (a) Projection of the period-sixteen limit-cycle on the  $a_1 - a_2$  plane; (b) the time evolution of  $a_1$ ; (c) FFT of the response:  $\mu = 0.969 \times 10^{-3}$ ;  $\sigma_2 = 0.969$ ;  $F = 2.84300574$ .

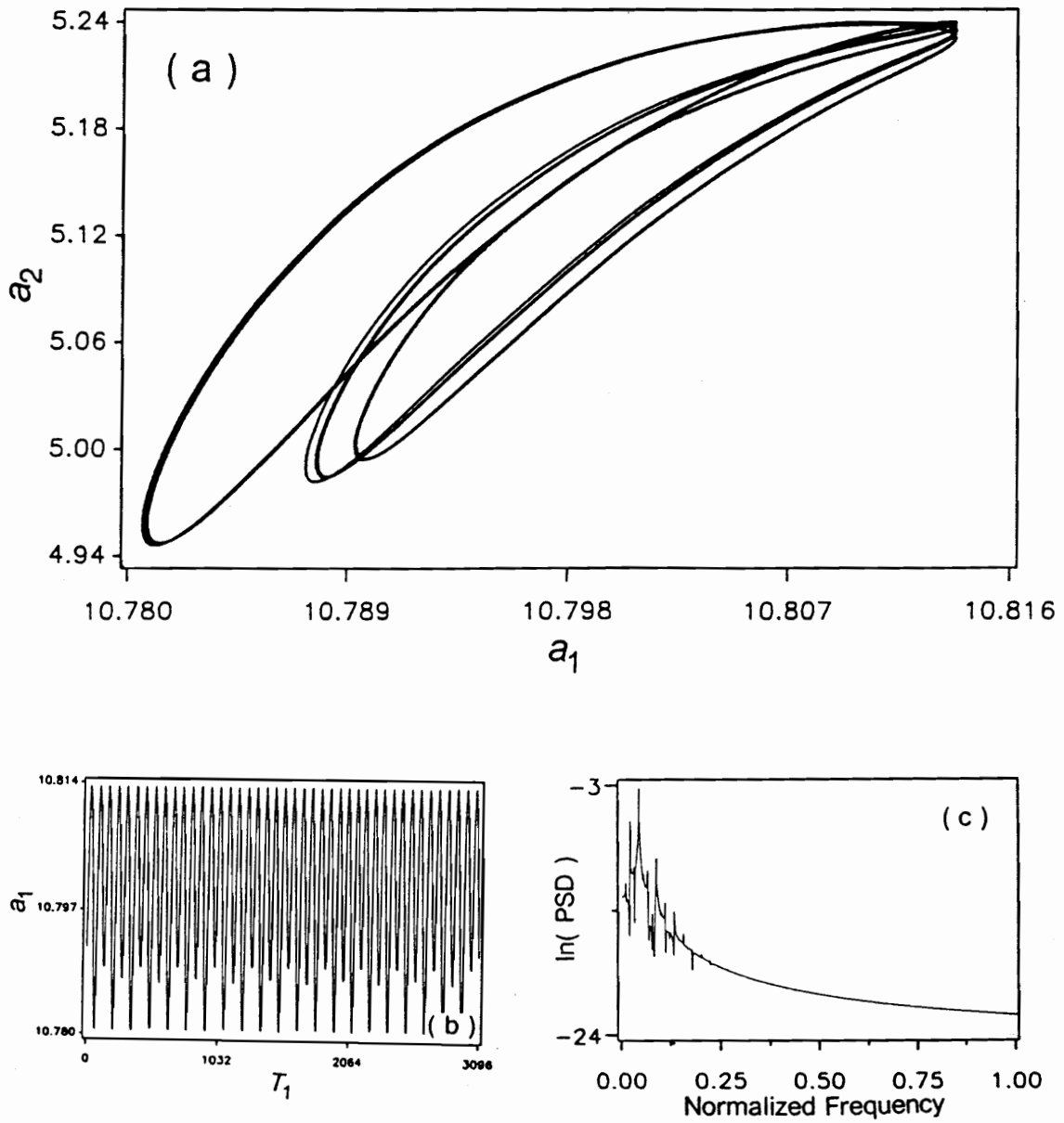


**Figure 4.11.** (a) Projection of the chaotic attractor on the  $a_1 - a_2$  plane; (b) the time evolution of  $a_1$ ; (c) FFT of the response:  $\mu = 0.969 \times 10^{-3}$ ;  $\sigma_2 = 0.969$ ;  $F = 2.84300582$ .

## 5. MODAL INTERACTION IN CIRCULAR PLATES

In this chapter, the dynamic analogue of the von Karman equations in polar form are used to study the axisymmetric response of a circular plate to a harmonic external excitation. The method of multiple scales is used to determine a set of first-order ordinary-differential equations governing the modulation of the phases and amplitudes of response in the presence of an internal or autoparametric resonance. A discussion of the stability of the steady-state solutions is given through a numerical example and a series of graphs. The results show the existence of period-doubling bifurcations leading to chaos in the solutions of the modulation equations.

### ***5.1. Nondimensionalization***

The equations governing the axisymmetric response of uniform circular plates in the absence of in-plane loads can be obtained from the dynamic analogue of von

Karman equations. When the damping term is included, the governing equations (2.57) and (2.58) can be written as follows:

$$\rho h \frac{\partial^2 w}{\partial t^2} + D \nabla^4 w = \frac{1}{r} \frac{\partial}{\partial r} \left( \frac{\partial F}{\partial r} \frac{\partial w}{\partial r} \right) - 2\mu \frac{\partial w}{\partial t} + q(r, t) \quad (5.1)$$

$$\nabla^4 F = - \frac{Eh}{2r} \frac{\partial}{\partial r} \left( \frac{\partial w}{\partial r} \right)^2 \quad (5.2)$$

where  $\mu$  is the damping coefficient and  $\nabla^4$  is the axisymmetric biharmonic operator defined by equation (2.59). The relations among  $F$ ,  $w$ , and the radial displacement  $u_r$  are

$$Eh \left[ \frac{\partial u_r}{\partial r} + \frac{1}{2} \left( \frac{\partial w}{\partial r} \right)^2 \right] = \frac{1}{r} \frac{\partial F}{\partial r} - \nu \frac{\partial^2 F}{\partial r^2} \quad (5.3)$$

$$Eh \frac{u_r}{r} = \frac{\partial^2 F}{\partial r^2} - \frac{\nu}{r} \frac{\partial F}{\partial r} \quad (5.4)$$

For convenience the following nondimensional variables denoted by an asterisk are introduced:

$$\begin{aligned} r &= Rr^*, & t &= R^2 \sqrt{\rho h / D} t^*, \\ u_r &= (h^4 / R^3) u^*, & \mu &= \frac{24(1 - \nu^2)}{R^4} \sqrt{\rho h^5 D} \mu^*, & w &= (h^2 / R) w^*, \\ q &= (D h^2 / R^5) q^*, & F &= (E h^5 / R^2) F^* \end{aligned}$$

where  $R$  is the radius of the plate. In terms of these nondimensional variables, equations (5.1)-(5.4) can be rewritten as

$$\frac{\partial^2 w}{\partial t^2} + \nabla^4 w = \varepsilon \left[ \frac{1}{r} \frac{\partial}{\partial r} \left( \frac{\partial w}{\partial r} \frac{\partial F}{\partial r} \right) - 2\mu \frac{\partial w}{\partial t} \right] + \varepsilon q \quad (5.5)$$

$$\nabla^4 F = -\frac{1}{2r} \frac{\partial}{\partial r} \left( \frac{\partial w}{\partial r} \right)^2 \quad (5.6)$$

$$\frac{\partial u}{\partial r} + \frac{1}{2} \left( \frac{\partial w}{\partial r} \right)^2 = \frac{1}{r} \frac{\partial F}{\partial r} - v \frac{\partial^2 F}{\partial r^2} \quad (5.7)$$

$$\frac{u}{r} = \frac{\partial^2 F}{\partial r^2} - \frac{v}{r} \frac{\partial F}{\partial r} \quad (5.8)$$

where  $\varepsilon = \frac{12(1-\nu^2)h^2}{R^2}$ ,  $q = \varepsilon q^*$ , and the asterisk was dropped for convenience of notation. A first integral of equation (5.6) is obtained by eliminating  $u$  from equations (5.7) and (5.8). The result is

$$\frac{1}{2} \left( \frac{\partial w}{\partial r} \right)^2 = \frac{1}{r} \frac{\partial F}{\partial r} - \frac{\partial^2 F}{\partial r^2} - r \frac{\partial^3 F}{\partial r^3} \quad (5.9)$$

Because we are considering the case of primary resonance, we put  $q = \varepsilon q^*$  so that the effect of the excitation is balanced by the effects of damping and nonlinearity.

The boundary conditions for a clamped circular plate are

$$w = \frac{\partial w}{\partial r} = u = 0 \quad \text{at } r = 1 \quad (5.10)$$

Putting  $u = 0$  in equation (5.8) yields

$$\frac{\partial^2 F}{\partial r^2} - v \frac{\partial F}{\partial r} = 0 \quad \text{at } r = 1 \quad (5.11)$$

In addition to the above boundary conditions,  $w$  and  $F$  are required to be finite at  $r = 0$ .

## 5.2. Method of Solution

The method of multiple scales (Nayfeh, 1973, 1981) is used to determine a uniformly valid first-order expansion of  $w$ . To this end, new time scales are introduced as follows:

$$T_k = \varepsilon^k t \text{ for } k = 0, 1, 2, \dots \quad (5.12)$$

In terms of these scales, the time derivatives become

$$\frac{\partial}{\partial t} = D_0 + \varepsilon D_1 + \dots, \quad \frac{\partial^2}{\partial t^2} = D_0^2 + \varepsilon(2D_0 D_1) + \dots \quad (5.13)$$

where

$$D_k = \frac{\partial}{\partial T_k} \text{ for } k = 0, 1, 2, \dots$$

Uniform expansions of  $w$  and  $F$  are sought in the form

$$w(r, t, \varepsilon) = w_0(r, T_0, T_1) + \varepsilon w_1(r, T_0, T_1) + \dots \quad (5.14)$$

$$F(r, t, \varepsilon) = F_0(r, T_0, T_1) + \varepsilon F_1(r, T_0, T_1) + \dots \quad (5.15)$$

Substituting equations (5.13)-(5.15) into equations (5.5) and (5.9) and equating like powers of  $\varepsilon$ , one obtains

$$D_0^2 w_0 + \nabla^4 w_0 = 0 \quad (5.16)$$

$$r \frac{\partial^3 F_0}{\partial r^3} + \frac{\partial^2 F_0}{\partial r^2} - \frac{1}{r} \frac{\partial F_0}{\partial r} = \frac{1}{2} \left( \frac{\partial w_0}{\partial r} \right)^2 \quad (5.17)$$

$$D_0^2 w_1 + \nabla^4 w_1 = -2D_0 D_1 w_0 - 2\mu D_0 w_0 + \frac{1}{r} \frac{\partial}{\partial r} \left( \frac{\partial F_0}{\partial r} \frac{\partial w_0}{\partial r} \right) + q \quad (5.18)$$

Substituting equations (5.14) and (5.15) into equations (5.10) and (5.11) and equating coefficients of like powers of  $\varepsilon$  yields

$$w_0 = \frac{\partial w_0}{\partial r} = 0 \text{ at } r = 1 \quad (5.19)$$

$$\frac{\partial^2 F_0}{\partial r^2} - \nu \frac{\partial F_0}{\partial r} = 0 \text{ at } r = 1 \quad (5.20)$$

$$w_1 = 0 \text{ and } \frac{\partial w_1}{\partial r} = 0 \text{ at } r = 1 \quad (5.21)$$

The bounded solution at  $r = 0$  of equation (5.16) that satisfies equation (5.19) is

$$w_0 = \sum_{m=1}^{\infty} \phi_m(r) [A_m(T_1) e^{i\omega_m T_0} + cc] \quad (5.22)$$

where cc stands for the complex conjugate of the preceding terms,

$$\phi_m(r) = I_0(\sqrt{\omega_m}) J_0(\sqrt{\omega_m} r) - I_0(\sqrt{\omega_m} r) J_0(\sqrt{\omega_m}) \quad (5.23)$$

$$\phi_m'(1) = I_0(\sqrt{\omega_m}) J_0'(\sqrt{\omega_m}) - I_0'(\sqrt{\omega_m}) J_0(\sqrt{\omega_m}) = 0 \quad (5.24)$$



and  $J_0$  and  $I_0$  are the Bessel and modified Bessel functions of order zero.

Substituting equations (5.22) and (5.23) into equation (5.17) yields

$$r \frac{\partial^3 F_0}{\partial r^3} + \frac{\partial^2 F_0}{\partial r^2} - \frac{1}{r} \frac{\partial F_0}{\partial r} = -\frac{1}{2} \sum_{m=1}^{\infty} \sum_{n=1}^{\infty} \Lambda_{mn} \phi_m'(r) \phi_n'(r) \quad (5.25)$$

where

$$\Lambda_{mn} = A_m A_n e^{i(\omega_m + \omega_n)T_0} + A_m \bar{A}_n e^{i(\omega_m - \omega_n)T_0} + cc \quad (5.26)$$

and the primes represent differentiation with respect to the argument. Because

$$\left( r^2 \frac{d}{dr^2} + r \frac{d}{dr} - 1 \right) J_1(\kappa_m r) = -\kappa_m^2 r^2 J_1(\kappa_m r) \quad (5.27)$$

it is convenient to express  $\frac{\partial F_0}{\partial r}$  as

$$\frac{\partial F_0}{\partial r} = \sum_{m=1}^{\infty} \eta_m(T_0, T_1) J_1(\xi_m r) \quad (5.28)$$

Using equation (5.20), we find that the  $\xi_m$  are given by

$$\xi_m J_0(\xi_m) - (1 + \nu) J_1(\xi_m) = 0 \quad (5.29)$$

Substitution of equation (5.28) into equation (5.25) yields

$$\sum_{m=1}^{\infty} \eta_m \left[ r J_1''(\xi_m r) + J_1'(\xi_m r) - \frac{1}{r} J_1(\xi_m r) \right] = -\frac{1}{2} \sum_{p=1}^{\infty} \sum_{q=1}^{\infty} \Lambda_{pq} \phi_p' \phi_q' \quad (5.30)$$

Multiplying both sides of equation (5.30) by  $J_1(\xi_n r)$  and integrating the result with respect to  $r$  from zero to one, one obtains

$$\eta_n = \sum_{q=1}^{\infty} \sum_{p=1}^{\infty} S_{npq} \Lambda_{pq} \quad (5.31)$$

where

$$S_{npq} = \frac{\int_0^1 \phi_q'(r) \phi_p'(r) J_1(\xi_n r) dr}{2\xi_n^2 \int_0^1 r J_1^2(\xi_n r) dr} = \frac{\int_0^1 \phi_q'(r) \phi_p'(r) J_1(\xi_n r) dr}{(\xi_n^2 - 1 + \nu^2) J_1^2(\xi_n)} \quad (5.32)$$

Then it follows that

$$\frac{\partial F_0}{\partial r} = \sum_{m=1}^{\infty} \sum_{p=1}^{\infty} \sum_{n=1}^{\infty} S_{mnp} \Lambda_{np} J_1(\xi_m r) \quad (5.33)$$

To proceed further, we need to specify the modes that are excited because all modes that are not excited directly by the load or indirectly excited through an internal or autoparametric resonance decay with time (Nayfeh and Mook, 1979). The first three natural frequencies (Leissa, 1969) are  $\omega_1 = 10.2158$ ,  $\omega_2 = 39.7711$ , and  $\omega_3 = 89.1041$ . Because  $\omega_1 + 2\omega_2 = 89.758 \approx \omega_3$ , an internal or autoparametric resonance involving the first three modes exists. To express quantitatively the nearness of this resonance, we introduce the detuning parameter  $\sigma_1$  defined according to

$$\omega_1 + 2\omega_2 - \omega_3 = .6538 = \varepsilon \sigma_1 \quad (5.34)$$

We consider the case in which one of these three modes is excited by a primary resonant excitation. Hence, all modes except these three decay with time due to damping. Hence, we set  $A_m = 0$  for all  $m \geq 4$  in equation (5.33) and obtain

$$\frac{\partial F_0}{\partial r} = \sum_{m=1}^{\infty} J_1(\xi_m r) \left( \sum_{n=1}^3 \sum_{p=1}^3 S_{mnp} \Lambda_{np} \right) = \sum_{n=1}^3 \sum_{p=1}^3 G_{np}(r) \Lambda_{np} \quad (5.35)$$

where

$$G_{np} = G_{np}(r) = \sum_{m=1}^{\infty} J_1(\xi_m r) S_{mnp} = G_{pn}(r) \quad (5.36)$$

Substitution of equations (5.22) and (5.35) into equation (5.18) yields

$$\begin{aligned} D_0^2 w_1 + \nabla^4 w_1 = & \sum_{m=1}^3 \left[ -2i\omega_m e^{i\omega_m T_0} (A_m' + \mu A_m) \right] \phi_m(r) \\ & + \sum_{m=1}^3 \sum_{n=1}^3 \sum_{p=1}^3 \hat{\alpha}_{mnp} \left[ A_m A_n A_p e^{i(\omega_m + \omega_n + \omega_p) T_0} \right. \\ & + A_m A_n \bar{A}_p e^{i(\omega_m + \omega_n - \omega_p) T_0} \\ & + A_m \bar{A}_n A_p e^{i(\omega_m - \omega_n + \omega_p) T_0} \\ & \left. + A_m \bar{A}_n \bar{A}_p e^{i(\omega_m - \omega_n - \omega_p) T_0} \right] + h e^{i\Omega T_0} + cc \end{aligned} \quad (5.37)$$

$$\hat{\alpha}_{mnp} = \frac{1}{r} \left[ G_{np}(r) \phi_m''(r) + G_{np}'(r) \phi_m'(r) \right] \quad (5.38)$$

The solution of  $w_1$  can be separated into two parts. The first part is a linear combination of the  $\exp(i\omega_s T_0)$ , which are assumed to be in the form of  $\sum \Phi_s(r, T_1) e^{i\omega_s T_0}$ , and the second one denoted by  $\hat{w}_1$  has no terms with any frequency  $\omega_m$  (Nayfeh and Asfar, 1986). Therefore

$$w_1 = \sum_{s=1}^{\infty} \Phi_s(r, T_1) e^{i\omega_s T_0} + \hat{w}_1 + cc \quad (5.39)$$

We assume that the driving frequency  $\Omega$  is near the  $j$ th natural frequency  $\omega_j$ . To express quantitatively the nearness of this resonance, we introduce the detuning parameter  $\sigma$  defined by

$$\Omega = \omega_j + \varepsilon \sigma \quad (5.40)$$

Substituting equation (5.39) into equation (5.37) and equating the coefficients of  $\exp(i\omega_m T_0)$  on both sides, one obtains

$$\begin{aligned} \nabla^4 \Phi_s - \omega_s^2 \Phi_s = & -2i\omega_s(A_s' + \mu A_s)\phi_s + h\delta_{js}e^{i\sigma T_1} + 3\hat{\alpha}_{sss}A_s^2\bar{A}_s \\ & + 2 \sum_{q=1, q \neq s}^3 A_q \bar{A}_q A_s (\hat{\alpha}_{sq q} + \hat{\alpha}_{qs q} + \hat{\alpha}_{qq s}) \\ & + (\hat{\alpha}_{221} + \hat{\alpha}_{212} + \hat{\alpha}_{122})\delta_{s3}A_1A_2^2e^{i\sigma_1 T_1} \\ & + (\hat{\alpha}_{322} + \hat{\alpha}_{232} + \hat{\alpha}_{223})\delta_{s1}A_3\bar{A}_2^2e^{-i\sigma_1 T_1} \\ & + (\hat{\alpha}_{123} + \hat{\alpha}_{231} + \hat{\alpha}_{312} + \hat{\alpha}_{321} + \hat{\alpha}_{132} \\ & + \hat{\alpha}_{213})\delta_{s2}\bar{A}_1\bar{A}_2A_3e^{-i\sigma_1 T_1} \end{aligned} \quad (5.41)$$

where  $\delta_{js}$  is the Kronecker delta. To apply the solvability condition (Nayfeh, 1981) to equation (5.41), one multiplies the right-hand side of equation (5.41) by  $r\phi_s$ , integrates from zero to one with respect to  $r$ , and obtains

$$\begin{aligned} & -2i\omega_s(A_s' + \mu_s A_s) + h_s e^{i\sigma T_1} \delta_{js} + 3\bar{A}_s A_s^2 \Gamma_{ssss} + 2 \sum_{q=1, q \neq s}^3 A_s A_q \bar{A}_q (\Gamma_{sqqs} + 2\Gamma_{qqss}) \\ & + (\Gamma_{122s} + 2\Gamma_{221s})\delta_{s3}A_1A_2^2e^{i\sigma_1 T_1} + (\Gamma_{322s} + 2\Gamma_{223s})\delta_{s1}A_3\bar{A}_2^2e^{-i\sigma_1 T_1} \\ & + (2\Gamma_{1232} + 2\Gamma_{2132} + 2\Gamma_{3122})\delta_{s2}\bar{A}_1\bar{A}_2A_3e^{-i\sigma_1 T_1} = 0 \end{aligned} \quad (5.42)$$

where

$$h_s = \int_0^1 r h \phi_s dr, \quad \Gamma_{mnp} = \int_0^1 r \hat{\alpha}_{mnp} \phi_s dr, \quad \mu_s = \int_0^1 r \mu \phi_s^2 dr \quad (5.43)$$

and

$$\begin{aligned} Q_1 &= \Gamma_{3221} + 2\Gamma_{2231} = 8Q, & Q_2 &= 2\Gamma_{1232} + 2\Gamma_{2132} + 2\Gamma_{3122} = 16Q, \\ Q_3 &= \Gamma_{1223} + 2\Gamma_{2213} = 8Q, & \alpha_{ij} &= (4 - 3\delta_{ij})\Gamma_{jjii} + 2\Gamma_{ijji} \end{aligned} \quad (5.44)$$

Introducing the polar form  $A_n = \frac{1}{2} a_n \exp(i\beta_n)$ , where the  $a_n(T_1)$  and  $\beta_n(T_1)$  are the amplitudes and phases, into equation (5.42) and separating real and imaginary parts, we obtain

$$\omega_1(a_1' + \mu_1 a_1) + Q a_3 a_2^2 \sin \gamma_1 - h_1 \delta_{j1} \sin \xi_{21} = 0 \quad (5.45)$$

$$\begin{aligned} \omega_1 a_1 \beta_1' + \frac{1}{8} (\alpha_{11} a_1^2 + \alpha_{12} a_2^2 + \alpha_{13} a_3^2) a_1 + Q a_3 a_2^2 \cos \gamma_1 \\ + h_1 \delta_{j1} \cos \xi_{21} = 0 \end{aligned} \quad (5.46)$$

$$\omega_2(a_2' + \mu_2 a_2) + 2Q a_1 a_2 a_3 \sin \gamma_1 - h_2 \delta_{j2} \sin \xi_{22} = 0 \quad (5.47)$$

$$\begin{aligned} \omega_2 \beta_2' a_2 + \frac{1}{8} (\alpha_{21} a_1^2 + \alpha_{22} a_2^2 + \alpha_{23} a_3^2) a_2 + 2Q a_1 a_2 a_3 \cos \gamma_1 \\ + h_2 \delta_{j2} \cos \xi_{22} = 0 \end{aligned} \quad (5.48)$$

$$\omega_3(a_3' + \mu_3 a_3) - Q a_1 a_2^2 \sin \gamma_1 - h_3 \delta_{j3} \sin \xi_{23} = 0 \quad (5.49)$$

$$\begin{aligned} \omega_3 \beta_3' a_3 + \frac{1}{8} (\alpha_{31} a_1^2 + \alpha_{32} a_2^2 + \alpha_{33} a_3^2) a_3 + Q a_1 a_2^2 \cos \gamma_1 \\ + h_3 \delta_{j3} \cos \xi_{23} = 0 \end{aligned} \quad (5.50)$$

where

$$\gamma_1 = \sigma_1 T_1 + 2\beta_2 + \beta_1 - \beta_3 \text{ and } \xi_{2k} = \sigma T_1 - \beta_k \quad (5.51)$$

Next, we discuss the steady-state solutions for the three cases:  $\Omega \approx \omega_1$ ,  $\Omega \approx \omega_2$ , and  $\Omega \approx \omega_3$ .

*Case I:*  $\Omega = \omega_1 + \varepsilon \sigma$  ( $j = 1$ )

It follows from equations (5.47) and (5.49) that the steady-state amplitudes satisfy

$$\frac{\omega_2 \mu_2 a_2}{\omega_3 \mu_3 a_3} = -\frac{2a_3}{a_2} \quad (5.52)$$

which implies  $a_2 = a_3 = 0$ . Moreover, a linear stability analysis of this solution shows that it is stable. Therefore, only the first mode is excited and to the first approximation,

$$w(r,t) = a_1 \phi_1(r) \cos(\Omega t - \xi_{21}) + \dots \quad (5.53)$$

*Case II:*  $\Omega = \omega_2 + \varepsilon \sigma$  ( $j = 2$ )

Similar to Case I one finds that in the steady state all modes except the second mode decay to zero and to the first approximation,

$$w(r,t) = a_2 \phi_2(r) \cos(\Omega t - \xi_{22}) + \dots \quad (5.54)$$

*Case III:*  $\Omega = \omega_3 + \varepsilon \sigma$  ( $j = 3$ )

In this case, equations (5.45)-(5.50) become

$$\omega_1(a_1' + \mu_1 a_1) + Q a_3 a_2^2 \sin \gamma_1 = 0 \quad (5.55)$$

$$\omega_2(a_2' + \mu_2 a_2) + 2Q a_1 a_2 a_3 \sin \gamma_1 = 0 \quad (5.56)$$

$$\omega_3(a_3' + \mu_3 a_3) - Q a_1 a_2^2 \sin \gamma_1 - h_3 \sin \gamma_2 = 0 \quad (5.57)$$

$$\omega_1 \beta_1' a_1 + \frac{1}{8} (\alpha_{11} a_1^2 + \alpha_{12} a_2^2 + \alpha_{13} a_3^2) a_1 + Q a_3 a_2^2 \cos \gamma_1 = 0 \quad (5.58)$$

$$\omega_2 \beta_2' a_2 + \frac{1}{8} (\alpha_{21} a_1^2 + \alpha_{22} a_2^2 + \alpha_{23} a_3^2) a_2 + 2Q a_1 a_2 a_3 \cos \gamma_1 = 0 \quad (5.59)$$

$$\omega_3 \beta_3' a_3 + \frac{1}{8} (\alpha_{31} a_1^2 + \alpha_{32} a_2^2 + \alpha_{33} a_3^2) a_3 + Q a_1 a_2^2 \cos \gamma_1 + h_3 \cos \gamma_2 = 0 \quad (5.60)$$

where  $\gamma_2 = \xi_{23}$ . In this case, there are two possibilities. First,  $a_1 = a_2 = 0$  and to the first approximation, the response consists of a one-mode solution in which  $a_3 \neq 0$ . Second, all three modes can participate in the response and to the first approximation,

$$w = \phi_1(r) a_1 \cos(\omega_1 t + \beta_1) + \phi_2(r) a_2 \cos(\omega_2 t + \beta_2) + \phi_3(r) a_3 \cos(\omega_3 t + \beta_3) + \dots \quad (5.61)$$

Nonperiodic steady-state solutions and the stability of the steady-state periodic solutions can be studied by transforming equations (5.55)-(5.60) into the autonomous form  $X' = F(X)$  as follows:

$$a_1' = -\mu_1 a_1 - \frac{Q}{\omega_1} a_2^2 a_3 \sin \gamma_1 \quad (5.62)$$

$$a_2' = -\mu_2 a_2 - \frac{2Q}{\omega_2} a_1 a_2 a_3 \sin \gamma_1 \quad (5.63)$$

$$a_3' = -\mu_3 a_3 + \frac{Q}{\omega_3} a_1 a_2^2 \sin \gamma_1 + \frac{h_3}{\omega_3} \sin \gamma_2 \quad (5.64)$$

$$\begin{aligned}
\gamma_1' = & \sigma_1 + a_1^2 \left( \frac{\alpha_{31}}{8\omega_3} - \frac{\alpha_{11}}{8\omega_1} - \frac{\alpha_{21}}{4\omega_2} \right) + a_2^2 \left( \frac{\alpha_{32}}{8\omega_3} - \frac{\alpha_{12}}{8\omega_1} - \frac{\alpha_{22}}{4\omega_2} \right) \\
& + a_3^2 \left( \frac{\alpha_{33}}{8\omega_3} - \frac{\alpha_{13}}{8\omega_1} - \frac{\alpha_{23}}{4\omega_2} \right) + \left( \frac{a_1 a_2^2}{\omega_3 a_3} - \frac{a_3 a_2^2}{\omega_1 a_1} - \frac{4a_1 a_3}{\omega_2} \right) Q \cos \gamma_1 \quad (5.65) \\
& + \frac{h_3}{\omega_3 a_3} \cos \gamma_2
\end{aligned}$$

$$\gamma_2' = \sigma + \frac{\alpha_{31} a_1^2 + \alpha_{32} a_2^2 + \alpha_{33} a_3^2}{8\omega_3} + \frac{Q}{\omega_3} \frac{a_1 a_2^2}{a_3} \cos \gamma_1 + \frac{h_3}{\omega_3 a_3} \cos \gamma_2 \quad (5.66a)$$

where  $\gamma_1$  is defined in equation (5.51). The fixed points of equations (5.62)-(5.66) are the solutions to the system  $F(X) = 0$ . Because the solution  $a_1 = a_2 = 0$  and  $a_3 \neq 0$  identically satisfies  $F(X) = 0$ , one-mode solution is possible. The stability of these steady-state solutions depends on the eigenvalues of the Jacobian of  $F(X)$ .

### 5.3. Numerical Results

Because Poisson's ratio for most metals is close to  $\frac{1}{3}$ , in the example given here the value  $\nu = \frac{1}{3}$  is used. The first eighteen values of  $\xi_m$ , the roots of equation (5.29), for  $\nu = \frac{1}{3}$  are



$$\xi_1 = 1.545, \quad \xi_2 = 5.266, \quad \xi_3 = 8.497, \quad \xi_4 = 11.677,$$

$$\xi_5 = 14.841, \quad \xi_6 = 17.997, \quad \xi_7 = 21.149, \quad \xi_8 = 24.298,$$

$$\xi_9 = 27.445, \quad \xi_{10} = 30.591, \quad \xi_{11} = 33.736, \quad \xi_{12} = 36.881,$$

$$\xi_{13} = 40.025, \quad \xi_{14} = 43.169, \quad \xi_{15} = 46.312, \quad \xi_{16} = 49.456$$

$$\xi_{17} = 52.599, \quad \xi_{18} = 55.742,$$

In calculating the  $\Gamma$ 's only the first eighteen  $\xi$ 's are used. The results are accurate up to six significant figures. The corresponding values of the  $\alpha_{ij}$  and  $Q_i$  are

$$\alpha_{11} = -162.22202, \quad \alpha_{12} = \alpha_{21} = -883.816, \quad \alpha_{31} = \alpha_{13} = -1644.77,$$

$$\alpha_{32} = \alpha_{23} = -14220.42, \quad \alpha_{22} = -5552.16, \quad \alpha_{33} = -34401.62,$$

$$Q_1 = Q_3 = -556.779, \quad Q_2 = 2Q_1 = -1113.558$$

The amplitudes of the steady-state response are plotted as a function of the detuning  $\varepsilon\sigma$  of the excitation in Figures 5.1a and 5.2a and as a function of the amplitude  $2\varepsilon h$  of the excitation in Figures 5.1b and 5.2b. For one-mode solutions,  $a_1 = a_2 = 0$ , an algebraic expression for  $a_3$  is found, then inverted, and finally plotted in Figure 5.1, which shows the jump phenomenon. For three-mode solutions the task of finding closed-form algebraic expressions for the  $a_n$  is difficult and hence a numerical algorithm is used. Because the Newton-Raphson iteration process is extremely sensitive to initial conditions for the problem on hand, an algorithm based

on homotopy (Watson et al., 1987) is used to find the values of the  $a_n$  for a fixed abscissa in Figure 5.2. Once the ordinate of a point is found, the system  $X' = F(X)$  is integrated along the curve to obtain other points for various values of the abscissa. This saves a lot of computer time because homotopy alone is very expensive.

It follows from Figure 5.2 that three-mode solutions are possible only for a certain range of parameters. Moreover, for small values of  $h$  the amplitude of the first two modes are much larger than that of the third mode. Because the stable and unstable branches in Figure 2a are very close to each other the detail for  $a_3$  is plotted in Figure 5.3. Similarly  $\gamma_1$  and  $\gamma_2$  are plotted in detail in Figures 5.4 and 5.5, respectively. As  $\varepsilon\sigma$  is decreased to 4.91, the stable branches lose their stability with a pair of complex conjugate eigenvalues crossing the imaginary axis into the right-half of the complex plane. In Figure 5.2b the solutions lose their stability as  $\varepsilon h$  is increased to  $\psi_1 = 1022$ . At this value the fixed points lose their stability with a pair of complex conjugate eigenvalues crossing the imaginary axis into the right-half of the complex plane. Therefore  $\psi_1$  is a Hopf bifurcation point (Seydel, 1988).

For values of  $\varepsilon h$  greater than but close to  $\psi_1$ , limit-cycle solutions are found. A typical projection of the trajectory of these limit-cycle solutions on the  $\gamma_2 - a_3$  plane along with corresponding time evolution and FFT are shown in Figure 5.6. Once the limit cycle and its period for a particular value of  $\varepsilon h$  is found the limit cycle and its period for another value of  $\varepsilon h$  is predicted by the computer algorithm of Apprile and Trick (1972). The algorithm is based on a Newton-Raphson iteration procedure and a numerical integration scheme. The stability of limit cycles is determined by applying Floquet theory (Nayfeh and Mook, 1979). Because the system is autonomous and periodic one of the Floquet multipliers is always +1. If the modulus of any other multiplier is greater than one then the orbit is unstable; otherwise it is stable (Seydel, 1988). The limit cycle is gradually deformed and its period is slowly

varied as  $\varepsilon h$  is increased until  $\varepsilon h$  approaches the value  $\psi_2 = 1073.37$  where the modulus of one of the Floquet multipliers becomes greater than unity. At this point the limit cycle is no longer stable. It is found that the period is abruptly doubled and the period two orbit is stable for a certain range of  $\varepsilon h$ . The process of period-doubling bifurcations is continued as  $\varepsilon h$  is increased, leading to a chaotic solution for the modulation equations, as shown in Figures 5.7-5.11.

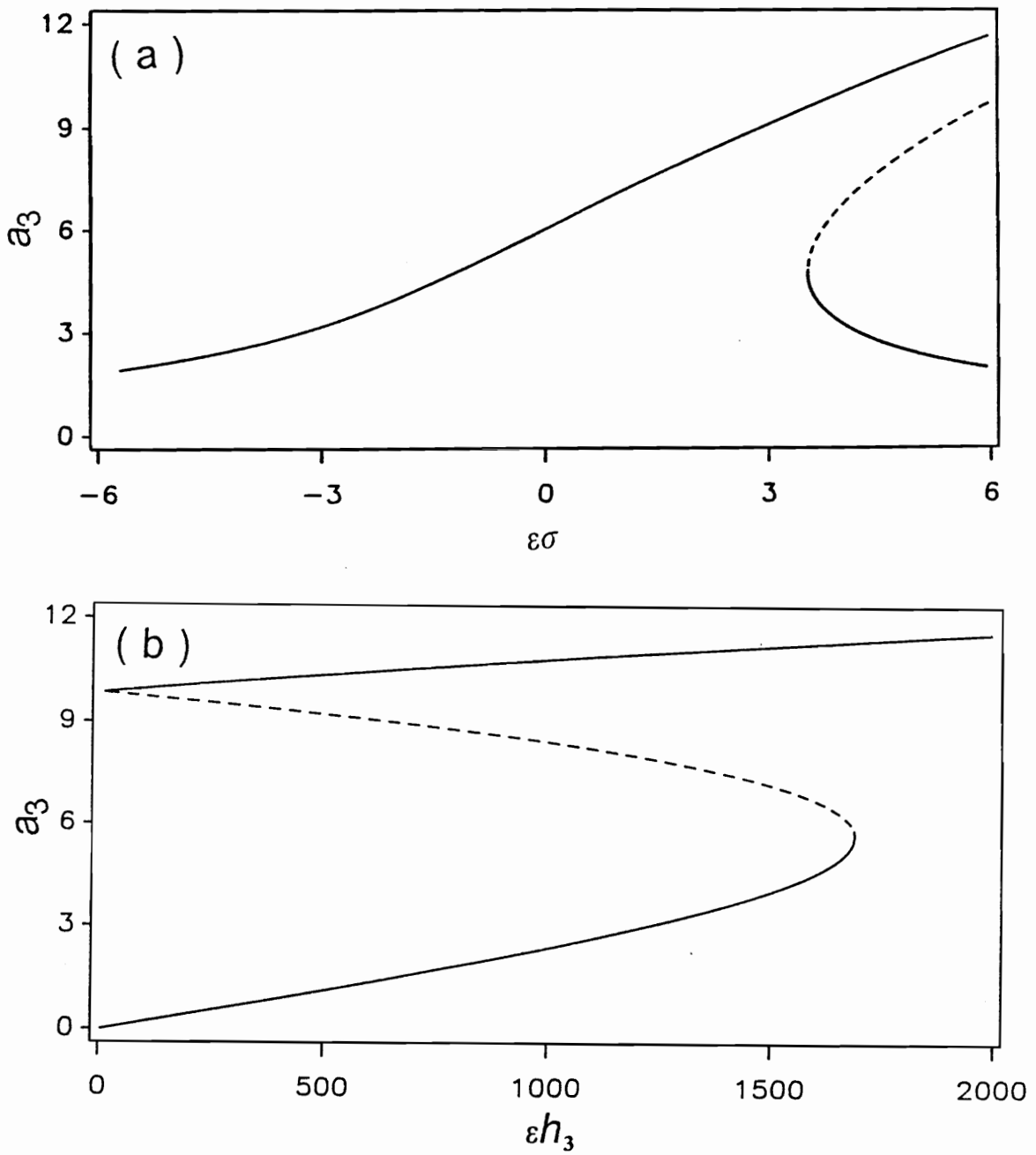


**Figure 5.1.** The amplitude of steady-state response for one-mode solution when  $\Omega \approx \omega_3$ , (a) as a function of the detuning of excitation for  $\varepsilon h = 1000$ , and (b) as a function of the amplitude of excitation for  $\varepsilon\sigma = 5$ . — stable; --- unstable;  $\varepsilon = 1.067 \times 10^{-3}$ ;  $\varepsilon\mu = .01$ .

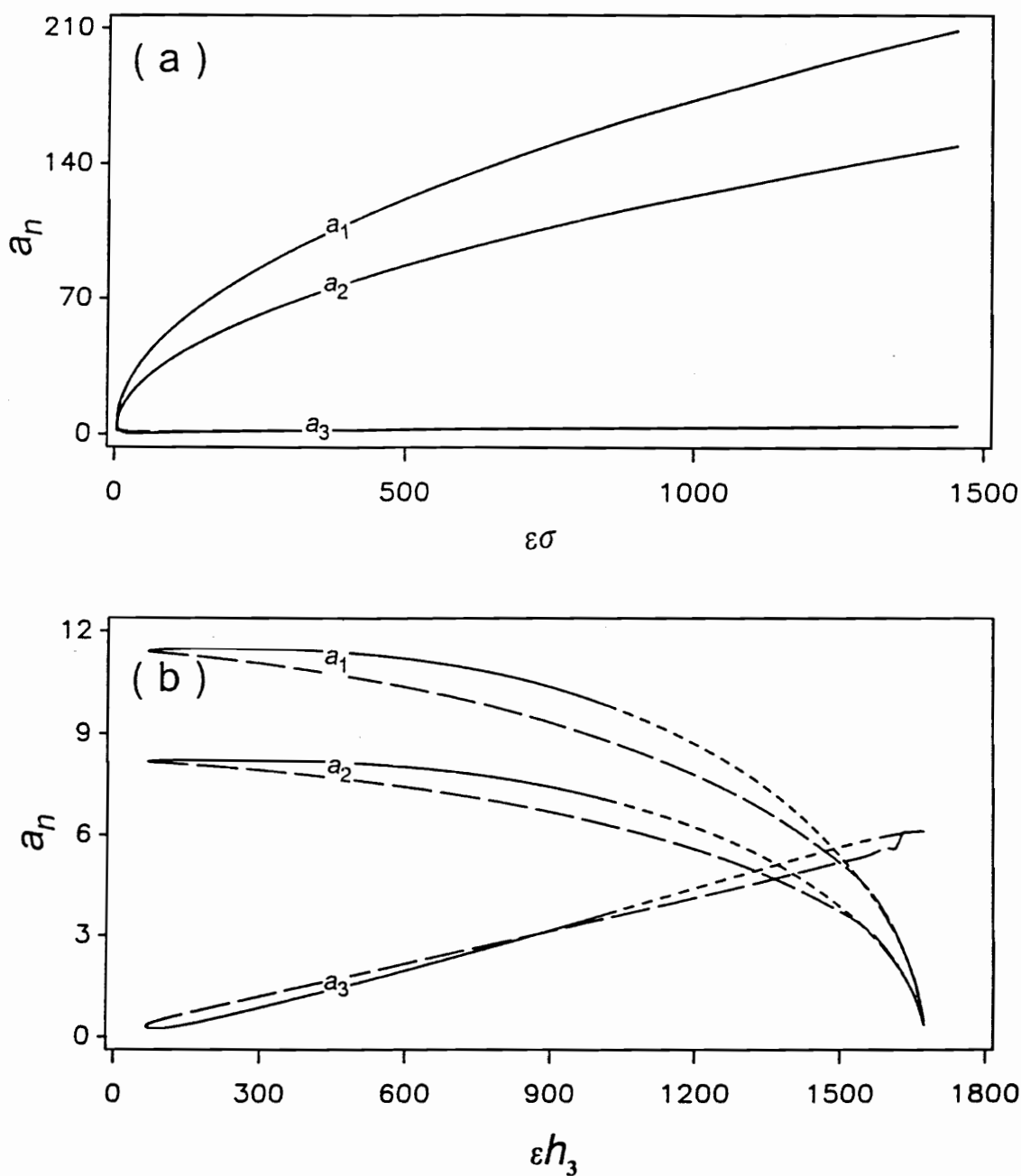


**Figure 5.2.** The amplitudes of steady-state response for three-mode solution when  $\Omega \approx \omega_3$ , (a) as a function of the detuning of excitation for  $\varepsilon h = 1000$ , and (b) as a function of the amplitude of excitation for  $\varepsilon \sigma = 5$ . — stable; --- unstable with real eigenvalues; - - -, unstable with complex conjugate pair of eigenvalues.  $\varepsilon = 1.067 \times 10^{-3}$ ;  $\varepsilon \mu = .01$ .

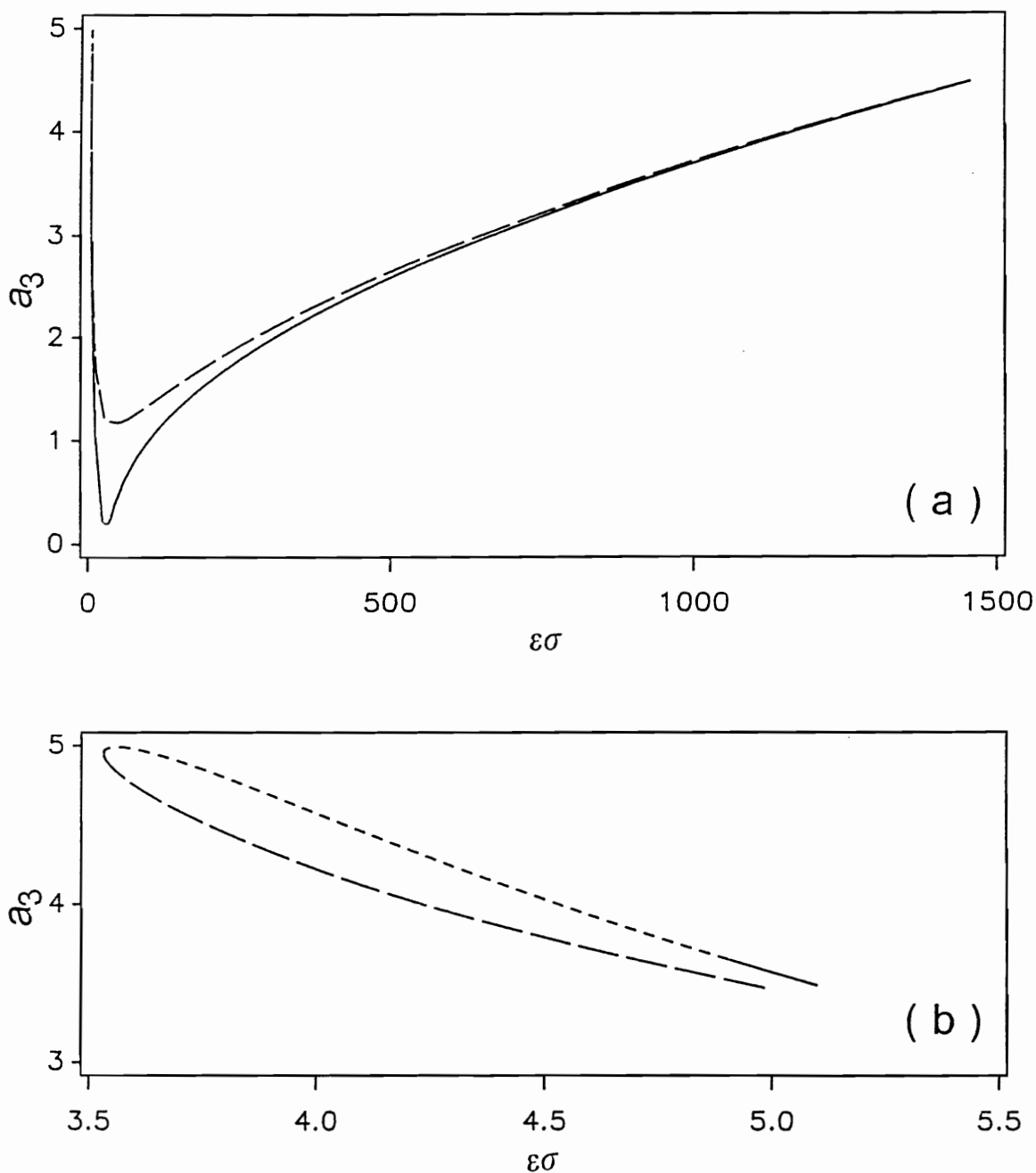


**Figure 5.3.** (a) The amplitude  $a_3$  of steady-state response for three-mode solution as a function of the detuning of excitation for  $\varepsilon h = 1000$ . (b) The detail of the left corner in (a). — stable; --- unstable with real eigenvalues; - - -, unstable with complex conjugate pair of eigenvalues.  $\varepsilon = 1.067 \times 10^{-3}$ ;  $\varepsilon \mu = .01$ .

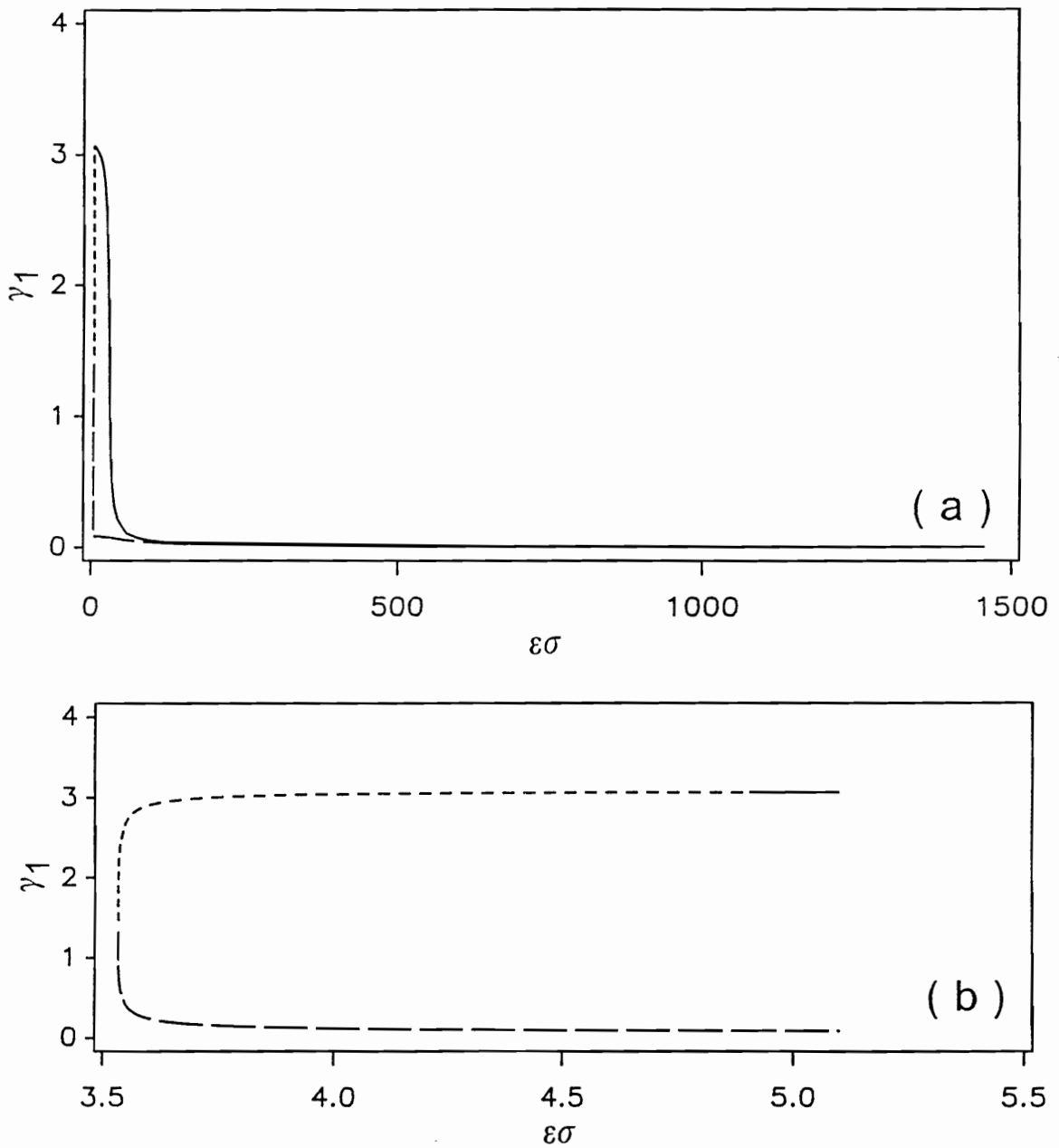


**Figure 5.4.** (a) The phase  $\gamma_1$  of steady-state response for three-mode solution as a function of the detuning of excitation for  $\varepsilon h = 1000$ . (b) The detail of the left corner in (a). — stable; --- unstable with real eigenvalues; - - -, unstable with complex conjugate pair of eigenvalues.  $\varepsilon = 1.067 \times 10^{-3}$ ;  $\varepsilon \mu = .01$ .

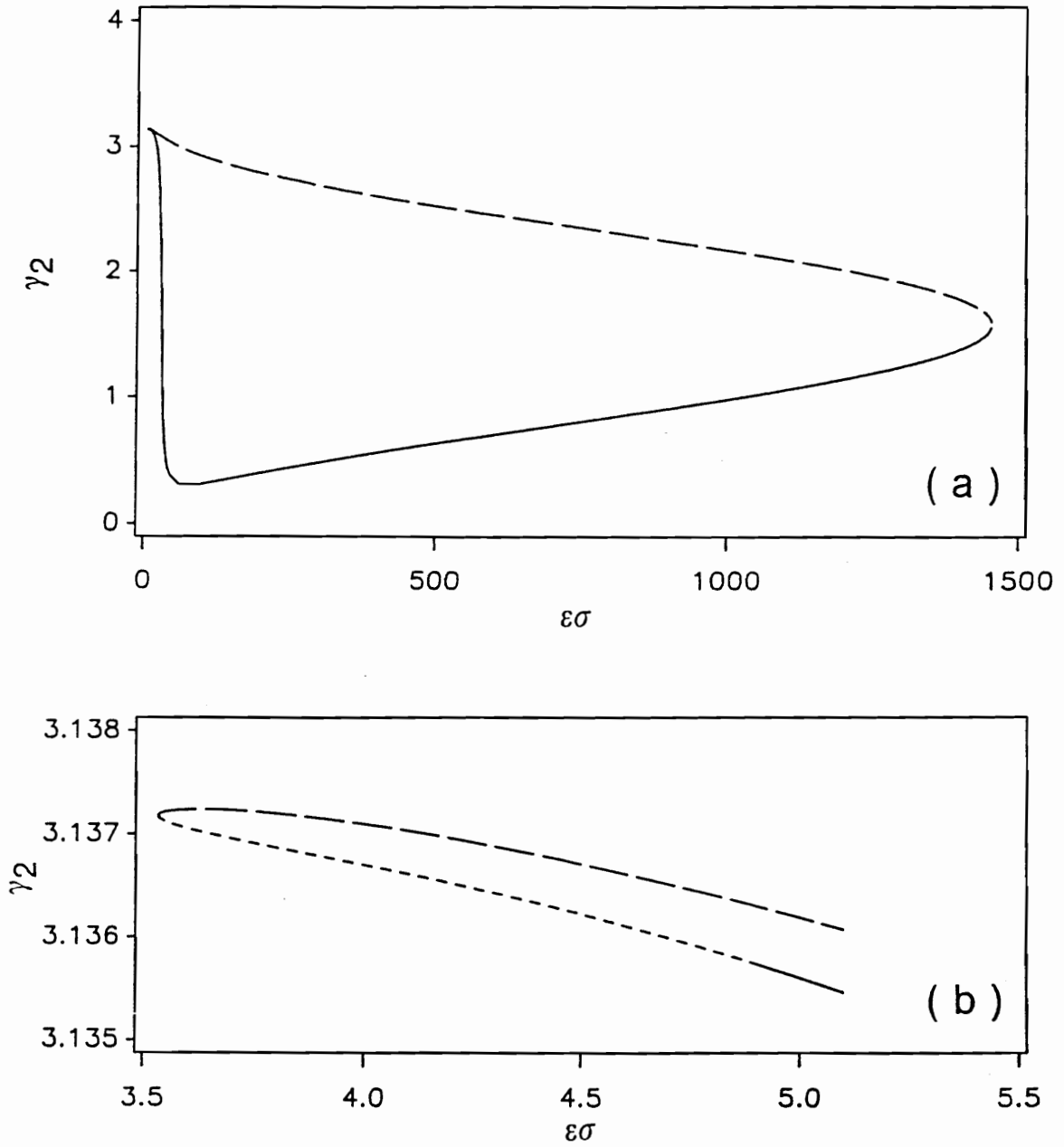


**Figure 5.5.** (a) The phase  $\gamma_2$  of steady-state response for three-mode solution as a function of the detuning of excitation for  $\varepsilon h = 1000$ . (b) The detail of the left corner in (a). — stable; --- unstable with real eigenvalues; - - -, unstable with complex conjugate pair of eigenvalues.  $\varepsilon = 1.067 \times 10^{-3}$ ;  $\varepsilon \mu = .01$ .



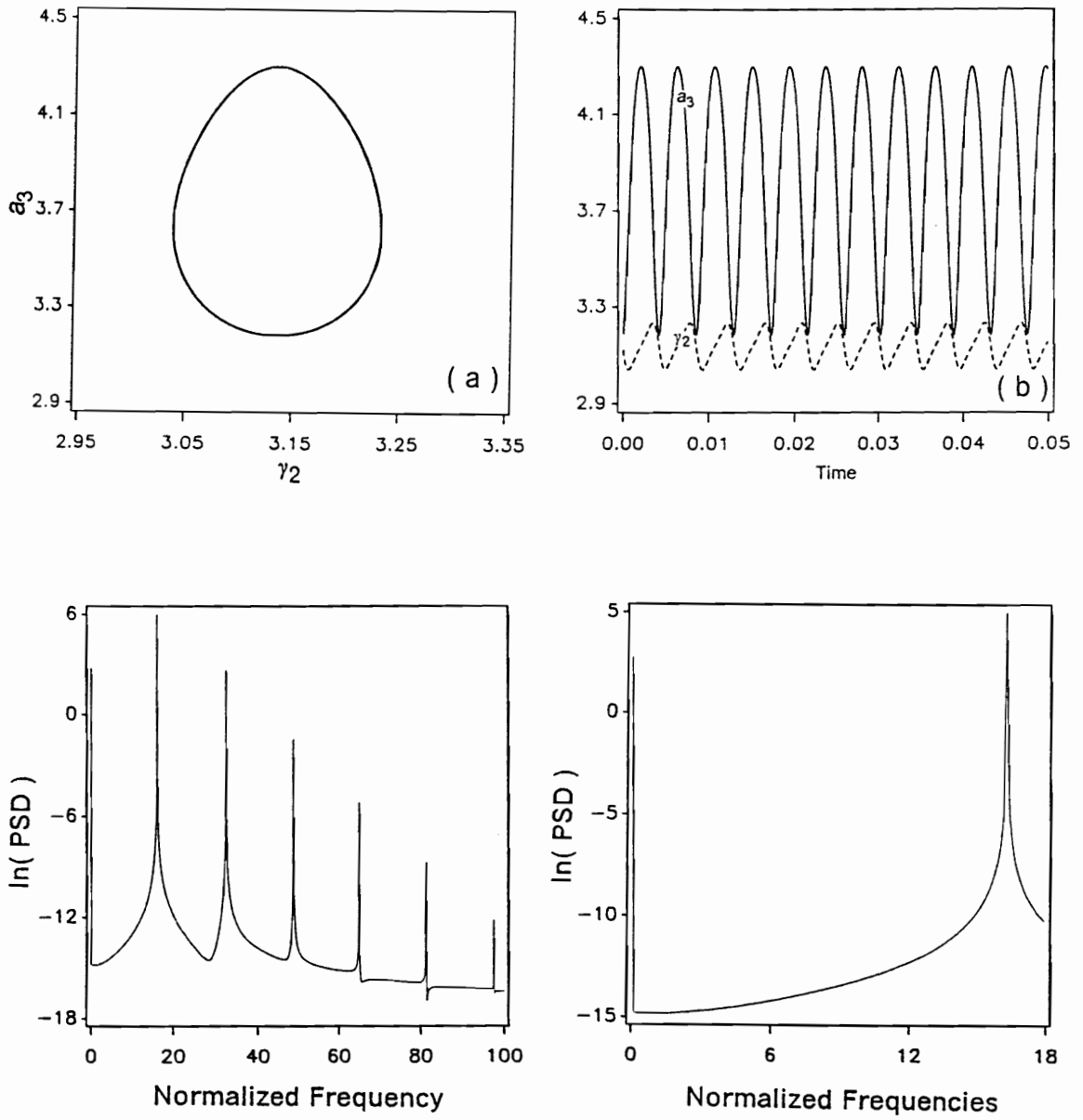


**Figure 5.6.** (a) Projection of the limit cycle solution trajectory on  $\gamma_2 - a_3$  plane, (b) the time evolution of  $\gamma_2$  and  $a_3$ , (c) FFT of the response, (d) the detail of FFT in (c).  $\epsilon\mu = .01$ ;  $\epsilon\sigma = 5.0$ ;  $\epsilon h = 1056.70$ ,  $\epsilon = 1.067 \times 10^{-3}$ .

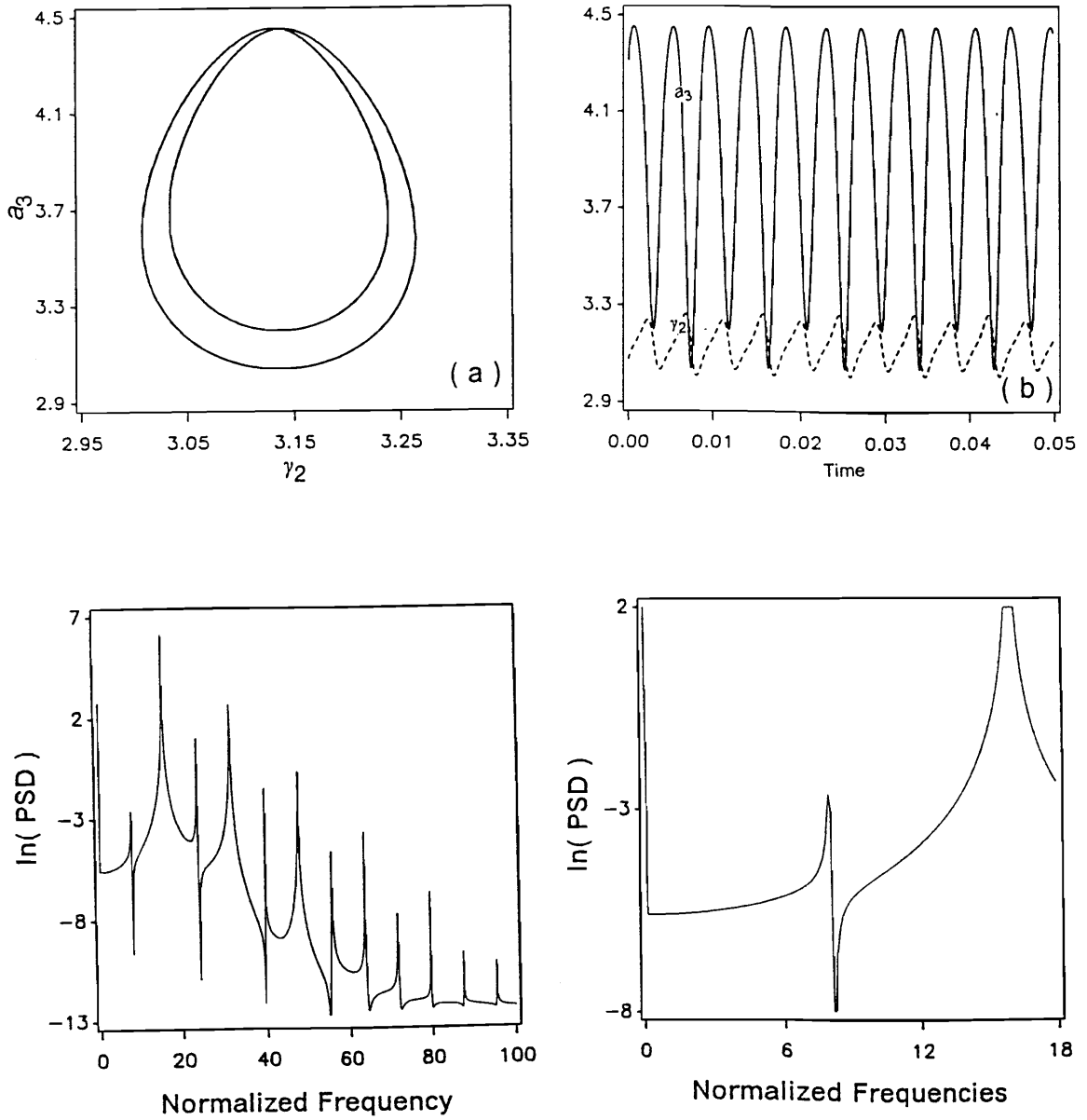


**Figure 5.7.** (a) Projection of the limit cycle solution trajectory on  $\gamma_2 - a_3$  plane, (b) the time evolution of  $\gamma_2$  and  $a_3$ , (c) FFT of the response, (d) the detail of FFT in (c).  $\varepsilon\mu = .01$ ;  $\varepsilon\sigma = 5.0$ ;  $\varepsilon h = 1075.00$ ,  $\varepsilon = 1.067 \times 10^{-3}$ .

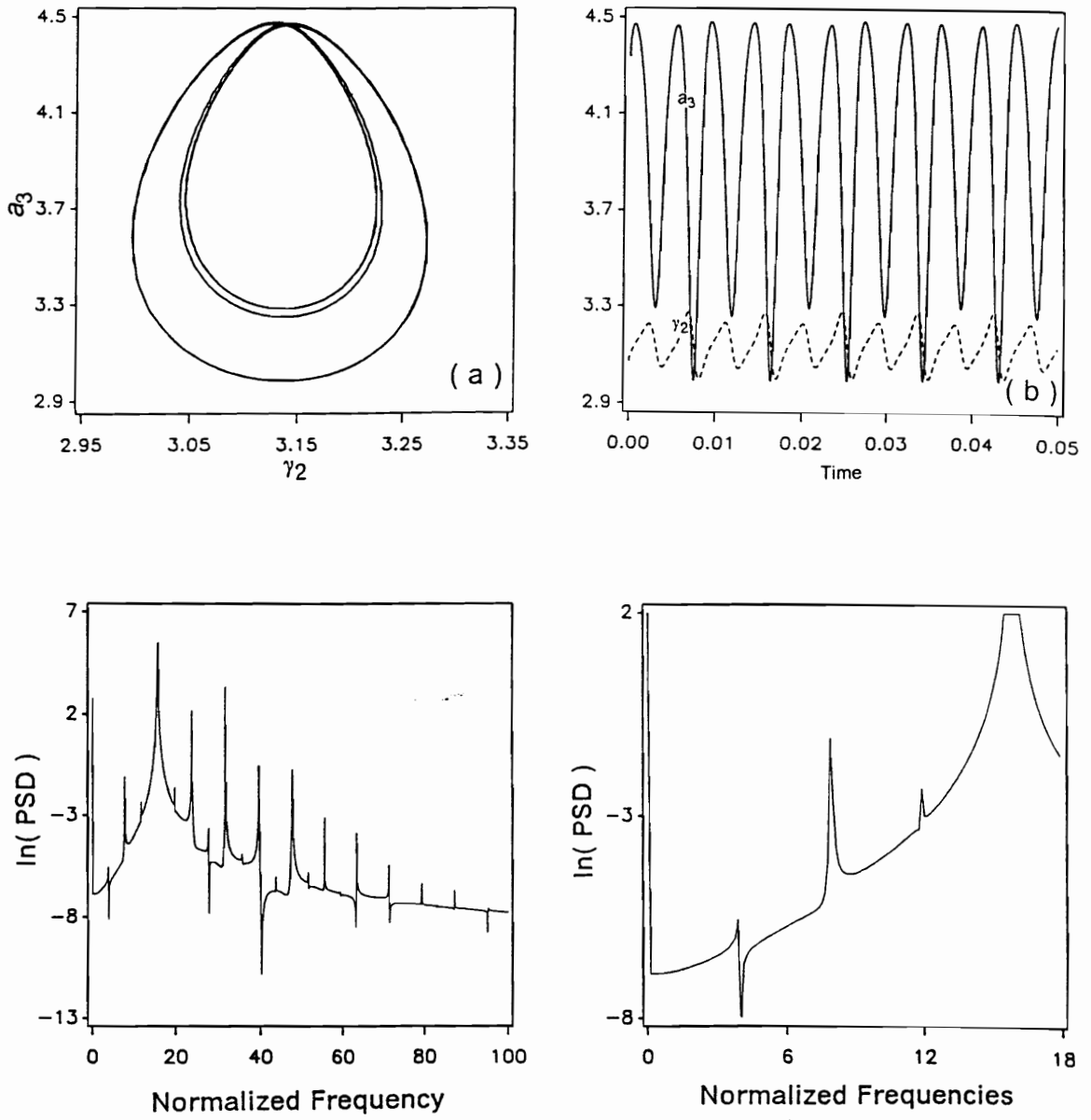


**Figure 5.8.** (a) Projection of the limit cycle solution trajectory on  $\gamma_2 - a_3$  plane, (b) the time evolution of  $\gamma_2$  and  $a_3$ , (c) FFT of the response, (d) the detail of FFT in (c).  $\varepsilon\mu = .01$ ;  $\varepsilon\sigma = 5.0$ ;  $\varepsilon h = 1078.74$ ,  $\varepsilon = 1.067 \times 10^{-3}$ .

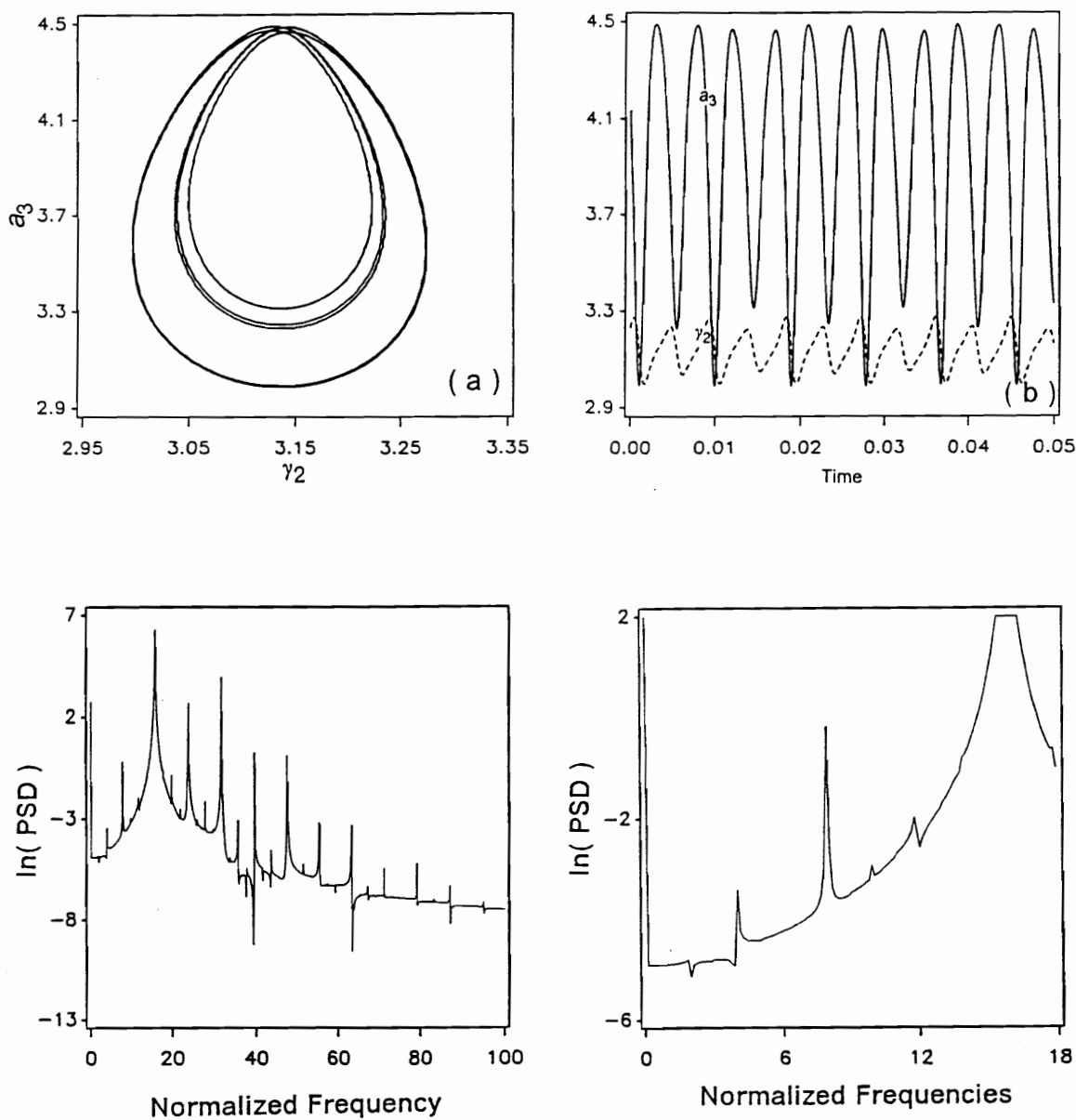


**Figure 5.9.** (a) Projection of the limit cycle solution trajectory on  $\gamma_2 - a_3$  plane, (b) the time evolution of  $\gamma_2$  and  $a_3$ , (c) FFT of the response, (d) the detail of FFT in (c).  $\varepsilon\mu = .01$ ;  $\varepsilon\sigma = 5.0$ ;  $\varepsilon h = 1079.270$ ,  $\varepsilon = 1.067 \times 10^{-3}$ .

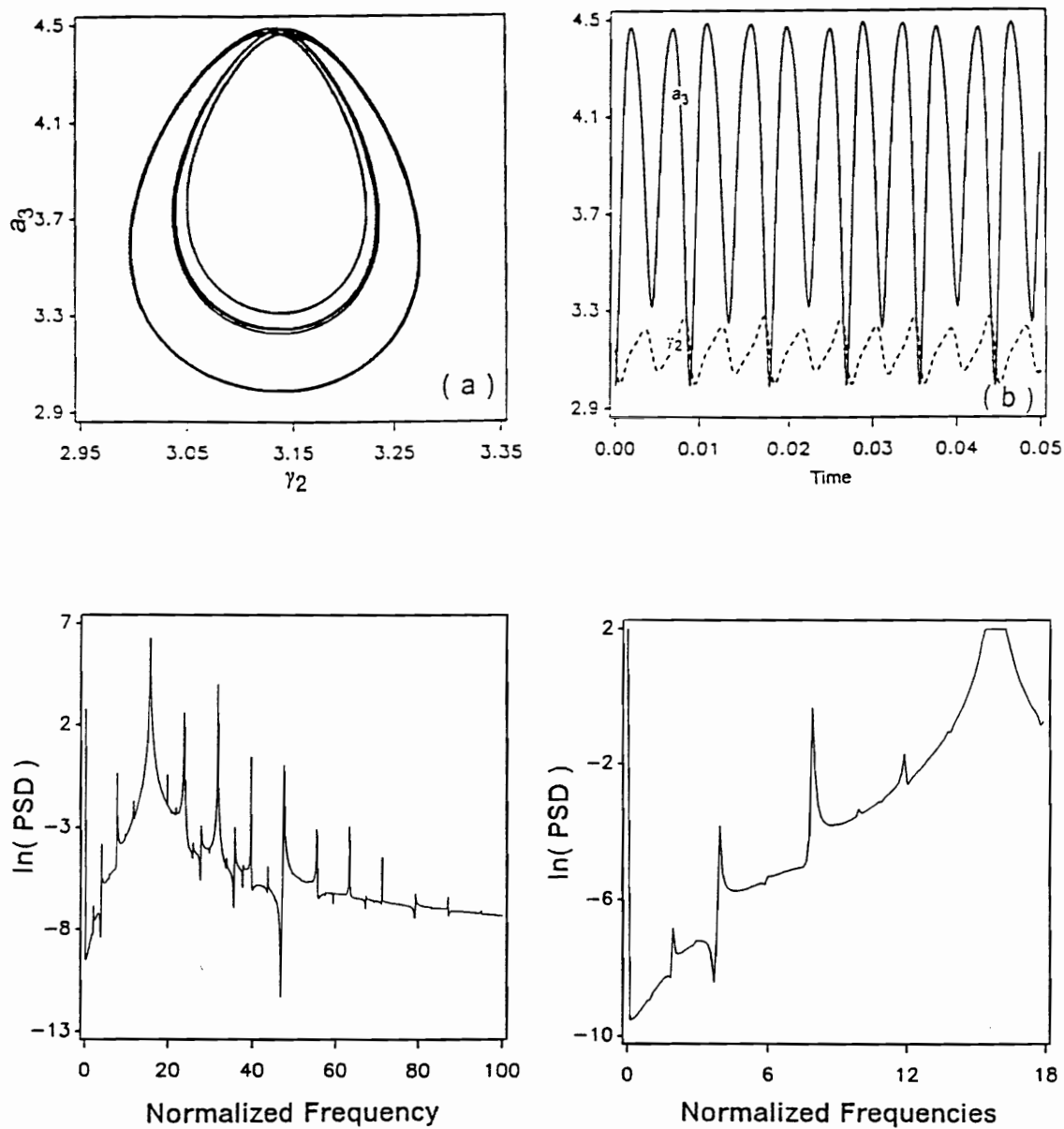


**Figure 5.10.** (a) Projection of the limit cycle solution trajectory on  $\gamma_2 - a_3$  plane, (b) the time evolution of  $\gamma_2$  and  $a_3$ , (c) FFT of the response, (d) the detail of FFT in (c).  $\varepsilon\mu = .01$ ;  $\varepsilon\sigma = 5.0$ ;  $\varepsilon h = 1079.297$ ,  $\varepsilon = 1.067 \times 10^{-3}$ .

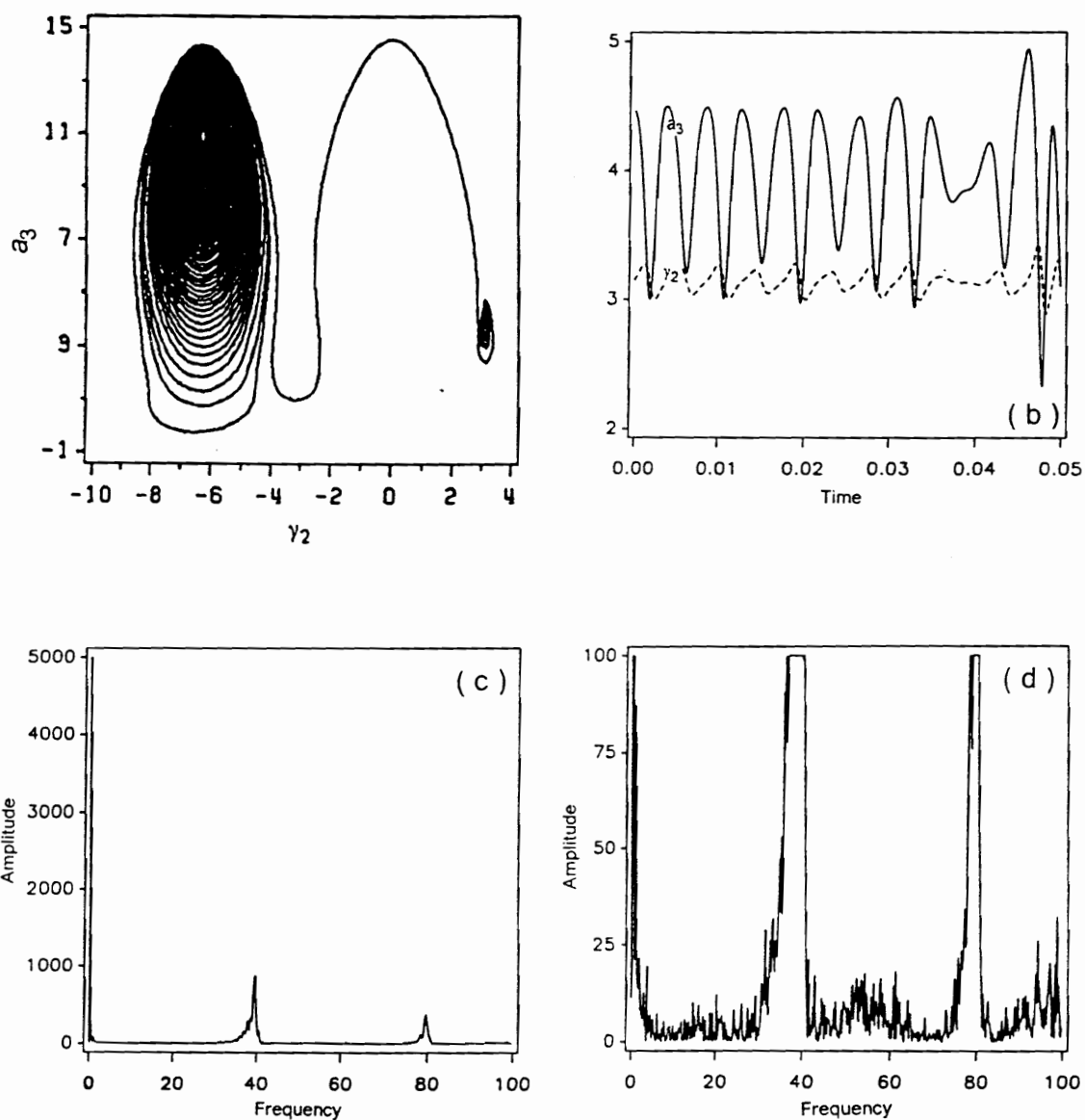


**Figure 5.11.** (a) Projection of the transient chaos trajectory on  $\gamma_2 - a_3$  plane, (b) the time evolution of  $\gamma_2$  and  $a_3$ , (c) FFT of the response, (d) the detail of FFT in (c).  $\varepsilon\mu = .01$ ;  $\varepsilon\sigma = 5.0$ ;  $\varepsilon h = 1079.301$ ,  $\varepsilon = 1.067 \times 10^{-3}$ .

## **6. SUMMARY AND RECOMMENDATIONS FOR FUTURE WORK**

### ***6.1. Present Study***

The method of virtual displacements is used to derive a set of five coupled nonlinear partial-differential equations governing the response of composite plates. The third-order shear-deformation theory of Reddy (1984a,b) and Bhimaraddi and Stevens (1984) is used to account for shear deformations. In this theory it is assumed that the transverse shear stresses are piecewise parabolic across the plate thickness and that the shear strains vanish at the top and bottom surfaces of the plate. The geometric nonlinearity of the von Karman type is considered and the effects of inplane and rotary inertias are also accounted for.

The governing partial-differential equations for the cases of free vibrations and linear stability are transformed into a set of five first-order ordinary-differential equations for the case of Levy-type solutions. The state-space concept is used and

the boundary conditions are applied to obtain equations for the natural frequencies and critical loads of the problem of free vibrations and linear stability, respectively. However, the straightforward application of the state-space concept is found to yield numerically ill-conditioned problems as the plate thickness is reduced. Various methods along with their advantages and disadvantages to overcome this problem are discussed. An initial value method with orthonormalization is selected. Through numerical examples it is shown that this method yields results that are in excellent agreement with previous results in the literature. It is shown that the method converges fast and yields all the frequencies and loads regardless of the plate thickness. The results are compared with the results obtained by using classical plate theory and it is shown that the application of CPT yields inaccurate results for thick plates.

The interaction of modes in shear-deformable rectangular composite plates subject to a harmonic external excitation is studied. A simply-supported plate is considered and a Navier-type solution is obtained for the linear problem. One of the natural frequencies is found to be near twice another one. Therefore, the case of two-to-one autoparametric resonance is investigated. The method of multiple scales is applied directly to the Lagrangian and four first-order ordinary-differential equations governing the modulation of the amplitudes and phases of the interacting modes are derived. The fixed points of these equations are determined. It is shown that in addition to a one-mode solution, two-mode solutions are possible. In the latter case, the mode which is indirectly excited through the internal resonance may dominate the response. The stability of the fixed points are determined and for certain plate and excitation parameter values, a Hopf bifurcation that gives birth to limit cycle solutions is found. The stability of these limit cycles is determined by



investigating the corresponding Floquet multipliers. It is shown that these limit cycles undergo a sequence of period-doubling bifurcations, leading to chaos.

The nonlinear response of axisymmetric circular plates in the presence of a combination resonance involving the first three modes is also investigated. The method of multiple scales is used to derive a set of ordinary-differential equations governing the modulation of amplitudes and phases. The fixed-point solutions and their stabilities are determined. It is shown that the excited mode is not necessarily the dominant one. As in the case of rectangular composite plates, a Hopf bifurcation is found. It is shown that the response may be (a) a nonlinear single- or three-mode periodic motion, (b) a nonlinear amplitude- and phase-modulated motion, or (c) a chaotically modulated motion.

## ***6.2. Recommendations for Future Work***

The nonlinear dynamic characteristics of plates are very rich subject and need extensive investigations. The study presented in this dissertation is just an infinitesimal piece of the research that the subject deserves. The following related topics are recommended for future study:

1. The use of Navier- and Levy-type solutions for composite plates is limited to certain stacking sequences, boundary conditions, etc.. In the case of generally laminated plates of arbitrary boundary conditions, another method such as finite-element method needs to be applied to solve the linear problem, which is the first approximation in a nonlinear analysis of the response of plates.

2. Composite plates used in many space vehicles and structures are sometimes designed to carry loads well beyond their buckling strength. Therefore, the postbuckling dynamics of composite plates needs to be investigated in detail.
3. The method of multiple scales is used in the nonlinear analysis of circular plates. These plates could also be analyzed by averaging the Lagrangian.
4. Modal interactions in plates needs to be investigated experimentally. Comparison of the theoretical and experimental results is a necessity.

We also recommend that the classical plate theory should be avoided in the analysis of thick and moderately thick composite plates.

## References

1. Aprille, T. J. and Trick, T. N. (1972). A computer algorithm to determine the steady-state response of nonlinear oscillators. *IEEE Transactions on Circuits Systems, CAS-4*, pp. 354-366.
2. Asfar, O. R., Masad, J. A., and Nayfeh, A. H. (1990). A method for calculating the stability of boundary layers. *Computers & Fluids*, Vol. 18, pp. 305-315.
3. Awrejcewicz, A. (1989). A route to chaos in a nonlinear oscillator with delay. *Acta Mechanica*, Vol. 77, pp. 111-120.
4. Balachandran, B. and Nayfeh, A. H. (1990). Nonlinear motion of a beam-mass structure. *Nonlinear Dynamics*, Vol. 1, pp. 39-61.
5. Banerjee, B. (1982). Large deflection of circular plates of variable thickness. *Journal of Applied Mechanics*, Vol. 49, pp. 243-245.
6. Banerjee, B. (1983). Large deflection of circular plates of variable thickness. *International Journal of Solids and Structures*, Vol. 19, pp. 179-183.
7. Bellman, R. E. and Kalaba, R. E. (1965). *Quasilinearization and Boundary-Value Problems*. American Elsevier, New York.
8. Bennett, J. A. (1971). Nonlinear vibration of simply supported angle ply laminated plates. *AIAA Journal*, Vol. 9, pp. 1997-2003.

9. Berger, H. M. (1955). A new approach to the analysis of large deflection of plates. *Journal of Applied Mechanics*, Vol. 22, pp. 465-472.
10. Bhimaraddi, A. and Stevens, L. K. (1984). Higher-order theory for free vibration of orthotropic, homogeneous, and laminated rectangular plates. *Journal of Applied Mechanics*, Vol. 51, pp. 195-198.
11. Brogan, W. L. (1974). *Modern Control Theory*. Quantum Publisher, New York.
12. Chandra, R. (1976). Large deflection vibration of cross-ply laminated plates with certain edge conditions. *Journal of Sound and Vibrations*, Vol. 47, pp. 509-514.
13. Chandra, R. and Raju, B. B. (1975). Large amplitude flexural vibration of cross-ply laminated composite plates. *Fiber Science and Technology*, Vol. 8, pp. 243-263.
14. Chia, C. Y. (1980). *Nonlinear Analysis of Plates*. McGraw-Hill, New York.
15. Chia, C. Y. and Prabhakara, M. K. (1976). Large deflection of unsymmetric cross-ply and angle-ply plates. *Journal of Mechanics and Engineering Science*, Vol. 18, pp. 179-183.
16. Chia, C. Y. and Prabhakara, M. K. (1978). A general mode approach to nonlinear flexural vibration of laminated rectangular plates. *Journal of Applied Mechanics*, Vol. 45, pp. 623-628.
17. Chow, S. N. and Hale, J. K. (1982). *Methods of Bifurcation Theory*. Springer-Verlag, New York.
18. Christensen, R. M. (1979). *Mechanics of Composite Materials*. Wiley-Interscience, New York.
19. Chu, H. N. and Herrmann, G. (1956). Influence of large amplitudes on free flexural vibrations of rectangular elastic plates. *Journal of Applied Mechanics*, Vol. 23, pp. 532-540.

20. Cohen, G. A. (1976). Analysis of multicircuit shells of revolution by the Field Method. *Computer Methods in Applied Mechanics and Engineering*, Vol. 8, pp. 301-318.
21. Cohen, G. A. (1982). Effect of transverse shear deformation on anisotropic plate buckling. *Journal of Composite Materials*, Vol. 16, pp. 301-312.
22. Conte, S. D. (1966). The numerical solution of linear boundary value problems. *Society for Industrial and Applied Mathematics Review*, Vol. 8, pp. 309-321.
23. Cooley, J. W. and Tukey, J. A. (1965). An algorithm for the machine calculation of complex Fourier series. *Mathematical Computations*, Vol. 19, pp. 297-301.
24. Davey, A. (1973). A simple numerical method for solving Orr-Sommerfeld problems. *Quarterly Journal of Mechanics and Applied Mathematics*, Vol. 26, pp. 401-411.
25. Eisley, J. G. (1964). Large amplitude vibration of buckled beams and plates. *AIAA Journal*, Vol. 2, pp. 2207-2209.
26. Eslami, H. and Kandil, O. (1989). Nonlinear forced vibration of orthotropic rectangular plates using the method of multiple scales. *AIAA Journal*, Vol. 27, pp. 955-967.
27. Evan-Iwanowski, R. M. (1976). *Resonance oscillations in mechanical systems*. Elsevier, New York.
28. Feiginbaum, M. J. (1979). The universal metric properties of nonlinear transformations. *Journal of Statistical Physics*, Vol. 21, pp. 669-706.
29. Feng, Z. C. and Sethna, P. R. (1989). Symmetry-breaking bifurcations in resonant surface waves. *Journal of Fluid Mechanics*, Vol. 199, pp. 495-518.
30. Franklin, J. N. (1968). *Matrix Theory*. Prentice-Hall, New Jersey.

31. Frederickson, R., Kaplan, J. L., Yorke, E. D., and Yorke, J. A. (1983). The Lyapunov dimension of strange attractors. *Journal of Differential Equations*, Vol. 49, pp. 185-207.
32. Gersting, J. M. and Jankowski, D. F. (1972). Numerical methods for Orr-Sommerfeld problems. *International Journal for Numerical Methods in Engineering*, Vol. 4, pp. 195-206.
33. Godunov, S. K. (1961). On the numerical solution of boundary-value problems for systems of linear ordinary differential equations. *Uspekhi Matematicheskikh Nauk*, Vol. 16, pp. 171-174.
34. Guckenheimer, J. and Holmes, P. J. (1983). *Nonlinear Oscillations, Dynamical Systems and Bifurcation of Vector Fields*. Springer-Verlag, New York.
35. Gurgoze, M. (1986). Parametric vibrations of a restrained beam with an end mass under displacement excitation. *Journal of Sound and Vibration*, Vol. 108, pp. 73-84.
36. Haddow, A. G., Barr, A. D. S., and Mook, D. T. (1984). Theoretical and experimental study of modal interaction in a two-degree-of-freedom structure. *Journal of Sound and Vibration*, Vol. 97, pp. 451-473.
37. Hale, J. K. (1963). *Oscillations in Nonlinear Systems*. McGraw-Hill, New York.
38. HaQuang, N. (1986). The response of multidegree-of-freedom systems with quadratic and cubic nonlinearities subjected to parametric and external excitation. Ph.D Dissertation, Virginia Polytechnic Institute and State University, Blacksburg, Virginia.
39. Hassard, B. D., Kazarinoff, N. D., and Wan, Y. H. (1981). *Theory and Application of Hopf Bifurcation*. Cambridge University Press, Cambridge.
40. Hatwal, H., Mallik, A. K., and Ghosh, A. (1983a). Forced nonlinear oscillations of an autoparametric system- part 1: periodic responses. *ASME Journal of Applied Mechanics*, Vol. 50, pp. 657-662.

41. Hatwal, H., Mallik, A. K., and Ghosh, A. (1983b). Forced nonlinear oscillations of an autoparametric system- part 1: chaotic responses. *ASME Journal of Applied Mechanics*, Vol. 50, pp. 663-668.
42. Huang, C. (1973). Finite amplitude vibrations of an orthotropic circular plate with an isotropic core. *AIAA Journal*, Vol. 12, pp. 388-390.
43. Huang, C. L. and Al-Khattat, I. M. (1977). Finite amplitude vibrations of a circular plate. *International Journal of Non-Linear Mechanics*, Vol. 12, pp. 297-306.
44. Huang, C. and Sandman, B. E. (1971). Large amplitude vibrations of a rigidly clamped circular plate. *International Journal of Non-Linear Mechanics*, Vol. 6, pp. 451-468.
45. Ibrahim, R. A. (1985). *Parametric Random Vibration*. Wiley-Interscience, New York.
46. looss, G. and Joseph, D. D. (1980). *Elementary Stability and Bifurcation Theory*. Springer-Verlag, New York.
47. Jones, R. M. (1975). *Mechanics of Composite Materials*. McGraw-Hill, New York.
48. Jordan, D. W. and Smith, P. (1977). *Nonlinear Ordinary Differential Equations*. Clarendon Press, Oxford.
49. Kalnins, A. (1964). Analysis of shells of revolution subjected to symmetrical and nonsymmetrical loads. *Journal of Applied Mechanics*, Vol. 31, pp. 467-476.
50. Khdeir, A. A. (1988). Free vibration of and buckling of symmetric cross-ply laminated plates by an exact method. *Journal of Sound and Vibration*, Vol. 126, pp. 447-461.
51. Khdeir, A. A. (1989). Free vibration and buckling of unsymmetric cross-ply laminated plates using a refined theory. *Journal of Sound and Vibration*, Vol. 128, pp. 377-395.

52. Kojima, H., Nagaya, J., Shiraishi, H., and Yamashita, A. (1985). Nonlinear vibrations of a beam with a mass subjected to alternating electromagnetic force. *Bulletin of Japan Society of Mechanical Engineers*, Vol. 18, pp. 468-475.
53. Kung, G. C. and Pao, Y. H. (1972). Nonlinear flexural vibration of a clamped circular plate. *Journal of Applied Mechanics*, Vol. 39, pp. 1050-1054.
54. Leissa, A. W. (1969). *Vibration of plates*. NASA-SP-160.
55. Leissa, A. W. (1987). A review of laminated composite plate buckling. *Applied Mechanics Reviews*, Vol. 40, pp. 575-591.
56. Levinson, M. (1980). An accurate simple theory of statics and dynamics of elastic plates. *Mechanics Research Communications*, Vol. 7, pp. 343-350.
57. Lo, K. H., Christensen, R. M., and Wu, E. M. (1977a). A high-order theory of plate deformation-part 1: homogeneous plates. *Journal of Applied Mechanics*, Vol. 44, pp. 663-668.
58. Lo, K. H., Christensen, R. M., and Wu, E. M. (1977b). A high-order theory of plate deformation, part 2: laminated plates. *Journal of Applied Mechanics*, Vol. 44, pp. 669-676.
59. Lobitz, D. W., Nayfeh, A. H., and Mook, D. T. (1977). Nonlinear analysis of vibrations of irregular plates. *Journal of Sound and Vibration*, Vol. 50, pp. 203-217.
60. Maganty, S. P. and Bickford, W. B. (1988). Influence of internal resonance on the non-linear oscillations of a circular ring under primary resonance conditions. *Journal of Sound and Vibration*, Vol. 122, pp. 521-547.
61. Marsden, J. E. and McCracken, M. (1976). *The Hopf Bifurcation and its Applications*. Springer-Verlag, New York.
62. Medwadowski, S. J. (1958). A refined theory of elastic, orthotropic plates. *Journal of Applied Mechanics*, Vol. 25, pp. 437-443.



63. Mei, C. (1973). Finite element displacement method for large amplitude free flexural vibrations of beams and plates. *Computers & Structures*, Vol. 3, pp. 163-174.
64. Miles, J. W. (1984a). Nonlinear Faraday resonance. *Journal of Fluid Mechanics*, Vol. 146, pp. 285-302.
65. Miles, J. W. (1984b). Resonantly forced motion of two quadratically coupled oscillators. *Physica D*, Vol. 13, pp. 247-260.
66. Miles, J. W. (1985). Parametric excitation of an internally resonant double pendulum. *Journal of Applied Mathematics and Physics (ZAMP)*, Vol. 36, pp. 337-345.
67. Mindlin, R. D. (1951). Influence of rotary inertia and shear on flexural motion of isotropic, elastic plates. *Journal of Applied Mechanics*, Vol. 18, pp. A31-A38.
68. Mook, D. T., Marshall, L. R., and Nayfeh, A. H. (1974). Subharmonic and superharmonic resonances in the pitch and roll modes of ship motions. *Journal of Hydrodynamics*, Vol. 8, pp. 32-40.
69. Moon, F. C. (1987). *Chaotic Vibrations, an Introduction for Applied Scientists and Engineers*. Wiley-Interscience, New York.
70. Murthy, M. V. V. (1981). An improved transverse shear deformation theory for laminated anisotropic plates. *NASA Technical Paper 1903*.
71. Narita, Y. and Leissa, A. W. (1990). Buckling studies for simply supported symmetrically laminated rectangular plates. *International Journal of Mechanical Science*, Vol. 32, pp. 909-924.
72. Nash, W. A. and Modeer, J. R. (1959). Certain approximate analysis of the nonlinear behavior of plates and shallow shells. *Proceedings of the Symposium on Theory of Thin Elastic Shells*. Wiley-Interscience, New York.
73. Nayfeh, A. H. (1973). *Perturbation Methods*. Wiley-Interscience, New York.

74. Nayfeh, A. H. (1981). Introduction to Perturbation Techniques. Wiley Interscience, New York.
75. Nayfeh, A. H. (1987a). Parametric excitation of two internally resonant oscillators. *Journal of Sound and Vibration*, Vol. 119, pp. 95-109.
76. Nayfeh, A. H. (1987b). Surface waves in closed basins under parametric and internal resonances. *Physics of Fluids*, Vol. 30, pp. 2976-2983.
77. Nayfeh, A. H. (1988). Numerical-perturbation methods in mechanics. *Computers & Structures*, Vol. 30, pp.185-204.
78. Nayfeh, A. H. and Asfar, K. R. (1986). Response of a bar constrained by a nonlinear spring to a harmonic excitation. *Journal of Sound and Vibration* Vol. 105, pp. 1-15.
79. Nayfeh, A. H. and Mook, D. T. (1979). *Nonlinear Oscillations*. Wiley-Interscience, New York.
80. Nayfeh, A. H., Mook, D. T., and Marshall, L. R. (1973). Nonlinear coupling of pitch and roll modes in ship motions. *Journal of Hydrodynamics*, Vol. 7, pp. 145-152.
81. Nayfeh, A. H. and Pai, P. F. (1989). Non-linear non-planar parametric responses of an inextensional beam. *International Journal of Non-Linear Mechanics*, Vol. 24, pp. 139-158.
82. Nayfeh, A. H. and Raouf, R. A. (1987). Non-linear oscillations of circular cylindrical shells. *International Journal of Solids and Structures*, Vol. 23, pp. 1625-1638.
83. Nayfeh, A. H., Raouf, R. A., and Nayfeh, J. F. (1990). Nonlinear response of infinitely long circular shells to subharmonic radial loads. *Journal of Applied Mechanics*, to appear.
84. Nayfeh, A. H. and Zavodney, L. D. (1986). The response of two-degree-of-freedom system with quadratic non-linearities to a combination parametric resonance. *Journal of Sound and Vibration*, Vol. 107, pp. 329-350.

85. Noble, B. and Daniel, J. W. (1977). Applied Linear Algebra. Prentice-Hall, New Jersey.
86. Noor, A. K. (1973a). Free vibration of multilayered composite plates. AIAA Journal, Vol. 11, pp. 1038-1039.
87. Noor, A. K. (1973b). Mixed finite-difference scheme for simply supported thick plates. Computers & Structures, Vol. 3, pp. 967-982.
88. Noor, A. K. (1975). Stability of multilayered composite plates. Fibre Science and Technology, Vol. 8, pp. 81-89.
89. Noor, A. K. and Hartley, S. J. (1977). Effects of shear deformation and anisotropy on the non-linear response of composite plates. Development in Composite Materials 1, G. Holister (ed.), pp. 55-65, Applied Science Publishers, Barking, Essex .
90. Nowinski, J. L. and Ohnabe, H. (1972). On certain inconsistencies in Berger equations for large deflection of plastic plates. International Journal Mech. Sci., Vol. 14, pp. 165-170.
91. Pagano, N. J. (1969). Exact solutions for composite laminates in cylindrical bending. Journal of Composite Materials, Vol. 3, pp. 398-411.
92. Pagano, N. J. (1970). Exact solutions for rectangular bidirectional composite and sandwich plates. Journal of Composite Materials, Vol. 4, pp. 20-34.
93. Pai, P. F. and Nayfeh, A. H. (1991a). Three-dimensional nonlinear vibration of composite beams. II. flapwise excitation. Nonlinear Dynamics, Vol. 2, pp. 1-34.
94. Pai, P. F. and Nayfeh, A. H. (1991b). Three-dimensional nonlinear vibration of composite beams. II. chordwise excitation. Nonlinear Dynamics, Vol. 2, pp. 137-156.
95. Prabhakara, M. K. and Chia, C. Y. (1977). Non-linear flexural vibrations of orthotropic rectangular plates. Journal of Sound and Vibration, Vol. 52, pp. 511-518.

96. Prathap, G. and Pandalai, K. A. V. (1979). Non-linear vibrations of transversely isotropic rectangular plates. *International Journal of Non-Linear Mechanics*, Vol. 13, pp. 285-294.
97. Rajgopal, S. V., Singh, G., Sadasiva Rao, Y. V. K., and Narayanan, S. (1986). Nonlinear vibration of sandwich plates. *Journal of Sound and Vibration*, Vol. 110, pp. 261-269.
98. Rao, G. V., raju, I. S., and Kanaka Raju, K. (1976). A finite element formulation for large amplitude flexural vibration of thin rectangular plates. *Computers & Structures*, Vol. 6, pp. 163-167.
99. Raouf, R. A. and Nayfeh, A. H. (1990a). One-to-one autoparametric resonances in infinitely long cylindrical shells. *Computers & Structures*, submitted for publication.
100. Raouf, R. A. and Nayfeh, A. H. (1990b). Nonlinear axisymmetric response of spherical shells to a radial harmonic excitation. *International Journal of Non-Linear Mechanics*, submitted for publication.
101. Reddy, J. N. (1984a). A refined nonlinear theory of plates with transverse shear deformation. *International Journal of Solids and Structures*, Vol. 20, pp. 881-896.
102. Reddy, J. N. (1984b). A simple higher-order theory for laminated composite plates. *Journal of Applied Mechanics*, Vol. 51, pp. 745-752.
103. Reddy, J. N. (1984c). *Energy and Variational Methods in Applied Mechanics*. Wiley, New York.
104. Reddy, J. N. (1990). A general non-linear third-order theory of plates with moderate thickness. *International Journal of Non-Linear Mechanics*, Vol. 25, pp. 677-686.
105. Reddy, J. N. and Chao, W. C. (1981a). Large deflection and large amplitude free vibrations of laminated composite material plates. *Computers & Structures*, Vol. 13, pp. 341-347.

106. Reddy, J. N. and Chao, W. C. (1981b). Nonlinear oscillations of laminated, anisotropic, thick rectangular plates. *Advances in Aerospace Structures and Materials*. The winter annual meeting of the American Society of Mechanical Engineering, Washington, D.C.
107. Reddy, J. N. and Khdeir, A. A. (1989). Buckling and vibration of laminated composite plates using various plate theories. *AIAA Journal*, Vol. 27, pp. 1808-1817.
108. Rehfield, L. W. (1974). Large amplitude forced vibration of elastic structures. *AIAA Journal*, Vol. 12, pp. 388-390.
109. Reissner, E. (1945). The effect of transverse shear deformation on the bending of elastic plates. *Journal of Applied Mechanics*, Vol. 12, pp. A69-A77.
110. Sathyamoorthy, M. (1978). Vibration of plates considering shear and rotary inertia. *AIAA Journal*, Vol. 16, pp. 285-286.
111. Sathyamoorthy, M. (1979). Effects of large amplitude, shear and rotatory inertia on vibration of rectangular plates. *Journal of Sound and Vibration*, Vol. 63, pp. 161-167.
112. Sathyamoorthy, M. (1981). Transverse shear and rotary inertia effects on nonlinear vibration of orthotropic circular plates. *Computers & Structures*, Vol. 14, pp. 129-134.
113. Sathyamoorthy, M. (1984a). Multiple mode non-linear dynamic analysis of thick orthotropic elliptic plates. *Journal of Sound and Vibration*, Vol. 96, pp. 353-361.
114. Sathyamoorthy, M. (1984b). Vibration of orthotropic thick plates. *AIAA Journal*, Vol. 22, pp.851-854.
115. Sathyamoorthy, M. and Chia, C. Y. (1980). Non-linear vibration of anisotropic rectangular plates including shear and rotatory inertia. *Fiber Science and Technology*, Vol. 13, pp. 337-361.

116. Sathyamoorthy, M. and Prasad, M. E. (1983). Multiple mode nonlinear analysis of circular plates. *Journal of Engineering Mechanics*, Vol. 109, pp. 1114-1123.
117. Schmidt, R. (1977). Refined non-linear theory of plates with transverse shear deformation. *Industrial Mathematics*, Vol. 27, pp. 23-38.
118. Schmidt, G. and Tondl, A. (1986). *Non-linear Vibrations*. Akademie-Verlag, Berlin.
119. Scott, M. R. (1974). On the conversion of boundary-value problems into stable initial-value problems via several invariant imbedding algorithms. Sandia Laboratories Report SAND74-0006.
120. Scott, M. R. and Watts, H. A. (1977). Computational solution of linear two-point boundary value problems and orthonormalization. *SIAM Journal on Numerical Analysis*, Vol. 14, pp. 40-70.
121. Seydel, R. (1988). *From Equilibrium to Chaos: Practical Bifurcation and Stability Analysis*. Elsevier, New York.
122. Shaw, J. and Shaw, S. W. (1989). The onset of chaos in a two-degree-of-freedom impacting system. *Journal of Applied Mechanics*, Vol. 56, pp. 168-174.
123. Singh, P. N., Sundararajan, V., and Das, Y. C. (1974). Large amplitude vibration of some moderately thick structural elements. *Journal of Sound and Vibration*, Vol. 36, pp. 375-387.
124. Singleton, R. C. (1969). An algorithm for computing the mixed radix fast Fourier transform. *IEEE Transactions on Audio and Electroacoustics*, AU-17, pp. 93-103.
125. Sivakumaran, K. S. and Chia, C. Y. (1985). Large-amplitude oscillations of unsymmetrically laminated anisotropic rectangular plates including shear, rotary inertia, and transverse normal stress. *Journal of Applied Mechanics*, Vol. 52, pp. 536-542.
126. Sokolnikoff, I. S. and Redheffer, R. M. (1966). *Mathematics of Physics and Modern Engineering*. McGraw-Hill, New York.

127. Sridhar, S., Mook, D. T., and Nayfeh, A. H. (1975). Non-linear resonances in the forced responses of plates, part I: symmetric response of circular plates. *Journal of Sound and Vibration*, Vol. 41, pp. 359-373.
128. Sridhar, S., Mook, D. T., and Nayfeh, A. H. (1978). Non-linear resonances in the forced responses of plates, part II: asymmetric responses of circular plates. *Journal of Sound and Vibration*, Vol. 59, pp. 159-170.
129. Srinivas, S. and Rao, A. K. (1970). Bending, vibration and buckling of simply-supported thick orthotropic rectangular plates and laminates. *International Journal of Solids and Structures*, Vol. 6, pp. 1463-1481.
130. Srinivas, S., Rao, C. V. J., and Rao, A. K. (1970). An exact analysis of vibration of simply supported homogeneous and laminated thick rectangular plates. *Journal of Sound and Vibration*, Vol. 12, pp. 187-199.
131. Stavsky, Y. (1965). On the theory of symmetrically heterogeneous plates having the same thickness variation of the elastic moduli. In *Topics in Applied Mechanics*, D. Abir, D. F. Ollendorff, and M. Reiner, Eds., American Elsevier, New York.
132. Streit, D. A., Bajaj, A. K., and Krousgrill, C. M. (1988). Combination parametric resonances leading to periodic and chaotic response in two-degree-of-freedom system with quadratic non-linearities. *Journal of Sound and Vibration*, Vol. 124, pp. 297-314.
133. Szemplinska-Stupnicka, W. (1978). The generalized harmonic balance method for determining the combination resonance in the parametric dynamic systems. *Journal of Sound and Vibration*, Vol. 58, pp. 347-361.
134. Thompson, J. M. T. and Stewart, H. B. (1986). *Nonlinear dynamics and chaos, geometric methods for engineers and scientists*. John Wiley and Sons Ltd., Great Britain.
135. Timoshenko, S. P. and Woinowsky-Krieger, S. (1959). *Theory of Plates and Shells*. McGraw-Hill, New York.

136. Tobias, S. A. (1958). Non-linear forced vibrations of circular disks. An experimental investigation. *Engineering*, Vol. 186, pp. 51-56.
137. Tsai, S. W. and Hahn, H. T. (1980). *Introduction to Composite Materials*. Technomic Publishing Co., Westport, CT.
138. Urabe, M. (1967). *Nonlinear Autonomous Oscillations*. Academic Press, New York and London.
139. Vanderbauwhede, A. (1982). *Local Bifurcations and Symmetry*. Pitman Books Ltd., Great Britain.
140. von Karman, T. (1910). Festigkeitsprobleme in maschinenbau. *Encyklopadie der Mathematischen Wissenschaften*, (P. R. Halmos, Ed.), American Mathematical Society, Vol. 3, pp. 211-385.
141. Wah, T. (1963). Large amplitude flexural vibrations of rectangular plates. *International Journal of Mechanical Sciences*, Vol. 5, pp. 425-438.
142. Watson, L. T., Billups, S. C., and Morgan, A. P. (1987). Hompack: a suite of codes for globally convergent homotopy algorithms. *ACM Transactions of Mathematical Software*, Vol. 13, pp. 281-310.
143. Wolf, A., Swift, J. B., Swinney, H. L., and Vastano, J. A. (1985). Determining Lyapunov exponents from a time series. *Physica-D*, Vol. 16, pp. 285-317.
144. Wu, C. I. and Vinson, J. R. (1969a). Influence of large amplitude, transverse shear deformation, and rotatory inertia on lateral vibrations of transversely isotropic plates. *Journal of Applied Mechanics*, Vol. 36, pp. 256-260.
145. Wu, C. I. and Vinson, J. R. (1969b). On the nonlinear oscillations of plates composed of composite materials. *Journal of Composite Materials*, Vol. 3, pp. 548-561.
146. Wu, C. I. and Vinson, J. R. (1971). Non-linear oscillations of laminated specially orthotropic plates with clamped and simply supported edges. *Journal of Acoustical Society of America*, Vol. 49, pp. 1561-1567.



147. Yamaki, N. (1967). Influence of large amplitudes on flexural vibrations of elastic plates. *Zeitschrift fur angewandte Mathematik und Mechanik*, Vol. 41, pp. 501-510.
148. Yamamoto, T. and Yasuda, K. (1977). On the internal resonance in a nonlinear two-degree-of-freedom system-forced vibrations near the lower resonance point when the natural frequencies are in the ratio 1:2. *Bulletin of Japan Society of Mechanical Engineers*, Vol. 20, pp. 168-175.
149. Yasuda, K. and Kushida, G. (1984). Nonlinear forced oscillations of a shallow spherical shell. *Bulletin of Japan Society of Mechanical Engineers*, Vol. 27, pp. 2233-2240.
150. Yasuda, K. and Torii, T. (1986). Nonlinear forced oscillations of a string, 2nd report: various types of responses near resonance points. *Bulletin of Japan Society of Mechanical Engineers*, Vol. 29, pp. 1253-1260.
151. Zavodney, L. D. and Nayfeh, A. H. (1988). The response of a single-degree-of-freedom system with quadratic and cubic non-linearities to a fundamental parametric resonance. *Journal of Sound and Vibration*, Vol. 120, pp. 63-93.

## Appendix A. The elements of the coefficient matrix in equation (3.10): free vibrations

The nonzero elements of the matrix  $\mathbf{A}(\omega)$  in equation (3.10) with the subscript  $m$  dropped are:

$$a_{1,2} = a_{3,4} = a_{5,6} = a_{6,7} = a_{7,8} = a_{9,10} = a_{11,12} = 1$$

$$a_{2,1} = \hat{D}_{66}(-I_1\omega^2 + \alpha^2 A_{11})/d_1$$

$$a_{2,4} = -\alpha \hat{D}_{66}(A_{12} + A_{66})/d_1$$

$$a_{2,5} = \alpha \hat{D}_{66}(I_2\omega^2 - \alpha^2 B_{11})/d_1$$

$$a_{2,9} = \hat{D}_{66}(-\bar{I}_2\omega^2 + \alpha^2 \hat{B}_{11})/d_1$$

$$a_{4,2} = \alpha \hat{D}_{22}(A_{12} + A_{66})/d_2$$

$$a_{4,3} = [\hat{D}_{22}(-I_1\omega^2 + \alpha^2 A_{66}) + \hat{B}_{22}\bar{I}_2\omega^2]/d_2$$

$$a_{4,6} = \{\hat{D}_{22}I_2\omega^2 - \hat{B}_{22}[\bar{I}_0\omega^2 - \alpha^2(\tilde{D}_{12} + 2\tilde{D}_{66})]\}/d_2$$

$$a_{4,8} = (\hat{D}_{22}B_{22} - \hat{B}_{22}\tilde{D}_{22})/d_2$$

$$a_{4,10} = -\alpha \hat{B}_{22}(\hat{D}_{12} + \hat{D}_{66})/d_2$$

$$a_{4,11} = [-\hat{D}_{22}\bar{I}_2\omega^2 - \hat{B}_{22}(-\bar{I}_3\omega^2 + \alpha^2 \hat{D}_{66} - D_{44})]/d_2$$

$$a_{10,1} = A_{66}(-\bar{I}_2\omega^2 + \alpha^2 \hat{B}_{11})/d_1$$

$$a_{10,5} = \alpha A_{66}(\bar{I}_0\omega^2 - \alpha^2 \tilde{D}_{11})/d_1$$

$$a_{10,7} = \alpha A_{66}(\tilde{D}_{12} + 2\tilde{D}_{66})/d_1$$

$$a_{10,9} = A_{66}(-\bar{l}_3\omega^2 + \alpha^2\hat{D}_{11} - D_{55}^*)/d_1$$

$$a_{10,12} = -\alpha A_{66}(\hat{D}_{12} + \hat{D}_{66})/d_1$$

$$a_{12,2} = -\alpha\hat{B}_{22}(A_{12} + A_{66})/d_2$$

$$a_{12,3} = -[A_{22}\bar{l}_2\omega^2 + \hat{B}_{22}(-l_1\omega^2 + \alpha^2 A_{66})]/d_2$$

$$a_{12,6} = \{A_{22}[\bar{l}_0\omega^2 - \alpha^2(\tilde{D}_{12} + 2\tilde{D}_{66})] - \hat{B}_{22}l_2\omega^2\}/d_2$$

$$a_{12,8} = (A_{22}\tilde{D}_{22} - \hat{B}_{22}B_{22})/d_2$$

$$a_{12,10} = \alpha A_{22}(\hat{D}_{12} + \hat{D}_{66})/d_2$$

$$a_{12,11} = [A_{22}(-\bar{l}_3\omega^2 + \alpha^2\hat{D}_{66} - D_{44}^*) + \hat{B}_{22}\bar{l}_2\omega^2]/d_2$$

$$a_{8,1} = (a_{2,1}d_4 + a_{10,1}d_5 + \alpha^3 B_{11} - \alpha l_2\omega^2)/d_3$$

$$a_{8,4} = [a_{2,4}d_4 + a_{10,4}d_5 + a_{4,3}B_{22} + a_{12,3}\tilde{D}_{22} + l_2\omega^2]/d_3$$

$$a_{8,5} = [a_{2,5}d_4 + a_{10,5}d_5 - \alpha^4 D_{11} + (l_1 + \alpha^2 l_3)\omega^2]/d_3$$

$$a_{8,7} = [a_{2,7}d_4 + a_{10,7}d_5 + a_{4,6}B_{22} + a_{12,6}\tilde{D}_{22} + \alpha^2(2D_{12} + 4D_{66}) - l_3\omega^2]/d_3$$

$$a_{8,9} = (a_{2,9}d_4 + a_{10,9}d_5 + \alpha^3\tilde{D}_{11} - \alpha\bar{l}_0\omega^2)/d_3$$

$$a_{8,12} = [a_{2,12}d_4 + a_{10,12}d_5 + a_{4,11}B_{22} + d_{12,11}\tilde{D}_{22} - \alpha^2(\tilde{D}_{12} + 2\tilde{D}_{66}) + \bar{l}_0\omega^2]/d_3$$

where

$$d_1 = A_{66}\hat{D}_{66}$$

$$d_2 = A_{22}\hat{D}_{22} - (\hat{B}_{22})^2$$

$$d_3 = D_{22} - a_{4,8}B_{22} - a_{12,8}\tilde{D}_{22}$$

$$d_4 = a_{4,2}B_{22} + a_{12,2}\tilde{D}_{22}$$

$$d_5 = a_{4,10}B_{22} + a_{12,10}\tilde{D}_{22} - \alpha(\tilde{D}_{12} + 2\tilde{D}_{66})$$

## Appendix B. The elements of boundary coefficient matrices in equation (3.11): free vibrations

The nonzero elements of  $\mathbf{R}_1$  and  $\mathbf{R}_2$  in equation (3.11) are:

i) Clamped edge

$$r_{1,1} = r_{2,3} = r_{3,5} = r_{4,6} = r_{5,9} = r_{6,11} = 1$$

ii) Simply supported edge

$$r_{1,1} = r_{1,5} = r_{3,9} = 1$$

$$r_{4,4} = A_{22}, \quad r_{4,7} = -B_{22}, \quad r_{4,12} = \hat{B}_{22}$$

$$r_{5,4} = B_{22}, \quad r_{5,7} = -D_{22}, \quad r_{5,12} = \hat{D}_{22}$$

$$r_{6,4} = E_{22}, \quad r_{6,7} = -F_{22}, \quad r_{6,12} = \frac{3}{4} h^2 \hat{F}_{22}$$

iii) Free edge

$$r_{1,1} = -\alpha A_{12}, \quad r_{1,4} = A_{22}, \quad r_{1,7} = -B_{22}, \quad r_{1,12} = \hat{B}_{22}$$

$$r_{2,4} = B_{22}, \quad r_{2,5} = \alpha^2 D_{12}, \quad r_{2,7} = -D_{22}, \quad r_{2,9} = -\alpha \tilde{D}_{12}, \quad r_{2,12} = \tilde{D}_{22}$$

$$r_{3,4} = \hat{B}_{22}, \quad r_{3,5} = \alpha^2 \tilde{D}_{12}, \quad r_{3,7} = -\tilde{D}_{22}, \quad r_{3,9} = -\alpha \hat{D}_{12}, \quad r_{3,12} = \hat{D}_{22}$$

$$r_{4,2} = A_{66}, \quad r_{4,3} = \alpha A_{66}$$

$$r_{5,6} = -2\alpha \tilde{D}_{66}, \quad r_{5,10} = \hat{D}_{66}, \quad r_{5,11} = \alpha \hat{D}_{66}$$

$$r_{6,2} = -\tilde{D}_{22} a_{12,2} - B_{22} a_{4,2}$$

$$r_{6,3} = -\tilde{D}_{22} a_{12,3} - B_{22} a_{4,3} - I_2 \omega^2$$

$$r_{6,6} = -\tilde{D}_{22} a_{12,6} - B_{22} a_{4,6} - \alpha^2 (D_{12} + 4D_{66}) + I_3 \omega^2$$

$$r_{6,8} = -\tilde{D}_{22}a_{12,8} - B_{22}a_{4,8} + D_{22}$$

$$r_{6,10} = -\tilde{D}_{22}a_{12,10} - B_{22}a_{4,10} + \alpha(\tilde{D}_{12} + 2\tilde{D}_{66})$$

$$r_{6,11} = -\tilde{D}_{22}a_{12,11} - B_{22}a_{4,11} + 2\alpha^2\tilde{D}_{66} - \bar{I}_0\omega^2$$

where  $a_{ij}$  are given in Appendix A and for convenience the subscript  $m$  of  $\omega$  and  $\alpha$  is dropped here.

## Appendix C. The elements of the coefficient matrix in equation (3.10): stability

The nonzero elements of the matrix  $\mathbf{A}(T_{11}, T_{22})$  in equation (3.10) with the subscript  $m$  dropped are:

$$a_{1,2} = a_{3,4} = a_{5,6} = a_{6,7} = a_{7,8} = a_{9,10} = a_{11,12} = 1$$

$$a_{2,1} = \alpha^2 \hat{D}_{66} A_{11} / d_1, \quad a_{2,4} = -\alpha \hat{D}_{66} (A_{12} + A_{66}) / d_1$$

$$a_{2,5} = -\alpha^3 \hat{D}_{66} B_{11} / d_1, \quad a_{2,9} = \alpha^2 \hat{D}_{66} \hat{B}_{11} / d_1$$

$$a_{4,2} = \alpha \hat{D}_{22} (A_{12} + A_{66}) / d_2, \quad a_{4,3} = \alpha^2 \hat{D}_{22} A_{66} / d_2$$

$$a_{4,6} = \alpha^2 \hat{B}_{22} (\tilde{D}_{12} + 2\tilde{D}_{66}) / d_2, \quad a_{4,8} = (\hat{D}_{22} B_{22} - \hat{B}_{22} \tilde{D}_{22}) / d_2$$

$$a_{4,10} = -\alpha \hat{D}_{22} (\hat{D}_{12} + \hat{D}_{66}) / d_2, \quad a_{4,11} = \hat{B}_{22} (-\alpha^2 \hat{D}_{66} + D_{44}^*) / d_2$$

$$a_{10,1} = \alpha^2 A_{66} \hat{B}_{11} / d_1, \quad a_{10,5} = -\alpha^3 A_{66} \tilde{D}_{11} / d_1, \quad a_{10,7} = \alpha A_{66} (\tilde{D}_{12} + 2\tilde{D}_{66}) / d_1$$

$$a_{10,9} = A_{66} (\alpha^2 \hat{D}_{11} - D_{55}^*) / d_1, \quad a_{10,12} = -\alpha A_{66} (\hat{D}_{12} + \hat{D}_{66}) / d_1$$

$$a_{12,2} = -\alpha \hat{B}_{22} (A_{12} + A_{66}) / d_2, \quad a_{12,3} = -\alpha^2 \hat{B}_{22} A_{66} / d_2$$

$$a_{12,6} = -\alpha^2 A_{22} (\tilde{D}_{12} + 2\tilde{D}_{66}) / d_2, \quad a_{12,8} = (A_{22} \tilde{D}_{22} - \hat{B}_{22} B_{22}) / d_2$$

$$a_{12,10} = \alpha A_{22} (\hat{D}_{12} + \hat{D}_{66}) / d_2, \quad a_{12,11} = A_{22} (\alpha^2 \hat{D}_{66} - D_{44}^*) / d_2$$

$$a_{8,1} = (a_{2,1} d_4 + a_{10,1} d_5 + \alpha^3 B_{11}) / d_3$$

$$a_{8,4} = (a_{2,4} d_4 + a_{10,4} d_5 + a_{4,3} B_{22} + a_{12,3} \tilde{D}_{22}) / d_3$$

$$a_{8,5} = [a_{2,5} d_4 + a_{10,5} d_5 - \alpha^4 D_{11} + \alpha^2 T_{11}] / d_3$$

$$a_{8,7} = [a_{2,7} d_4 + a_{10,7} d_5 + a_{4,6} B_{22} + a_{12,6} \tilde{D}_{22} + \alpha^2 (2D_{12} + 4D_{66}) - T_{22}] / d_3$$

$$a_{8,9} = (a_{2,9}d_4 + a_{10,9}d_5 + \alpha^3\tilde{D}_{11})/d_3$$

$$a_{8,12} = [a_{2,12}d_4 + a_{10,12}d_5 + a_{4,11}B_{22} + d_{12,11}\tilde{D}_{22} - \alpha^2(\tilde{D}_{12} + 2\tilde{D}_{66})]/d_3$$

where

$$d_1 = A_{66}\hat{D}_{66}$$

$$d_2 = A_{22}\hat{D}_{22} - (\hat{B}_{22})^2$$

$$d_3 = D_{22} - a_{4,8}B_{22} - a_{12,8}\tilde{D}_{22}$$

$$d_4 = a_{4,2}B_{22} + a_{12,2}\tilde{D}_{22}$$

$$d_5 = a_{4,10}B_{22} + a_{12,10}\tilde{D}_{22} - \alpha(\tilde{D}_{12} + 2\tilde{D}_{66})$$

## Appendix D. The elements of boundary coefficient matrices in equation (3.11): stability

The nonzero elements of  $\mathbf{R}_1$  and  $\mathbf{R}_2$  in equation (3.11) are:

i) Clamped edge

$$r_{1,1} = r_{2,3} = r_{3,5} = r_{4,6} = r_{5,9} = r_{6,11} = 1$$

ii) Simply supported edge

$$r_{1,1} = r_{1,5} = r_{3,9} = 1$$

$$r_{4,4} = A_{22}, \quad r_{4,7} = -B_{22}, \quad r_{4,12} = \hat{B}_{22}$$

$$r_{5,4} = B_{22}, \quad r_{5,7} = -D_{22}, \quad r_{5,12} = \hat{D}_{22}$$

$$r_{6,4} = E_{22}, \quad r_{6,7} = -F_{22}, \quad r_{6,12} = F_{22} - \frac{4}{3h^2} H_{22}$$

iii) Free edge

$$r_{1,1} = -\alpha A_{12}, \quad r_{1,4} = A_{22}, \quad r_{1,7} = -B_{22}, \quad r_{1,12} = \hat{B}_{22}$$

$$r_{2,4} = B_{22}, \quad r_{2,5} = \alpha^2 D_{12}, \quad r_{2,7} = -D_{22}, \quad r_{2,9} = -\alpha \tilde{D}_{12}, \quad r_{2,12} = \tilde{D}_{22}$$

$$r_{3,4} = \hat{B}_{22}, \quad r_{3,5} = \alpha^2 \tilde{D}_{12}, \quad r_{3,7} = -\tilde{D}_{22}, \quad r_{2,9} = -\alpha \hat{D}_{12}, \quad r_{3,12} = \hat{D}_{22}$$

$$r_{4,2} = A_{66}, \quad r_{4,3} = \alpha A_{66}$$

$$r_{5,6} = -2\alpha \tilde{D}_{66}, \quad r_{5,10} = \hat{D}_{66}, \quad r_{5,11} = \alpha \hat{D}_{66}$$

$$r_{6,2} = -\tilde{D}_{22} a_{12,2} - B_{22} a_{4,2}, \quad r_{6,3} = -\tilde{D}_{22} a_{12,3} - B_{22} a_{4,3}$$

$$r_{6,6} = -\tilde{D}_{22} a_{12,6} - B_{22} a_{4,6} - \alpha^2 (D_{12} + 4D_{66}) + T_{22}$$

$$r_{6,8} = -\tilde{D}_{22} a_{12,8} - B_{22} a_{4,8} + D_{22}$$



$$r_{6,10} = -\tilde{D}_{22}a_{12,10} - B_{22}a_{4,10} + \alpha(\tilde{D}_{12} + 2\tilde{D}_{66})$$

$$r_{6,11} = -\tilde{D}_{22}a_{12,11} - B_{22}a_{4,11} + 2\alpha^2\tilde{D}_{66}$$

where  $a_{i,j}$  are given in Appendix C and for convenience the subscript  $m$  of  $\alpha$  is dropped here.

## Appendix E. The constant coefficients in equation (4.16)

$$\alpha_0 = \frac{2ab}{3\pi^2}, \quad \alpha_1 = \alpha_2 = 0$$

$$\begin{aligned} \alpha_3 = & \frac{\omega_1}{2} \int_0^b \int_0^a \left\{ l_1 (g_{11}^2 + g_{21}^2 + g_{31}^2) + \bar{l}_3 (g_{41}^2 + g_{51}^2) \right. \\ & \left. - 2\bar{l}_0 \left( \frac{\partial g_{31}}{\partial x} g_{41} + \frac{\partial g_{31}}{\partial y} g_{51} \right) + l_3 \left[ \left( \frac{\partial g_{31}}{\partial x} \right)^2 + \left( \frac{\partial g_{31}}{\partial y} \right)^2 \right] \right\} dx dy \end{aligned}$$

$$\begin{aligned} \alpha_4 = & \frac{\omega_2}{2} \int_0^b \int_0^a \left\{ l_1 (g_{12}^2 + g_{22}^2 + g_{32}^2) + \bar{l}_3 (g_{42}^2 + g_{52}^2) \right. \\ & \left. - 2\bar{l}_0 \left( \frac{\partial g_{32}}{\partial x} g_{42} + \frac{\partial g_{32}}{\partial y} g_{52} \right) + l_3 \left[ \left( \frac{\partial g_{32}}{\partial x} \right)^2 + \left( \frac{\partial g_{32}}{\partial y} \right)^2 \right] \right\} dx dy \end{aligned}$$

$$\begin{aligned}
\alpha_5 = & \frac{1}{2} \int_0^b \int_0^a \left\{ A_{11} \left[ 2 \frac{\partial g_{11}}{\partial x} \frac{\partial g_{31}}{\partial x} \frac{\partial g_{32}}{\partial x} + \frac{\partial g_{12}}{\partial x} \left( \frac{\partial g_{31}}{\partial x} \right)^2 \right] \right. \\
& + A_{22} \left[ 2 \frac{\partial g_{21}}{\partial y} \frac{\partial g_{31}}{\partial y} \frac{\partial g_{32}}{\partial y} + \frac{\partial g_{22}}{\partial y} \left( \frac{\partial g_{31}}{\partial y} \right)^2 \right] \\
& + 2A_{66} \left( \frac{\partial g_{11}}{\partial y} \frac{\partial g_{31}}{\partial x} \frac{\partial g_{32}}{\partial y} + \frac{\partial g_{11}}{\partial y} \frac{\partial g_{32}}{\partial x} \frac{\partial g_{31}}{\partial y} \right. \\
& + \frac{\partial g_{21}}{\partial x} \frac{\partial g_{31}}{\partial x} \frac{\partial g_{32}}{\partial y} + \frac{\partial g_{21}}{\partial x} \frac{\partial g_{32}}{\partial x} \frac{\partial g_{31}}{\partial y} \\
& \left. \left. + \frac{\partial g_{12}}{\partial y} \frac{\partial g_{31}}{\partial x} \frac{\partial g_{31}}{\partial y} + \frac{\partial g_{22}}{\partial x} \frac{\partial g_{31}}{\partial x} \frac{\partial g_{31}}{\partial y} \right) \right. \\
& + A_{12} \left[ 2 \frac{\partial g_{11}}{\partial x} \frac{\partial g_{31}}{\partial y} \frac{\partial g_{32}}{\partial y} + 2 \frac{\partial g_{21}}{\partial y} \frac{\partial g_{31}}{\partial x} \frac{\partial g_{32}}{\partial x} \right. \\
& \left. + \frac{\partial g_{22}}{\partial y} \left( \frac{\partial g_{32}}{\partial x} \right)^2 + \frac{\partial g_{12}}{\partial x} \left( \frac{\partial g_{31}}{\partial y} \right)^2 \right] \\
& + \hat{B}_{11} \left[ \frac{\partial g_{42}}{\partial x} \left( \frac{\partial g_{31}}{\partial x} \right)^2 + 2 \frac{\partial g_{31}}{\partial x} \frac{\partial g_{32}}{\partial x} \frac{\partial g_{41}}{\partial x} \right] \\
& + \hat{B}_{22} \left[ \frac{\partial g_{52}}{\partial y} \left( \frac{\partial g_{31}}{\partial y} \right)^2 + 2 \frac{\partial g_{31}}{\partial y} \frac{\partial g_{32}}{\partial y} \frac{\partial g_{51}}{\partial y} \right] \\
& - B_{11} \left[ \frac{\partial^2 g_{32}}{\partial x^2} \left( \frac{\partial g_{31}}{\partial x} \right)^2 + 2 \frac{\partial^2 g_{31}}{\partial x^2} \frac{\partial g_{31}}{\partial x} \frac{\partial g_{32}}{\partial x} \right] \\
& \left. - B_{22} \left[ \frac{\partial^2 g_{32}}{\partial y^2} \left( \frac{\partial g_{31}}{\partial y} \right)^2 + 2 \frac{\partial^2 g_{31}}{\partial y^2} \frac{\partial g_{31}}{\partial y} \frac{\partial g_{32}}{\partial y} \right] \right\} dx dy
\end{aligned}$$

$$\begin{aligned}
\alpha_6 = & \frac{3}{8} \int_0^b \int_0^a \left[ A_{11} \left( \frac{\partial g_{31}}{\partial x} \right)^4 + A_{22} \left( \frac{\partial g_{31}}{\partial y} \right)^4 \right. \\
& \left. + 2(A_{12} + 2A_{66}) \left( \frac{\partial g_{31}}{\partial x} \right)^2 \left( \frac{\partial g_{31}}{\partial y} \right)^2 \right] dx dy
\end{aligned}$$

$$\begin{aligned}
\alpha_7 = & \frac{3}{8} \int_0^b \int_0^a \left[ A_{11} \left( \frac{\partial g_{32}}{\partial x} \right)^4 + A_{22} \left( \frac{\partial g_{32}}{\partial y} \right)^4 \right. \\
& \left. + 2(A_{12} + 2A_{66}) \left( \frac{\partial g_{32}}{\partial x} \right)^2 \left( \frac{\partial g_{32}}{\partial y} \right)^2 \right] dx dy
\end{aligned}$$

$$\begin{aligned}
\alpha_8 = & \frac{1}{2} \int_0^b \int_0^a \left\{ 3A_{11} \left( \frac{\partial g_{31}}{\partial x} \right)^2 \left( \frac{\partial g_{32}}{\partial x} \right)^2 + 3A_{22} \left( \frac{\partial g_{31}}{\partial y} \right)^2 \left( \frac{\partial g_{32}}{\partial y} \right)^2 \right. \\
& + (A_{12} + 2A_{66}) \left[ \left( \frac{g_{31}}{\partial x} \right)^2 \left( \frac{\partial g_{32}}{\partial y} \right)^2 + \left( \frac{\partial g_{32}}{\partial x} \right)^2 \left( \frac{\partial g_{31}}{\partial y} \right)^2 \right. \\
& \left. \left. + 4 \frac{\partial g_{31}}{\partial x} \frac{\partial g_{32}}{\partial x} \frac{\partial g_{31}}{\partial y} \frac{\partial g_{32}}{\partial y} \right] \right\} dx dy
\end{aligned}$$

## Appendix F. The elements of the Jacobian matrices

The elements of the Jacobian matrix  $\mathbf{J}_1$  associated with equations (4.30) are:

$$J_{11} = -\mu_1 - \Lambda_1 q_2 - 2\Lambda_3 p_1 q_1$$

$$J_{12} = \frac{1}{2}(\sigma_1 + \sigma_2) + \Lambda_1 p_2 - \Lambda_3(p_1^2 + 3q_1^2) - \Lambda_5(p_2^2 + q_2^2)$$

$$J_{13} = \Lambda_1 q_1 - 2\Lambda_5 p_2 q_1$$

$$J_{14} = -\Lambda_1 p_1 - 2\Lambda_5 q_1 q_2$$

$$J_{21} = -\frac{1}{2}(\sigma_1 + \sigma_2) + \Lambda_1 p_2 + \Lambda_3(3p_1^2 + q_1^2) + \Lambda_5(p_2^2 + q_2^2)$$

$$J_{22} = -\mu_1 + \Lambda_1 q_2 + 2\Lambda_3 p_1 q_1$$

$$J_{23} = \Lambda_1 p_1 + 2\Lambda_5 p_1 p_2$$

$$J_{24} = \Lambda_1 q_1 + 2\Lambda_5 p_1 q_2$$

$$J_{31} = -2\Lambda_2 q_1 - 2\Lambda_6 p_1 q_2$$

$$J_{32} = -2\Lambda_2 p_1 - 2\Lambda_6 q_1 q_2$$

$$J_{33} = -\mu_2 - 2\Lambda_4 p_2 q_2$$

$$J_{34} = \sigma_2 - \Lambda_4(p_2^2 + 3q_2^2) - \Lambda_6(p_1^2 + q_1^2)$$

$$J_{41} = 2\Lambda_2 p_1 + 2\Lambda_6 p_1 p_2$$

$$J_{42} = -2\Lambda_2 q_1 + 2\Lambda_6 p_2 q_1$$

$$J_{43} = -\sigma_2 + \Lambda_4(3p_2^2 + q_2^2) + \Lambda_6(p_1^2 + q_1^2)$$

$$J_{44} = -\mu_2 + 2\Lambda_4 p_2 q_2$$

The elements of the Jacobian matrix  $\mathbf{J}_2$  associated with equations (5.38) are:

$$J_{11} = -\mu_1 - \Lambda_1 a_2 \sin \gamma_1$$

$$J_{21} = 2\Lambda_2 a_1 \sin \gamma_1$$

$$J_{31} = 2\Lambda_2 a_1 \cos \gamma_1 / a_2 + 2(\Lambda_6 - 2\Lambda_3) a_1$$

$$J_{41} = -2\Lambda_2 a_1 \cos \gamma_1 / a_2 - 2\Lambda_6 a_1$$

$$J_{12} = -\Lambda_1 a_1 \sin \gamma_1$$

$$J_{22} = -\mu_2$$

$$J_{32} = (F \cos \gamma_2 - \Lambda_2 a_1^2 \cos \gamma_1) / a_2^2 + 2(\Lambda_4 - 2\Lambda_5) a_2 - 2\Lambda_1 \cos \gamma_1$$

$$J_{42} = (-F \cos \gamma_2 + \Lambda_2 a_1^2 \cos \gamma_1) / a_2^2 - 2\Lambda_4 a_2$$

$$J_{13} = -\Lambda_1 a_1 a_2 \cos \gamma_1$$

$$J_{23} = \Lambda_2 a_1^2 \cos \gamma_1$$

$$J_{33} = (2\Lambda_1 a_2^2 - \Lambda_2 a_1^2) \sin \gamma_1 / a_2$$

$$J_{43} = \Lambda_2 a_1^2 \sin \gamma_1 / a_2$$

$$J_{14} = 0$$

$$J_{24} = F \cos \gamma_2$$

$$J_{34} = F \sin \gamma_2 / a_2$$

$$J_{44} = -F \sin \gamma_2 / a_2$$

## **VITA**

The author, Mohammad Jafar Hadian, was born in Iran on September, 6, 1956. He obtained a Bachelor Degree in Civil Engineering from the University of Nebraska in 1981. He earned two Master Degrees, one in Structural Engineering (1982) and another in Applied Mathematics (1985), from the University of Nebraska. He joined Virginia Polytechnic Institute and State University in 1985 and received a Doctor of Philosophy in Engineering Mechanics in May 1991.